

A quarter-million years of paleoenvironmental change at Bear Lake, Utah and Idaho

Darrell S. Kaufman

Jordon Bright

Department of Geology, Box 4099, Northern Arizona University, Flagstaff, Arizona 86011, USA

Walter E. Dean

Joseph G. Rosenbaum

U.S. Geological Survey, Box 25046, MS 980 Federal Center, Denver, Colorado 80225, USA

Katrina Moser

University of Western Ontario, Department of Geography, London, Ontario N5Y 2S9, Canada

R. Scott Anderson

Center for Environmental Sciences and Education, Northern Arizona University, Flagstaff, Arizona 86011, USA

Steven M. Colman

Large Lakes Observatory and Department of Geological Sciences, University of Minnesota, Duluth, Minnesota 02543, USA

Clifford W. Heil Jr.

School of Oceanography, University of Rhode Island, South Ferry Road, Narragansett, Rhode Island 02882, USA

Gonzalo Jiménez-Moreno

Center for Environmental Sciences and Education, Northern Arizona University, Flagstaff, Arizona 86011, USA

Marith C. Reheis

Kathleen R. Simmons

U.S. Geological Survey, Box 25046, MS 980 Federal Center, Denver, Colorado 80225, USA

ABSTRACT

A continuous, 120-m-long core (BL00-1) from Bear Lake, Utah and Idaho, contains evidence of hydrologic and environmental change over the last two glacial-interglacial cycles. The core was taken at 41.95°N, 111.31°W, near the depocenter of the 60-m-deep, spring-fed, alkaline lake, where carbonate-bearing sediment has accumulated continuously. Chronological control is poor but indicates an average sedimentation rate of 0.54 mm yr⁻¹. Analyses have been completed at multi-centennial to millennial scales, including (in order of decreasing temporal resolution) sediment magnetic properties,

oxygen and carbon isotopes on bulk-sediment carbonate, organic- and inorganic-carbon contents, palynology; mineralogy (X-ray diffraction), strontium isotopes on bulk carbonate, ostracode taxonomy, oxygen and carbon isotopes on ostracodes, and diatom assemblages. Massive silty clay and marl constitute most of the core, with variable carbonate content (average = $31 \pm 19\%$) and oxygen-isotopic values ($\delta^{18}\text{O}$ ranging from -18‰ to -5‰ in bulk carbonate). These variations, as well as fluctuations of biological indicators, reflect changes in the water and sediment discharged from the glaciated headwaters of the dominant tributary, Bear River, and the processes that influenced sediment delivery to the core site, including lake-level changes. Although its influence has varied, Bear River has remained a tributary to Bear Lake during most of the last quarter-million years. The lake disconnected from the river and, except for a few brief excursions, retracted into a topographically closed basin during global interglaciations (during parts of marine isotope stages 7, 5, and 1). These intervals contain up to 80% endogenic aragonite with high $\delta^{18}\text{O}$ values (average = $-5.8 \pm 1.7\text{‰}$), indicative of strongly evaporitic conditions. Interglacial intervals also are dominated by small, benthic/tychoplanktic fragilarioid species indicative of reduced habitat availability associated with low lake levels, and they contain increased high-desert shrub and *Juniperus* pollen and decreased forest and forest-woodland pollen. The $^{87}\text{Sr}/^{86}\text{Sr}$ values (>0.7100) also increase, and the ratio of quartz to dolomite decreases, as expected in the absence of Bear River inflow. The changing paleoenvironments inferred from BL00-1 generally are consistent with other regional and global records of glacial-interglacial fluctuations; the diversity of paleoenvironmental conditions inferred from BL00-1 also reflects the influence of catchment-scale processes.

INTRODUCTION

Bear Lake, Utah and Idaho, is one of the longest-lived extant lakes on the North American continent. The half-graben that contains the lake is filled with an estimated 3 km of sediment (Evans et al., 2003). High-resolution seismic-reflection profiles of the upper 250 m reveal well-layered sediment with few unconformities (Colman, 2006). The upper part of the sedimentary sequence was recovered in a 120-m-long composite core drilled in 2000 (BL00-1; Dean et al., 2002). Sediment deposited in Bear Lake is strongly influenced by variable production of endogenic carbonate within the lake, by fluctuating input of fluvial and glacial-fluvial products from its headwaters in the Uinta Mountains and local catchment, and by periodic retraction of the lake into a topographically closed basin. These, in turn, are influenced by climatic and non-climatic processes. The extent to which changes in the lacustrine deposits can accurately be ascribed to particular causes depends on a multi-parameter investigation of its physical, chemical, and biological composition. The purpose of this chapter is to synthesize the available data on BL00-1, and to summarize our current understanding of paleoenvironmental change over the last two glacial-interglacial cycles at Bear Lake.

To date, most analyses of BL00-1 are based on sampling on the scale of decimeters (centuries) to meters (millennia). More detailed, centimeter-scale analyses have been completed on shorter cores from the lake (see overview of the lake-coring campaign by Rosenbaum and Kaufman, this volume). Our interpretations of BL00-1 rely heavily on analyses of these shorter cores, which in some cases benefited from parameters that were not measured

in BL00-1 (e.g., elemental geochemistry; Rosenbaum et al., this volume). They also rely on an understanding of the modern composition and fluxes of sediment and water to the lake (e.g., Dean et al., 2007; Bright, this volume, Chapter 4). The rerouting of Bear River water into Bear Lake ca. 1912 had a pervasive effect on the lake. This event affords a whole-lake experiment on the response of lake sediment to a major hydrological change. The reader is referred to the other chapters and journal articles for a more detailed account of the methods and interpretations that are summarized in this chapter. The other works place the BL00-1 core site into a lake- and drainage-basin-wide context.

Setting

Bear Lake is located in an intermontane basin straddling the northeastern Great Basin and the Rocky Mountain physiographic provinces along the Utah-Idaho state border (Fig. 1). The primary surface-water inflow to Bear Lake Valley is the Bear River, which drains the northwest sector of the Uinta Mountains southeast of the lake. Within historical times, the river was not connected directly to the lake, but bypassed the lake en route to Great Salt Lake, located 100 km southwest of Bear Lake. When separated from Bear River, the primary surface inflows are streams that drain eastward from the Bear River Range, which are fed by springs that emerge from cavernous Paleozoic carbonate rocks. This "local" surface catchment area is relatively small, encompassing $\sim 1300 \text{ km}^2$, or about five times the surface area of the lake (280 km^2). When Bear River is a tributary to the lake, the drainage basin area expands by a factor of six. Reheis et al. (this volume)

discuss mechanisms that might have caused Bear River to swing into and out of Bear Lake. Bear Lake Valley currently contains an alkaline lake (Bear Lake) that is confined to the southern end of the valley, with an overflow threshold at an elevation of 1805 m above sea level (asl). The lake is ~30 km long and 10 km wide, with a maximum depth of 63 m. The physical, chemical, and biological limnology of the lake is reviewed by Dean et al. (this volume).

At present, Bear Lake is nearly in hydrologic balance, and only a small increase in effective moisture would be required to cause the lake to overflow (Bright et al., 2006; Bright, this volume, Chapter 4). Intermittent overflow is also indicated by Lamarra et al.'s (1986) hydrological balance modeling, which showed that, without the diversion of Bear River, Bear Lake would have exceeded its threshold ~24% of the time during the 60 years prior to 1984. Furthermore, McConnell et al. (1957) provided historical reports

of northward drainage, and Reheis et al. (this volume) described north-trending channels that were active during the Holocene. With a transgression of just a few meters, the northern shoreline of Bear Lake would capture the channel of Bear River. Once the shoreline intersected the river, surface-water inflow to the lake would more than double, and the water residence time would be reduced by an order of magnitude. To disconnect the river from the lake requires the lake shoreline to regress south of where the river enters the valley. Climate-induced desiccation could cause a regression, as could erosion of the lake outlet where it previously fed now-abandoned, north-flowing channels. If the elevation of this outlet lowered, then lake level would lower despite inflow of the Bear River. In summary, the lake can alternate between topographically open (overflowing) and closed states. The lake may overflow without input from Bear River, but when the lake expands, it necessarily is

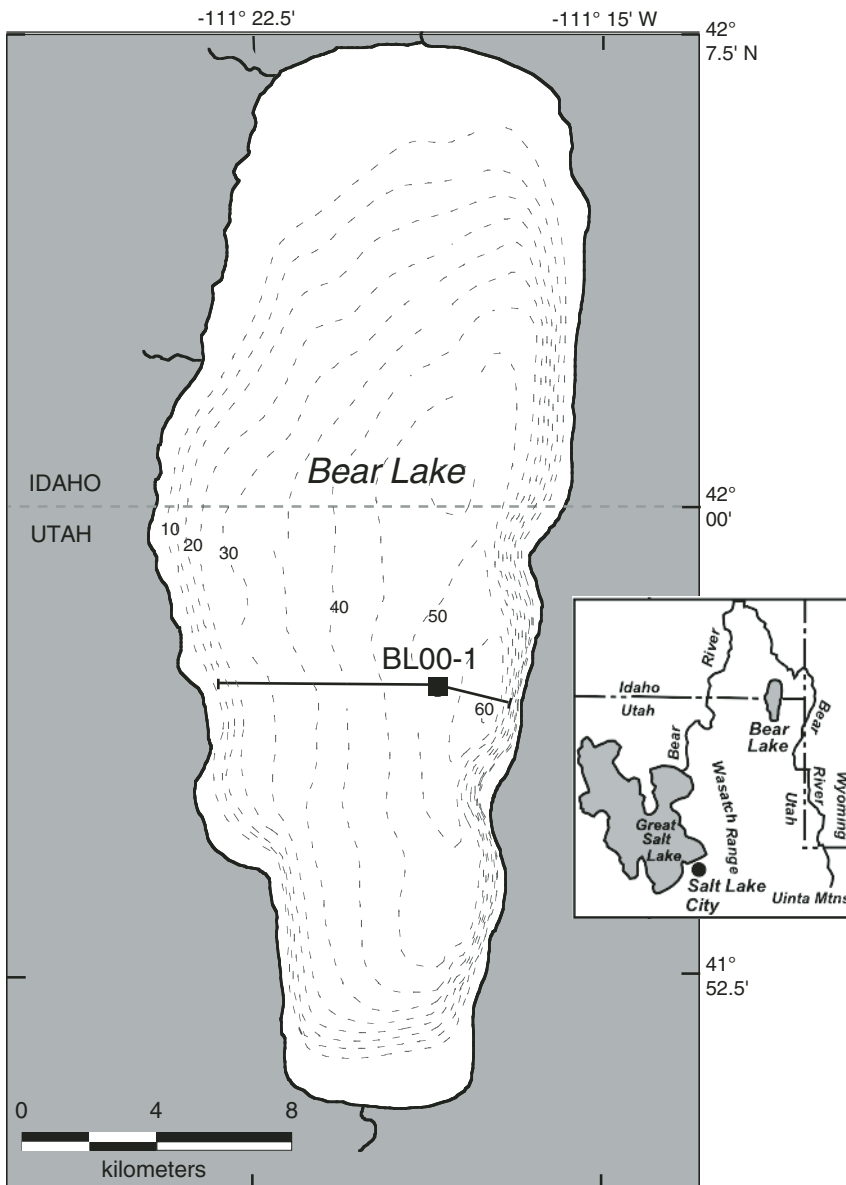


Figure 1. Location map showing Bear Lake and BL00-1 core site. Solid line is track of acoustic profile shown in Figure 2. Bathymetry (dotted lines) in meters from Denny and Colman (2003).

connected with the river. Lake-level changes in Bear Lake Valley are controlled by climatic changes as well as tectonic effects and the dynamics of erosion and deposition of the outlet stream that control the elevation of the basin threshold.

The core site (BL00-1; 41.9517°N, 111.3083°W) is in 54.8 m water depth (relative to full lake [1805 m asl]) near the lake depocenter, where sedimentation rates are highest. Acoustic subbottom profiles show that the stratigraphic units are laterally continuous and thin westward from the core site (Fig. 2; Colman, 2006). The site was located ~1.5 km west of the deepest part of the lake with the intent of reducing the impact of subaqueous mass wasting associated with the steep fault-bounded eastern margin of the lake. Two holes offset by a few meters were drilled by the GLAD800 (Global Lake Drilling to 800 m) platform during its trial engineering tests in September 2000 (http://dosecc.org/html/utah_lakes.html; Dean et al., 2002). Continuous coring in 2- or 3-m-long segments produced ~100 m of sediment from one hole (BL00-1D) and 121.07 m from the second (BL00-1E), both with essentially 100% recovery. Core breaks were offset vertically to provide a continuous record. Fluctuations in magnetic susceptibility were used to correlate between the holes, resulting in a composite record (hereafter, "BL00-1") based on the depth scale of BL00-1E.

SUMMARY OF PRIMARY FINDINGS

Geochronology

The currently accepted age model for BL00-1 was developed by Colman et al. (2006) (Fig. 3). The model is based on ^{14}C

ages from shorter cores (Colman et al., this volume) projected onto the upper part of BL00-1 on the basis of correlations by magnetic susceptibility and other stratigraphic markers. Numerical age control beyond the range of ^{14}C dating includes one magnetic excursion correlated with the Laschamp excursion (Heil et al., this volume), and a single uranium-series age on aragonite from the last interglaciation (Colman et al., 2006). Amino acid racemization and tephrochronology support the overall sedimentation rates determined by the other three techniques (Colman et al., 2006). In addition, peaks and troughs in the carbonate content and stable isotope composition of BL00-1 can be correlated with those of the well-dated oxygen isotope record of vein calcite from Devils Hole (Winograd et al., 1992), located ~700 km southwest of Bear Lake. The correlations provide the only available age control for the lower half of the core, and they impose an age for Termination II that is ~12,000 years older than that inferred for the global marine oxygen isotope record. As emphasized by Colman et al. (2006), tuning the BL00-1 chronology to Devils Hole limits our ability to infer the timing of events from BL00-1 independently of the assumption that climate change is registered simultaneously at Bear Lake and Devils Hole.

To avoid the limitations of an age model predicated on climate correlations, for this synthesis we adopt an age model based on four secure ages only, and the assumption of a linear sedimentation rate (Fig. 3). The four points used to determine the sedimentation rate are (1) the surface (0 m below lake floor [blf] = 0 yr = A.D. 2000); (2) the prominent peak in sediment magnetic properties, which has been ascribed to glacier flour production (Rosenbaum and Heil, this volume) and dated by ^{14}C (Colman et

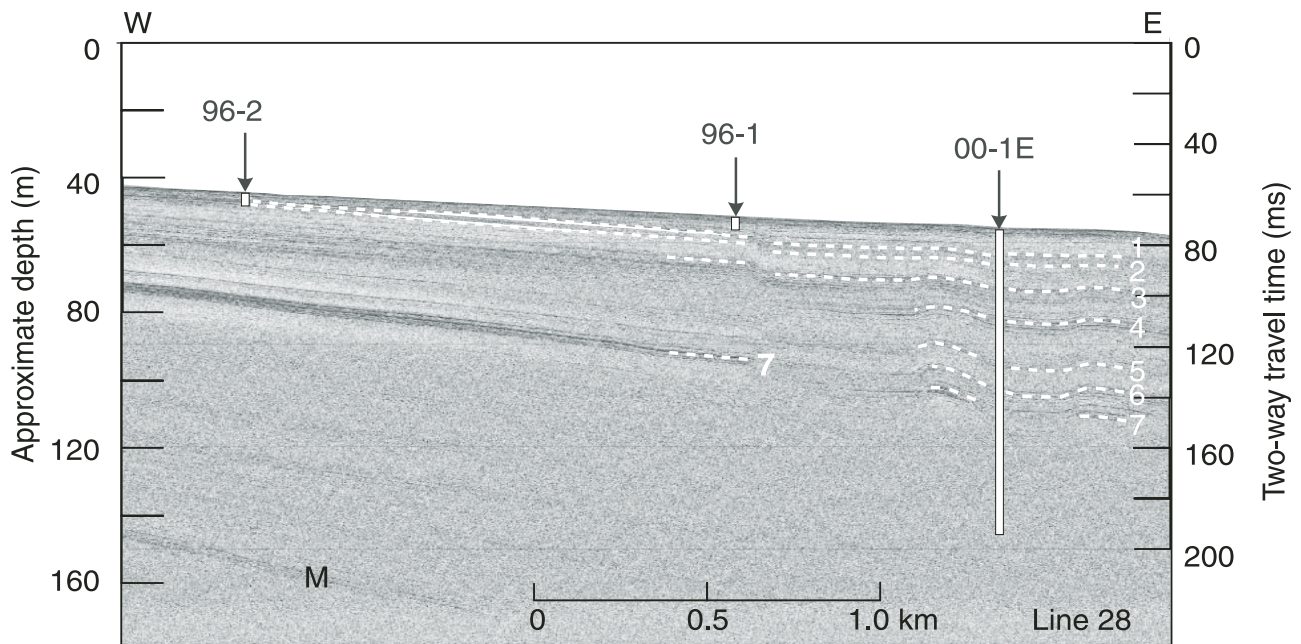


Figure 2. Acoustic profile along section line through core site BL00-1E (from Colman, 2006). Numbered dashed lines mark prominent reflectors. Approximate depths are calculated from two-way travel time, assuming a sound velocity of 1500 m s^{-1} . 96-2 and 96-1 are locations of gravity cores collected in 1996 and discussed elsewhere in this volume. M—multiple reflection.

al., this volume) (11.38 m blf = 18.52 cal ka); (3) the correlated Laschamp excursion (26.5 m blf = 41 ka; Heil et al., this volume); and (4) the uranium-series age (67 m blf = 127.7 ka; Colman et al., 2006). A least-squares linear regression with y-intercept forced through zero results in an average sedimentation rate of 0.54 mm yr^{-1} over the upper half of the core ($r^2 = 0.990$), which we extrapolate over the lower half. This rate is identical to the average rate over the entire core based on the original age model of Colman et al. (2006) and, like the original model, is supported by the available tephrochronology.

The ages based on this simple linear model are approximate. The average absolute difference between the Devils-Hole-tuned and the linear age models is 4900 years as evaluated at 1 m intervals, with the largest differences (up to 12,000 yr) centered on 80 m blf. This difference is less than the average age uncertainty of $\pm 11,000$ years for the original age model based on the 95% confidence intervals of the spline-fitting procedure used by Colman et al. (2006). We emphasize the importance of the broad age uncertainties for BL00-1, even though errors are not stated along with the approximate ages cited in this chapter. This chapter deals with trends over the entire 120-m-long core based on an approximate time scale with uncertainties of several millennia. References

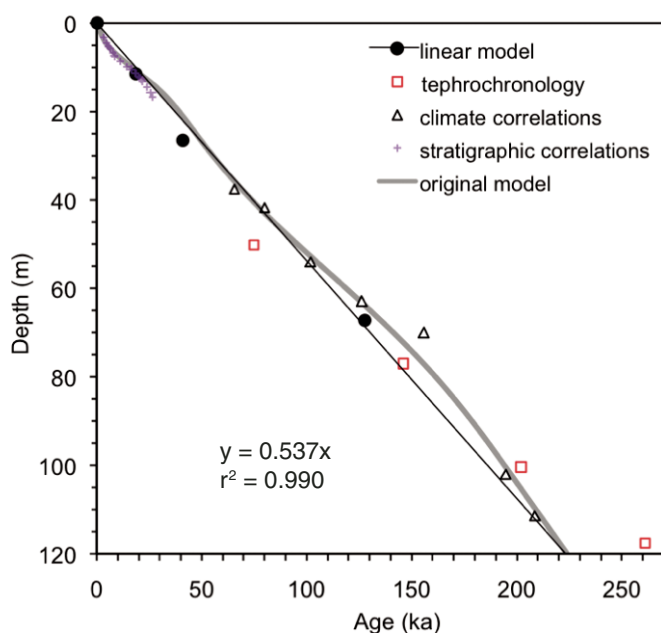


Figure 3. Geochronology of core BL00-1. The age model used in this chapter is based on the least-squares linear regression through the four points from the upper half of the core (solid circles) and is independent of any assumptions about regional or global climate correlations (see text for discussion). The original age model of Colman et al. (2006; thick gray curve) was tuned to correlate with the chronology from Devils Hole (triangles). Tephra ages (squares) are discussed by Colman et al. (2006); stratigraphic correlations based on ^{14}C ages from piston cores (small plus signs) over the upper 20 m are described by Colman et al. (this volume), and are not used in this chapter.

to marine oxygen isotope stages (MIS) are for convenience and do not imply strict correlations to the record of global ice volume.

Colman et al. (this volume) present a detailed age model for the top 20 m of BL00-1 (last 30,000 years), which is well constrained by ^{14}C in other piston cores and transferred to BL00-1 on the basis of correlations of stratigraphic horizons. The ^{14}C chronology shows that the average linear sedimentation rate is too low over the Holocene (Fig. 3); ages generated by the linear model are as much as 5000 years too old during the early Holocene (5–10 m blf). The linear model coincides with the ^{14}C chronology during the last local glacial maximum (11 m blf), but is 7000 years too old at the depth of the presumed Laschamp excursion (26.5 m blf).

Lithostratigraphy

The cores were curated at the Limnological Research Center (LRC), University of Minnesota, where they were processed according to standard initial core description (ICD) procedure (<http://lrc.geo.umn.edu/corefac-icd.htm>). The results of whole-core logging of porosity, bulk density, magnetic susceptibility, and P-wave velocity are available digitally, along with visual descriptions of the lithostratigraphy and photographs of each split-core segment (<http://www.ngdc.noaa.gov/mgg/curator/curator.html>). Smear slides were made at levels where lithology changed, and the observations were incorporated into the descriptions of the cores.

Briefly, the sediment consists mainly of massive gray to greenish-gray silty clay with carbonate contents ranging from calcareous silty clay (<30% CaCO_3) to marl (>30% CaCO_3) (Fig. 4). Most of the CaCO_3 is low-Mg calcite, but two of the marl units consist almost entirely of aragonite, and a third is aragonite-bearing. Most units contain centimeter-scale bands distinguished by degree of bioturbation or color, which probably reflect differences in the content of sulfide minerals, organic matter, and CaCO_3 abundance. The sedimentary sequence is subdivided into seven primary units (Fig. 4), which roughly coincide with the mineral magnetic zonation of Heil et al. (this volume): Unit 1 (from the base of the core to 101 m blf) is marl, composed mostly of aragonite near the top of the unit (103.1–101.6 m blf), with calcite below. Unit 2 (101–67 m blf) is calcareous silty clay. Unit 3 (67–61 m blf) is aragonitic marl. Unit 4 (61–40 m blf) is marl. Unit 5 (40–17 m blf) is calcareous clay. Unit 6 (17–10 m blf) is reddish-gray silty clay. Unit 7 (10–0 m blf) is light-gray aragonitic marl.

Organic and Inorganic Carbon

A total of 334 samples, at an average spacing of ~ 36 cm through core BL00-1, were analyzed by coulometry (e.g., Engleman et al., 1985) to measure the total carbon and inorganic carbon (IC) contents. Organic carbon (OC) was calculated as the difference between the two values, and weight percent CaCO_3 was calculated by dividing IC by the fraction of carbon in CaCO_3 (0.12). The same technique was used by Dean (this volume) and Dean et al. (2006, 2007) to analyze sediment from shorter piston cores. The results are tabulated in Appendix A and are shown in

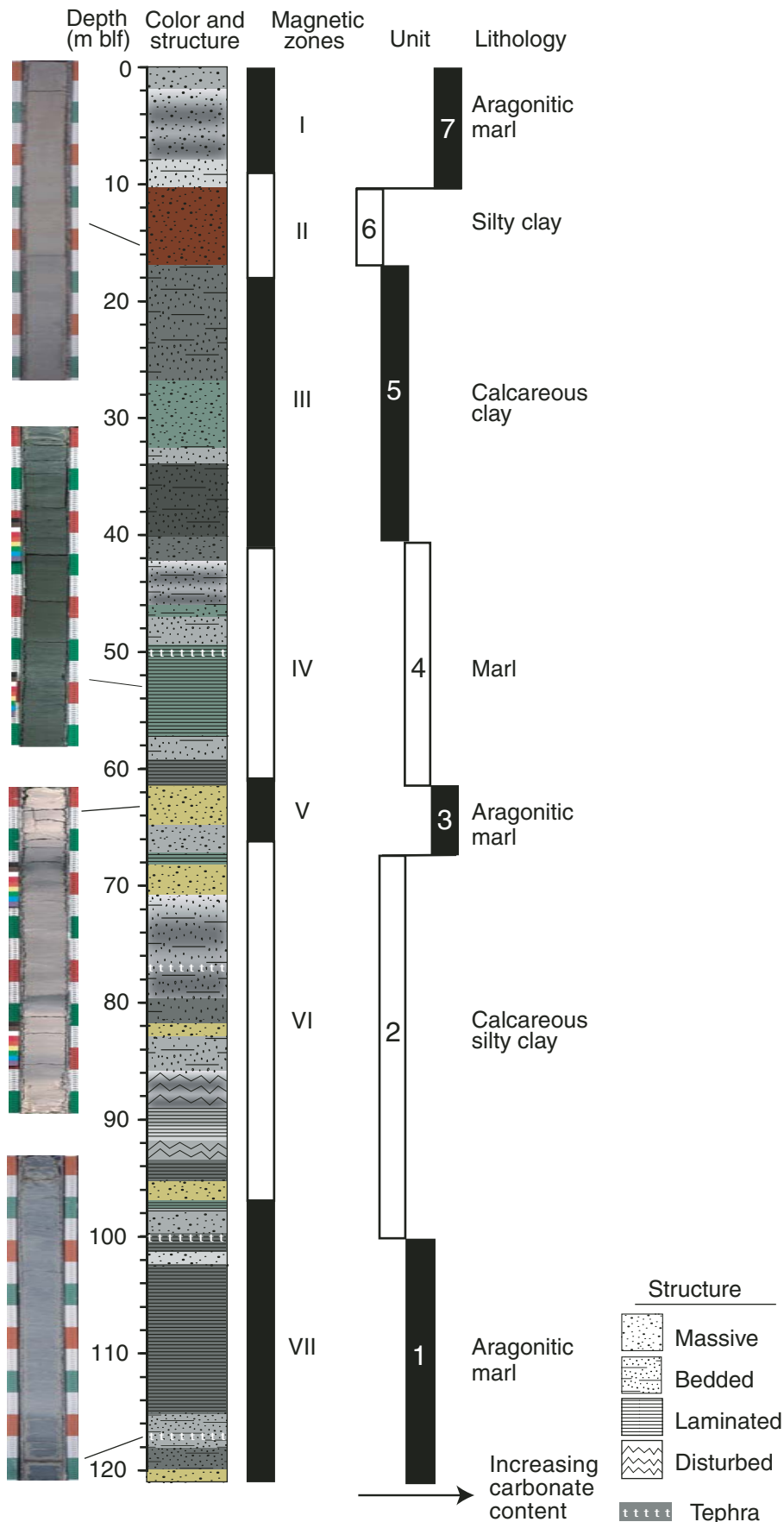


Figure 4. Lithostratigraphy of core BL00-1 dividing the core into seven lithologic units as summarized from the initial core descriptions (<http://www.ngdc.noaa.gov/mgg/curator/curator.html>). Depths are in meters below lake floor (m blf). Core photographs of four selected colors and features are shown on the left. Colors on lithologic log, including shades of gray, denote mud colors, but are not accurate representations. Magnetic zones (I–VII) are based on mineral magnetic properties discussed by Heil et al. (this volume).

Figure 5, together with the results of other analyses, where the sample depth has been transferred to age based on a linear sedimentation rate of 0.54 mm yr^{-1} (Fig. 3).

The abundance of OC in Bear Lake sediment reflects the flux of organic matter delivered to the lake and produced within the water column, relative to the rate at which it is decomposed. The CaCO_3 content is controlled primarily by the production rate of endogenic carbonate, and secondarily by the flux of allogenic carbonate delivered to the lake, reworking of previously deposited carbonate, carbonate dissolution, and dilution by the non-carbonate lithic input. The type and rate of endogenic carbonate produced by Bear Lake water are dictated by a variety of hydro-geochemical factors reviewed by Dean (this volume).

The CaCO_3 content in BL00-1 averages $31 \pm 19\%$ over the core ($n = 334$). Six intervals (111.7–109.0, 103.5–100.1, 67.4–61.4, 56.6–52.5, 41.9–41.2, and 8.9–0 m blf) constituting 29% of the samples, contain distinctly higher CaCO_3 contents that exceed 40% (average = $57 \pm 11\%$; $n = 97$). Trends in CaCO_3 content mimic the global marine oxygen isotope record. The substages of MIS 5 are expressed clearly by the total CaCO_3 content (Fig. 5). Sediment deposited during MIS 7 exhibits two prominent peaks that are correlated with substages 7c and 7a, and the later part of substage 7e is indicated by increasing CaCO_3 content of the lowest four samples. The X-ray diffraction analyses (discussed below) indicate that five CaCO_3 -rich intervals contain aragonite. They are correlated with the peak interglacial intervals, MIS 7c, 7a, 5e, 5c, and 1.

The OC content of BL00-1 sediment averages $1.3 \pm 0.7\%$. The OC and CaCO_3 contents are not inversely related, as might be expected through a dilution effect, but show a weak positive correlation ($r = 0.16$; $p = 0.07$). The OC content tends to be slightly higher in the aragonite-rich intervals (median = 1.2%) compared with the calcite-dominated intervals (median = 1.0%).

Mineralogy

The relative abundance of the common minerals that make up Bear Lake sediment was analyzed by X-ray diffraction (XRD). A total of 329 samples (nearly all of the levels analyzed by coulometry) were analyzed according to standard techniques (e.g., Moore and Reynolds, 1989), which are described by Dean et al. (2006) for the 1996 cores. In addition, the silt-plus-clay fractions (<53 μm ; hereafter “mud”) of 53 samples of fluvial sediment collected from the bed (27 samples) and flood-plain banks (26 samples) of modern streams were also analyzed by XRD; the results of these and other analyses of physical properties of fluvial sediment are presented by Rosenbaum et al. (this volume). Results for quartz, calcite, aragonite, dolomite, and feldspar from BL00-1 samples are reported as a percentage of the sum of the main XRD peak intensities (Appendix A). These percentage values are not accurate representations of the concentration of mineral abundances and should be interpreted cautiously because they do not account for different X-ray mass absorption characteristics of different minerals.

Quartz is the dominant mineral in Bear Lake sediment (average = $50 \pm 16\%$ over the entire core), except in the six CaCO_3 -rich

intervals. Quartz abundance estimated from XRD peak intensities is inversely related to the abundance of CaCO_3 as measured independently by coulometry, indicating the effect of dilution ($r = -0.87$, $p < 0.001$ for the correlation between log-transformed quartz versus CaCO_3 for the entire core) (Fig. 6). The XRD results also show that, of the six CaCO_3 -rich ($\text{CaCO}_3 > 40\%$) intervals, four are dominated by aragonite: 103.1–101.6, 67.4–61.0, 55.8–55.3, and 8.4–0 m blf, and a fifth interval contains some aragonite (111.0–110.5 m blf). Of these, aragonite is most abundant in the uppermost interval (Holocene) and least abundant in the lowermost (MIS 7c), possibly due in part to diagenetic conversion of aragonite to low-Mg calcite. One of the carbonate-rich intervals (MIS 5a) does not contain aragonite.

Most of the stream-sediment samples that we analyzed are also dominated by quartz. Mud carried by the Bear River in proximity to Bear Lake tends to contain a higher proportion of quartz (average = 80%) than that in the local tributaries (average = 65%) (Fig. 7). Perhaps the clearest mineralogical distinction of sediment carried by local streams is the dolomite content. Local stream mud contains an average of ~17% dolomite, with a higher proportion (25%) in the west-side streams, compared to 5% for Bear River mud. Dolomite is a significant constituent of Bear Lake sediment, averaging ~7% (when excluding the CaCO_3 -rich intervals), and is thought to be entirely allogenic (Dean et al., 2006; Rosenbaum et al., this volume). The relative percentages of quartz and dolomite track each other closely (Fig. 5) because they both derive from allogenic sources, and because they are related inversely to the relative percentage of calcite, the second most abundant mineral.

We examined downcore trends in two mineral constituents (Fig. 5). First, the relative abundance of quartz might serve as an indicator of the input of the allogenic component relative to endogenic carbonate, although the carbonate has both allogenic and endogenic sources that vary in proportion through the core. Second, the ratio of quartz to dolomite might provide some information on the relative importance of input from the Bear River, which is depleted in dolomite, versus input from local streams, which carry a higher proportion of dolomite (Fig. 7).

In summary, the mineralogy of Bear Lake sediment is controlled by the production rate of endogenic carbonate and the extent to which it is diluted by allogenic input. Aragonite formation depends on whether the lake water contains sufficient Mg, which appears to be the case only when Bear Lake is isolated from Bear River (Dean et al., 2007; Dean, this volume). Aragonite is preserved in five intervals of BL00-1, and these have been correlated with peak interglaciations of MIS 7c, 7a, 5e, 5c, and 1. Quartz is the dominant mineral in the carbonate-poor lake sediment and stream mud. An increase in the discharge of the Bear River relative to local streams might have the dual effect of increasing the flux of quartz and decreasing the production of endogenic carbonate, because water carried by the Bear River tends to have a lower solute content than the local streams and springs (Dean et al., 2007; Bright, this volume, Chapter 4). An increase of Bear River discharge relative to local discharge should also be indicated by

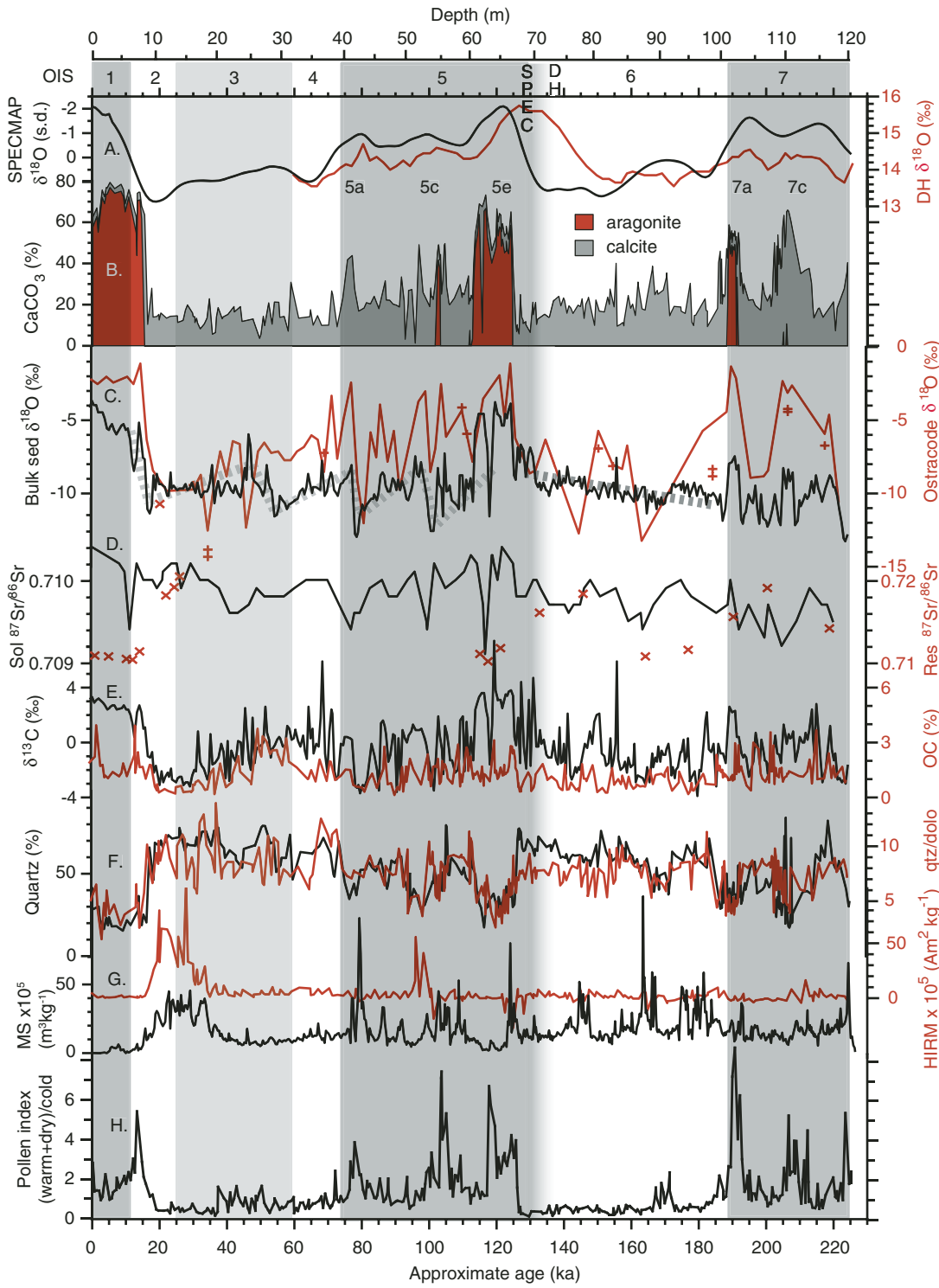


Figure 5. Downcore plots of mineralogical, isotopic, and magnetic properties of core BL00-1. Gray and white vertical intervals with numbers delimit marine isotope stages (MIS) according to SPECMAP chronology (SPEC = onset of MIS 5e in SPECMAP chronology; DH = onset of MIS 5e in Devils Hole chronology). Age model for BL00-1 is based on a linear sedimentation rate of 0.54 mm yr⁻¹ (Fig. 3). (A) Oxygen isotope values (δ¹⁸O) based on SPECMAP (black, standard deviation [s.d.] units) and Devils Hole calcite (red). (B) Calcite (gray) and aragonite (red) content, where the total CaCO₃ weight % is based on total inorganic carbon analysis and the relative proportion of the two mineral phases is based on X-ray diffraction (XRD) peak heights. (C) δ¹⁸O values in bulk-sediment carbonate (black), and ostracode calcite (red line—*Cardona* sp. 1; red crosses—*Cythereissa lacustris*); gray dashed lines highlight trends discussed in text. (D) Strontium-isotope ratios for 5M-acetic-acid-soluble fraction (sol—black), and insoluble residue fraction (res—red Xs). (E) Carbon isotope ratios (δ¹³C) in bulk-sediment carbonate (black), and organic carbon (OC) content (red). (F) Approximate quartz percentage (black), and ratio of quartz to dolomite (qtz/dolo) (red) based on XRD peak intensities. (G) Magnetic susceptibility (MS) (black); and hard isothermal remanent magnetization (HIRM) (red). (H) Pollen index calculated as the ratio of “dry” (*Ambrosia*, Chenopodiaceae-*Amaranthus*, and *Sarcobatus*) plus “warm” (*Quercus* and *Juniperus*) to cold (*Picea*, other Asteraceae, and *Eriogonum*) pollen indicators. All data are listed in Appendices, except magnetic properties and pollen abundances.

the ratio of quartz to dolomite in Bear Lake sediment, which is independent of endogenic carbonate production.

Sediment Magnetic Properties

The magnetic properties of Bear Lake sediment have been studied in samples from the shorter piston cores (Rosenbaum and Heil, this volume) and in continuous channel samples from BL00-1 (Heil et al., this volume). The magnetic properties of stream sediment in the Bear Lake drainage basin also have been characterized (Dean et al., 2006; Rosenbaum et al., this volume). Here we focus on two key magnetic properties from BL00-1 (Fig. 5): magnetic susceptibility (MS) and hard isothermal remnant magnetization (HIRM). MS commonly reflects the content of ferrimagnetic minerals (e.g., magnetite, titanomagnetite, and greigite), whereas HIRM is a measure of high-coercivity minerals (e.g., hematite and goethite). Variations in these properties in Bear Lake sediment can be explained largely by (1) post-depositional destruction of detrital Fe-oxide minerals, (2) dilution of magnetic minerals by non-magnetic endogenic CaCO_3 , and (3) post-depositional formation of greigite (a ferrimagnetic Fe-sulfide mineral).

Magnetic properties of BL00-1 are highly variable. The most important magnetic minerals in much of the cored section are detrital titanohematite and authigenic greigite. Petrographic observations (Reynolds and Rosenbaum, 2005) indicate that most detrital magnetite has been destroyed (either dissolved or converted to pyrite), although a small quantity is present in some samples, mostly protected inside rock fragments. Variations in MS arise largely from differences in the quantity of authigenic greigite, which varies greatly, probably reflecting changes in salinity (i.e., availability of sulfate).

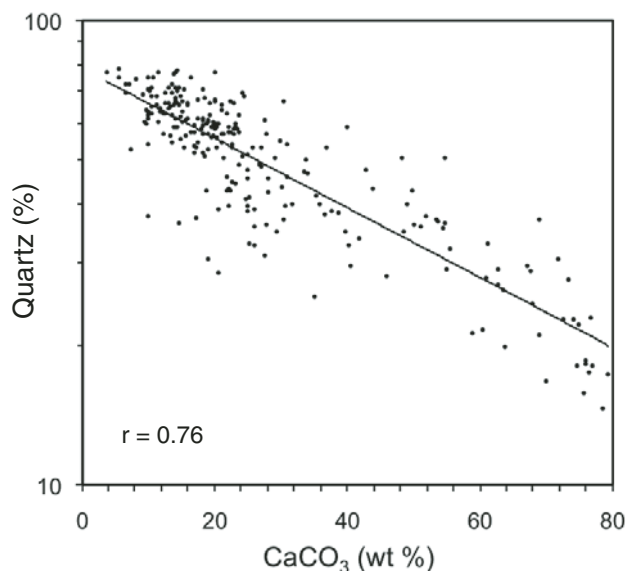


Figure 6. Percent CaCO_3 measured by coulometry versus quartz abundance estimated from X-ray diffraction peak intensities in samples from core BL00-1.

Two intervals exhibit exceptionally low values of MS and HIRM: from 66 to 61 m blf (MIS 5e) and from 9 to 0 m blf (younger than 15 ka). These reflect extensive alteration of detrital Fe-oxide minerals and dilution by high CaCO_3 contents. In contrast, the sediment from 18 to 9 m blf (MIS 2) exhibits high values of both MS and HIRM due to low CaCO_3 content and high magnetic mineral content. This is the only interval in which detrital Fe-oxide minerals are well preserved, and corresponds to high content of hematite-rich glacial flour from the headwaters of the Bear River in the Uinta Mountains (Rosenbaum and Heil, this volume). The preservation of the Fe-oxides in this interval reflects some combination of fresh water, rapid deposition, and perhaps greater quantities of detrital Fe-oxides.

Oxygen and Carbon Isotopes

Bright et al. (2006) reported the results of oxygen and carbon isotopic analyses from BL00-1. They analyzed bulk-sediment carbonate of 375 samples spaced at an average interval of 32 cm across the core (~700-year resolution). To compare the isotopic composition of purely endogenic carbonate with the bulk sediment, they also analyzed calcite in ostracode valves (*Candona* sp. 1; Bright et al., 2005) from 78 levels, mainly from the upper half of the core, where valves are better preserved. In addition, in this study we present new results on *Cytherissa* valves from 13 core levels to compare with the results on *Candona*. Values for the ratios of $^{18}\text{O}/^{16}\text{O}$ and $^{13}\text{C}/^{12}\text{C}$ are reported using standard permil (‰) δ notation, where the standards Vienna Standard Mean Ocean Water (VSMOW) and Vienna Pee Dee Belemnite (VPDB) were used for water and carbonate, respectively. Additional context for interpreting the downcore changes in $\delta^{18}\text{O}$ and $\delta^{13}\text{C}$ from BL00-1 is provided by (1) the isotopic composition of water that

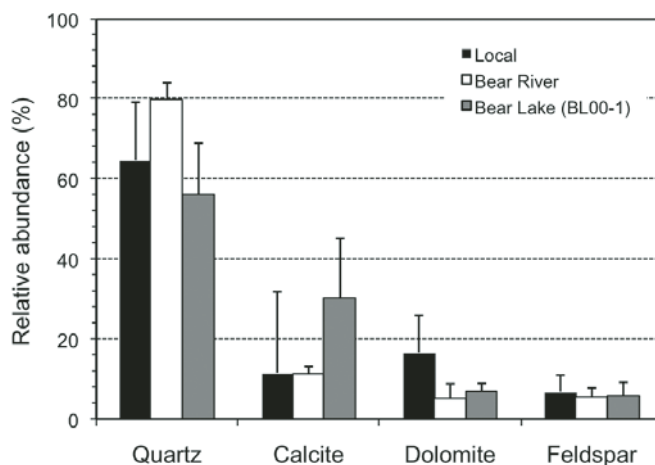


Figure 7. Average mineral assemblages for Bear Lake, Bear River, and local stream sources based on X-ray diffraction peak intensities. Bulk sediment was analyzed from BL00-1; the silt+clay fraction was analyzed from samples from Bear River and local streams. Errors bars are 1σ . Data for stream sediments are summarized from Rosenbaum et al. (this volume).

presently feeds the lake (Bright, this volume, Chapter 4), (2) the isotopic shift in shallow surface cores that span the ca. 1912 diversion of Bear River water into Bear Lake (Dean et al., 2007), and (3) the results of more detailed analyses of shorter cores taken in 1996 (Dean et al., 2006). The oxygen isotope composition of carbonate in Bear Lake sediment provides insights into the sources of water and the hydrologic budget of the lake, whereas the carbon isotopes reflect changes in the biologic activity as well as the hydrologic budget. We focus here on the $\delta^{18}\text{O}$ results because our understanding of the factors that control isotopic composition is better for oxygen than for carbon.

The $\delta^{18}\text{O}$ values range broadly, from about -13‰ to -5‰ in the bulk-sediment carbonate (Fig. 5; Appendix B). Enrichment in ^{18}O is significantly greater in the five intervals that contain aragonite (average = $-5.9 \pm 1.6\text{‰}$, $n = 52$) than in the rest of the core (average = $-9.8 \pm 1.1\text{‰}$, $n = 322$), an increase that cannot be attributed solely to the offset in mineralogic fractionation. The $\delta^{13}\text{C}$ values exhibit a similarly broad range, from about -4‰ to 7‰ , with higher values in the aragonite-bearing intervals ($2.4 \pm 0.9\text{‰}$) compared with the rest of the core ($-0.7 \pm 1.6\text{‰}$). The two isotopes correlate more strongly in the aragonite-bearing intervals ($r = 0.89$; $p < 0.001$) than over the rest of the core ($r = 0.42$; $p < 0.001$) (Fig. 8A), although the extent of the correlation varies among the oxygen isotope stages (Bright et al., 2006). The $\delta^{13}\text{C}$ values also correlate positively with OC content ($r = 0.40$; $p < 0.001$) (Fig. 5).

The $\delta^{18}\text{O}$ value of calcite in *Candona* is nearly always higher than that in the enclosing bulk-sediment carbonate (average difference = $2.8 \pm 2.4\text{‰}$, $n = 78$) (Fig. 5), as expected from the vital effect (e.g., $+2.2\text{‰}$ for *Candona*; von Grafenstien et al., 1999). The new results on *Cytherissa* generally agree with those of *Candona*. Excluding the ten results from the aragonite-bearing intervals, the $\delta^{18}\text{O}$ values of ostracodes ($-7.1 \pm 2.6\text{‰}$, $n = 66$) vary more than the $\delta^{18}\text{O}$ of the enclosing bulk sediment ($-9.8 \pm 1.0\text{‰}$, $n = 66$), with the ostracodes typically within the range of -12‰ to -2‰ , and the bulk carbonate within the range of -9‰ to -11‰ (Fig. 8B). The lower variability in the isotopic composition of bulk carbonate probably reflects the influence of allogenic carbonate. When the aragonitic intervals are excluded, the correlation between $\delta^{18}\text{O}$ of ostracode and bulk-sediment carbonate is relatively weak ($r = 0.33$; $p = 0.01$). The lower variability in the $\delta^{18}\text{O}$ values of bulk sediment might also result from greater time-averaging than for the ostracode samples, which comprised several valves.

Values of $\delta^{18}\text{O}$ and $\delta^{13}\text{C}$ in rocks, stream sediment, and water from the Bear Lake tributaries have been presented previously, and are summarized here (Table 1). The Paleozoic limestone and dolomite that underlie the Bear River Range, and the Mesozoic carbonate rock within the Bear Lake Plateau to the east, have $\delta^{18}\text{O}$ values ranging from -5.1 to -13.3‰ , and averaging $-8.2 \pm 2.7\text{‰}$ ($n = 9$) (Bright et al., 2006). In contrast, mud carried by local streams contains carbonate with much lower $\delta^{18}\text{O}$ values. Bright et al. (2006) reported an average value of $-13.6 \pm 1.3\text{‰}$ ($n = 7$), whereas Dean et al. (2006; their Table 2) reported values based on a slightly more extensive data set: The average $\delta^{18}\text{O}$ value for west-side streams is $-14.3 \pm 1.1\text{‰}$ ($n = 5$; after excluding

Hobble Creek, which is not on the west side, and the one outlier from Paris Creek); the average $\delta^{18}\text{O}$ value for east-side streams is $-12.5 \pm 1.0\text{‰}$ ($n = 5$; this value is different than reported by Dean et al. [2006, p. 107] but is correct). CaCO_3 in mud carried by the Bear River north of the Uinta Mountains has slightly higher $\delta^{18}\text{O}$ values than CaCO_3 in mud from local streams ($-11.6 \pm 1.3\text{‰}$, $n = 11$). The results on the alluvial mud probably more closely reflect the allogenic input than do spot analyses on bedrock units. They are lower than the values in the rocks (-8.2‰) because the streams carry detrital tufa grains derived with $\delta^{18}\text{O}$ values of around -16‰ (Bright et al., 2006), closer to that of present-day water, which averages -46.8‰ VPDB ($= -17.3 \pm 0.7\text{‰}$ VSMOW, $n = 40$) for

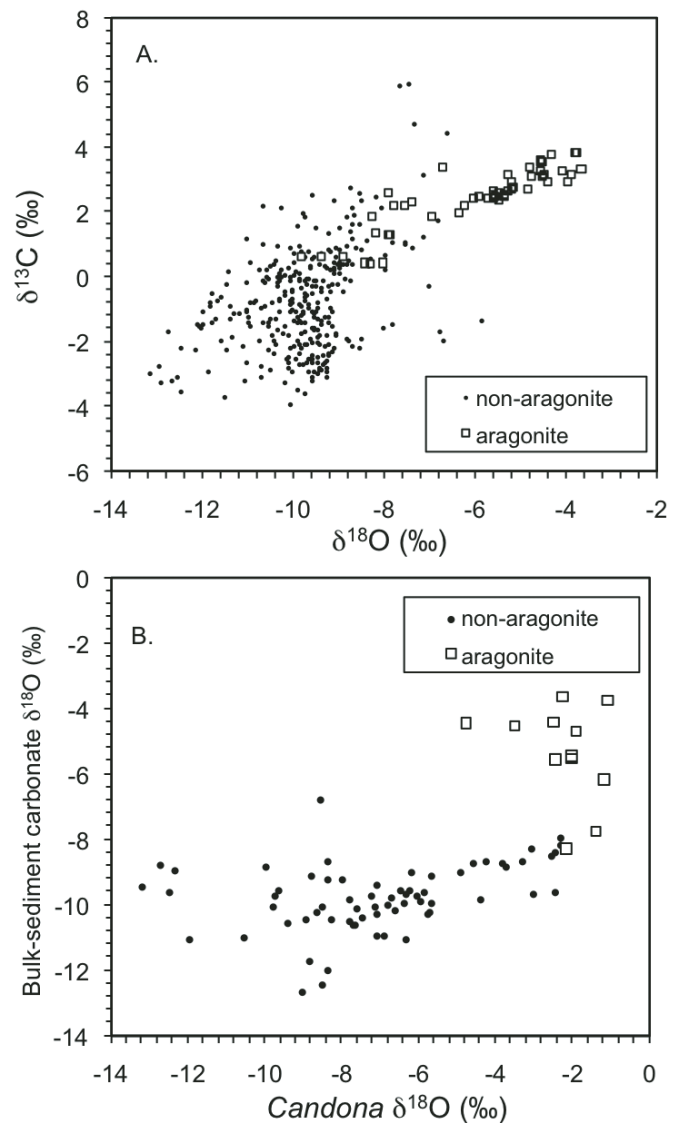


Figure 8. Stable isotope ratios from core BL00-1. (A) Cross plot of oxygen ($\delta^{18}\text{O}$) and carbon ($\delta^{13}\text{C}$) isotope ratios in bulk-sediment carbonate. (B) $\delta^{18}\text{O}$ in ostracode (*Candona*) calcite versus those in enclosing bulk sediment (includes allogenic and endogenic carbonates). Data from Bright et al. (2006), and listed in Appendix B.

TABLE 1. AVERAGE VALUES FOR OXYGEN, CARBON, AND STRONTIUM ISOTOPE RATIOS IN WATER, SEDIMENT, AND ROCKS FROM BEAR LAKE AREA

Province	Material	$\delta^{18}\text{O}^{\dagger}$	$\pm 1\sigma$	n	$\delta^{13}\text{C}^{\ddagger}$	$\pm 1\sigma$	n	Soluble fraction or water $^{87}\text{Sr}/^{86}\text{Sr}^{\#}$	$\pm 1\sigma$	n	Residue fraction $^{87}\text{Sr}/^{86}\text{Sr}^{\#}$	$\pm 1\sigma$	n
West side	Spring and stream water	-17.4	0.7	30	-9.7	0.2	6	0.71084	0.00074	26	-	-	-
East side	Spring and stream water	-17.0	0.8	10	-9.2	1.2	2	0.70975	0.00113	20	-	-	-
Bear River	Stream water	-16.3	0.4	4	-8.9	-	1	0.70823	0.00050	6	-	-	-
Bear Lake	Lake water	-8.1	0.1	4	-2.2	-	1	0.70919	0.00002	11	-	-	-
East & west sides	Carbonate rocks	-8.2	2.7	9	0.4	1.4	9	0.70881	0.00102	16	-	-	-
West side	Stream sediment (<53 μm bulk)	-12.5	1.0	5	-5.3	1.1	5	0.71015	0.00015	4	0.71042	0.00346	16
East side	Stream sediment (<53 μm bulk)	-12.5	1.0	5	-5.3	1.1	5	0.70866	0.00088	3	0.71999	0.00262	4
East & west sides	Stream sediment (<53 μm bulk)	-13.6	1.3	7	-5.8	1.1	7	0.70951	0.00095	7	0.71325	0.00143	3
Bear River	Stream sediment (<53 μm bulk)	-11.6	1.3	11	-5.1	0.8	11	0.71027	0.00085	12	0.71710	0.00413	7
East & west sides	Stream sediment (picked tufa grains)	-15.7	0.4	3	-6.5	0.8	3	0.71054	0.00040	2	0.72451	0.00796	12

Note: Oxygen and carbon isotopes values are ‰ relative to Vienna standard mean ocean water for water and Vienna Pee Dee belemnite for carbonate.
n—number of samples used to calculate mean and standard deviation.
[†]Data used to calculate mean values for O and C isotope ratios are listed in Bright et al. (2006).
[‡]Data used to calculate mean values for Sr isotope ratios are from: stream water (Bright, this volume, Chapter 4); carbonate rocks—soluble (Bright, this volume, Chapter 4); carbonate rocks—residue (this study); Bear Lake water (Dean et al., 2007); stream sediment soluble fraction (Dean, this volume); stream sediment residue fraction and tufa grains (this paper).

local streams and -45.9‰ VPDB ($= -16.3 \pm 0.4\text{‰}$ VSMOW, $n = 4$) for the Bear River (Bright et al., 2006). Values of $\delta^{18}\text{O}$ in bulk carbonate in BL00-1 are almost always higher than those in bulk carbonate in modern stream mud, suggesting that the allo-genic component of the bulk sediment moderates the fluctuations in the isotopic composition of endogenic carbonate, but that allo-genic carbonate is not sufficiently abundant to entirely overwhelm the endogenic component.

In summary, the isotopic composition of Bear Lake water and sediment has fluctuated considerably over the last two glacial-interglacial cycles. Values of $\delta^{18}\text{O}$ and $\delta^{13}\text{C}$ were higher during interglacial intervals, when fractionation was clearly controlled by evaporative effects. Such effects are consistent with the presence, if not dominance, of aragonite, among other indicators of a topographically closed-basin lake which are discussed elsewhere in this volume. Outside of the aragonitic intervals, ostra-code calcite exhibits larger fluctuations in $\delta^{18}\text{O}$ values than does the bulk-sediment carbonate, and can be interpreted without the uncertainty that results from fluctuating carbonate detritus. Ostra-codes are more abundant in the upper half of the core, however, and the sampling resolution is presently too coarse throughout to allow detailed interpretation.

Strontium Isotopes

Sr isotopes ($^{87}\text{Sr}/^{86}\text{Sr}$) have been analyzed from the 5M-acetic-acid-soluble (hereafter “soluble”) fraction of bulk sediment at an average spacing of 1.3 m in BL00-1. In addition, $^{87}\text{Sr}/^{86}\text{Sr}$ was analyzed in the acetic-acid-insoluble (hereafter “residue”) fraction of 20 samples scattered across the core. The methods and precision of Sr isotope analyses of Bear Lake sediment by thermal ion-ization mass spectrometry are given by Dean et al. (2006, 2007). The interpretation of Sr isotope results, like those for the O and C isotopes, is guided by an understanding of the modern water and sediment input to the lake, and by more detailed analyses of other cores (e.g., Dean et al., 2006, 2007). Like O isotopes, Sr isotopes can provide insights into the source area of water; unlike O iso-topes, Sr isotopes are not complicated by the fractionation effects that are influenced by temperature and evaporation.

Values of $^{87}\text{Sr}/^{86}\text{Sr}$ of the soluble fraction of sediment samples from BL00-1 range from 0.7091 to 0.7104, and average 0.7099 ± 0.0003 ($n = 93$) (Fig. 5; Appendix B). These values are bracketed by the two primary sources of water to the lake: the Bear River with present-day $^{87}\text{Sr}/^{86}\text{Sr}$ values averaging 0.7082 ± 0.0005 ($n = 6$), and local stream water, which averages 0.7104 ± 0.0011 ($n = 46$) (Bright, this volume, Chapter 4; note: Dean et al. (2007) listed a subset of these values, focusing on sites where additional solute data were also available). The $^{87}\text{Sr}/^{86}\text{Sr}$ value of endogenic carbonate that precipitates in Bear Lake depends directly on the $^{87}\text{Sr}/^{86}\text{Sr}$ value of the lake water. In turn, this depends on the flux of Sr, which is controlled by its concentration and the discharge from the various inflow sources. On the basis of the data that are presently available, west- and south-side surface-water sources account for greater Sr flux than

east-side sources, and they are more radiogenic (west-side average = 0.7108 ± 0.0007 , $n = 26$ compared with east-side average = 0.7098 ± 0.0011 , $n = 20$) (Table 1). Bear River water tends to have a higher Sr concentration than the local streams (Bright, this volume, Chapter 4), and is probably the dominant solute source of Sr when it discharges into the lake.

Although the $^{87}\text{Sr}/^{86}\text{Sr}$ value of soluble Bear Lake sediment can be accounted for by various mixtures of water from Bear River and local stream sources, the analyses of bulk sediment are also influenced by the composition and abundance of soluble allogenic components. The $^{87}\text{Sr}/^{86}\text{Sr}$ value of the Paleozoic and Jurassic carbonate bedrock units in the local drainage basin averages 0.7088 ± 0.0010 ($n = 16$) (Bright, this volume, Chapter 4; Dean et al. (2006) calculated an average value of 0.7092, $n = 20$, but included data from units that do not crop out in the local drainage), slightly lower than the average value of the soluble fraction of sediment samples in BL00-1 (0.7099 ± 0.0003). The $^{87}\text{Sr}/^{86}\text{Sr}$ value of the soluble fraction of mud ($<0.53 \mu\text{m}$) collected from the bed of local streams reflects the composition of the carbonate rocks in the catchments. The value is higher for west-side streams (0.7101 ± 0.0001 , $n = 4$) than for east-side streams (0.7087 ± 0.0009 , $n = 3$) (Dean, this volume). The Bear River carries mud with the highest $^{87}\text{Sr}/^{86}\text{Sr}$ values in the Bear Lake drainage (0.7103 ± 0.0009 ; $n = 12$) (Dean, this volume). The $^{87}\text{Sr}/^{86}\text{Sr}$ values are higher for the residue fraction of the fluvial mud than for the soluble fraction, averaging 0.7272 ± 0.0076 ($n = 19$), and the values from the two fractions correlate ($r = 0.60$, $n = 12$) (Dean, this volume). Data on Sr concentrations in the two fractions are not available; presumably Sr is enriched in the soluble fraction.

The $^{87}\text{Sr}/^{86}\text{Sr}$ values of soluble Bear Lake sediment generally track the $\delta^{18}\text{O}$ values of the bulk-sediment carbonate (Fig. 5). The enrichment of both ^{18}O and ^{87}Sr in the aragonitic zones probably reflects the absence of Bear River input, which increases the water residence time and the consequent evaporative influence on $\delta^{18}\text{O}$ and eliminates the dominant source of solutes with low $^{87}\text{Sr}/^{86}\text{Sr}$ values. Without the input of solutes and clastic sediment from the Bear River, the soluble components of Bear Lake sediment acquire the $^{87}\text{Sr}/^{86}\text{Sr}$ value of west-side inflow. With the input of the Bear River, the $^{87}\text{Sr}/^{86}\text{Sr}$ value of the endogenic carbonate in Bear Lake decreases, whereas the $^{87}\text{Sr}/^{86}\text{Sr}$ value of the allogenic component increases. The net effect therefore depends on the balance of the two components, and we do not know the relative difference in the concentration of Sr in the endogenic and allogenic components.

The $^{87}\text{Sr}/^{86}\text{Sr}$ values for the residue fraction of lake sediment tend to track the relative proportion of quartz in BL00-1 (Fig. 5). This supports the interpretation that the quartz-rich units are dominated by sediment delivered by the Bear River, which carries mud with high $^{87}\text{Sr}/^{86}\text{Sr}$ values. Half of the samples from BL00-1 analyzed for the residue fraction yielded $^{87}\text{Sr}/^{86}\text{Sr}$ values less than 0.7119, which is lower than any value measured in stream sediment from the drainage basin (Dean, this volume). The source of the low $^{87}\text{Sr}/^{86}\text{Sr}$ values in the residue fraction is not clear, although the carbonate bedrock units that crop out in the Bear Lake drain-

age, especially the Jurassic units on Bear Lake Plateau, tend to have lower values than indicated by the analyses of stream sediment data (average = 0.7109 ± 0.0037 , $n = 18$; Table 1).

Ostracodes

A discussion of the ostracodes from Bear Lake sediment—most of them endemic—along with photomicrographs of the valves, is presented by Bright (this volume, Chapter 8; Bright et al., 2005). We processed 138 sediment samples, with an average spacing of 88 cm and an average mass of 54 g, according to methods outlined by Bright (this volume, Chapter 8). Whole ($>80\%$ complete) adult ostracode valves $>150 \mu\text{m}$ were counted and identified to genus, and where possible, to species level. In addition, the presence of juvenile valves was noted for *Cytherissa lacustris*, the only taxon for which paleoenvironmental inferences can be made, but the valves were not counted. The presence of only juveniles is assumed to indicate that the species was living in the lake, but in low numbers, or possibly that the environment at the core site was poor for ostracode longevity.

Adult ostracode valves were recovered in 85 (62%) of the samples, and an additional 16 samples contained fragmented or juvenile valves of *Cytherissa*. In all, 2355 valves were counted, of which 93% are *Candona* spp. Valves are more abundant in the upper half of the core; 94% are from the top 65 m. Only 19 samples contained >1 valve per gram of sediment (vpg), and about half of these were within the Holocene section (Fig. 9; Appendix C). The ostracode fauna consists of one unidentified genus, several unnamed species of *Candona*, two unnamed species of *Limnocythere*, and *Cytherissa lacustris*. With the exception of *Cytherissa lacustris*, all of the ostracode species are endemic (Bright, this volume, Chapter 8). The greater abundance of valves in the upper half of the core, and especially in the Holocene aragonite-rich mud, is probably a result of post-depositional preservation. Little can be inferred about paleohydrologic conditions from the abundances of the endemic forms; many taxa cross lithostratigraphic boundaries and seem to have inhabited the lake whether it was generating aragonite in a topographically closed basin, or whether it was receiving input from the Bear River.

Cytherissa lacustris is an extant species with known environmental tolerances (Bradbury and Forester, 2002). This species inhabits dilute ($\text{TDS} < 365 \text{ mg L}^{-1}$) boreal lakes typically under the influence of polar-high and subpolar-low air masses. Lakes that support *C. lacustris* are stable, well oxygenated, and display little if any seasonal variation. The species' modern distribution is confined to northern Canada, Alaska, and a few isolated localities in the northern conterminous United States. Its presence in Pleistocene lake sediment from the western United States coincides with glacial periods, when the polar and subpolar air masses were forced southward by large ice sheets over northern North America (e.g., Bradbury and Forester, 2002). *C. lacustris* is absent from four of the five aragonite-bearing intervals, consistent with its preference for dilute lakes formed during glacial intervals. It is present, however, in sediment that correlates with the interglacial

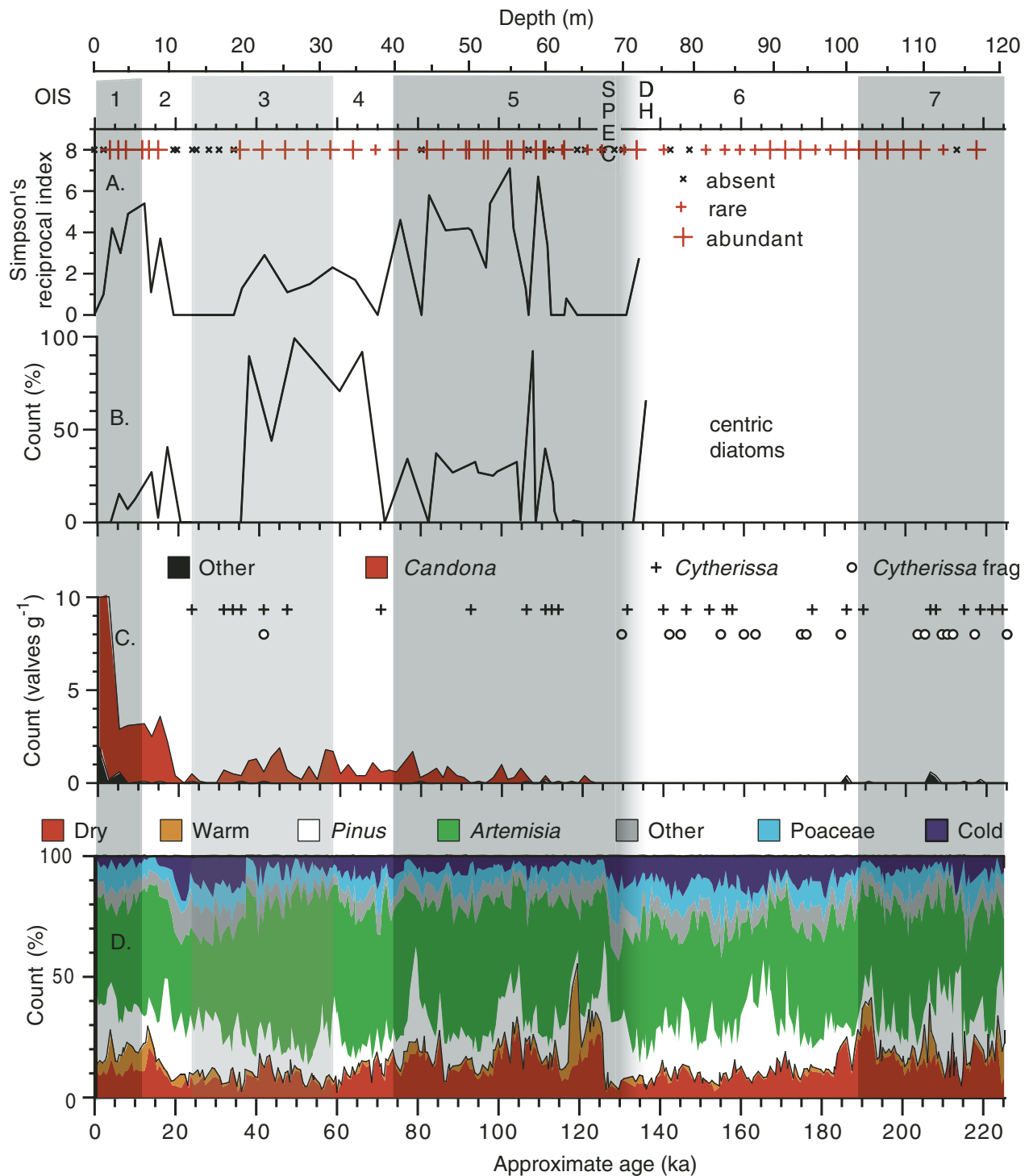


Figure 9. Paleobiological data from core BL00-1 with time scale and isotope stages as described for Figure 5. (A) Diatom diversity based on the Simpson's reciprocal index; plot symbols at top indicate relative abundance of diatoms (rare—dissolved or broken diatoms that were difficult or impossible to count). (B) Percent centric diatoms (approximately equivalent to % planktic diatoms, except that many of the non-centric planktic diatoms [$<1\%$ in any given sample] were counted as either tycho planktic or planktic). (C) Abundance of all ostracode *Candona* spp. and other whole, adult ostracode taxa, with the presence of *Cytherissa lacustris* shown as whole (plus signs), and as fragmented or juvenile (open circles). (D) Relative percentages of selected pollen taxa where “dry” = *Ambrosia*, *Chenopodiaceae-Amaranthus*, and *Sarcobatus*, “warm” = *Quercus* and *Juniperus*, and “cold” = *Picea*, other Asteraceae, and *Eriogonum*. Abbreviations are the same as for Figure 5. Diatom and ostracode data are listed in Appendices C and D; pollen data are from Jiménez-Moreno et al. (2007) and are available from the North American Pollen Database (<http://www.ncdc.noaa.gov/paleo/napd.html>).

MIS 7c. To our knowledge, this is the first documented case of *C. lacustris* in the western contiguous United States during peak global interglacial conditions.

Pollen

The recent pollen study of BL00-1 by Jiménez-Moreno et al. (2007) provides one of the most detailed and continuous records of Quaternary vegetation change in North America, and Doner (this volume) analyzed pollen in a short piston core from the lake (BL96-2) extending back 19,000 yr. Pollen from BL00-1 was analyzed in 359 samples (intervals of 30 cm = ~600-yr resolution), each comprising 2 cm³. A minimum of 300 grains of terrestrial pollen were identified to the lowest taxonomic level possible, usually genus but sometimes family. The pollen data are available through the North American Pollen Database (<http://www.ncdc.noaa.gov/paleo/napd.html>).

Preservation of pollen in BL00-1 is excellent, with generally high concentrations averaging >40,000 grains cm⁻³. The assemblage is dominated by *Artemisia* (sagebrush), which averages 46% of the grains throughout the core. *Pinus* (pine) is the second most abundant type, averaging 17%. Other pollen types generally constitute <10% each, and their interpretation is discussed by Jiménez-Moreno et al. (2007). Here (Fig. 9), we summarize the pollen data by combining taxa that indicate similar climatic conditions. “Dry” indicators include *Ambrosia* (ragweed), Chenopodiaceae-*Amaranthus* (saltbush), and *Sarcobatus* (greasewood); “warm” indicators include *Quercus* (oak) and *Juniperus* (juniper); and “cold” indicators are *Picea* (spruce), other Asteraceae (sunflower family), and *Eriogonum* (buckwheat).

The pollen assemblages in BL00-1 can be subdivided into two general types: glacial and interglacial. The pollen spectra from interglacial periods contain higher percentages of “warm” and “dry” indicators, with higher *Juniperus* percentages during the early part of each interglacial interval. Vegetation interpretations suggest that valley bottoms were occupied by salt-tolerant, high-desert shrubs, and that *Juniperus* woodlands expanded locally during interglaciations. Pollen spectra of glacial intervals generally have higher percentages of “cold” indicators, suggesting that forest or forest-woodland conditions prevailed.

The pollen data can be further summarized by using a ratio of the “warm” plus “dry” indicators (“warm+dry”) to “cold” indicators (Fig. 5). This index is nearly identical to the relative abundance of “warm-arid” taxa emphasized by Jiménez-Moreno et al. (2007), but the ratio avoids issues related to closed-array percentage data while integrating information on the abundance of cold indicators. Sediment deposited during glacial intervals generally contains fewer pollen grains of “warm+dry” indicator taxa than “cold” taxa (i.e., index values [(warm+dry)/cold] < 1), whereas interglacial periods are typified by more “warm+dry” than “cold” pollen grains (i.e., index values >1). Overall, the penultimate glacial period (MIS 6) shows lower index values, reflecting a higher proportion of *Picea* pollen than during the last glacial cycle (MIS 4–2), and suggesting that MIS 6 was generally colder. The high-

est index values are associated with peak interglacial substages, especially MIS 7a, 5e, and 5c. Index values for the early Holocene are intermediate among the peak interglacial intervals.

Diatoms

Diatoms were analyzed from 49 samples (25 core catcher samples and 24 core samples) from the upper 73 m of BL00-1 (Fig. 9; Appendix D). Of the samples analyzed, 28 (57%) contained sufficient diatoms for meaningful counts. Core catcher samples were also analyzed from below 78 m blf to assess qualitatively the relative abundance of diatoms. Samples were processed following standard methods, as described by Moser and Kimball (this volume). Diatom taxonomy was based primarily on Krammer and Lange-Bertalot (1986–1991). Because the main goal of this study was to infer climatic and hydrologic change, the diatom data are summarized using two indices: (1) percentage planktic diatoms, with higher percentages typically associated with higher lake levels (Wolfin and Duthie, 1999), and (2) species diversity, which has been suggested to increase with greater habitat variability and nutrient availability (Douglas et al., 1994). Simpson’s reciprocal index (SRI; Simpson, 1949) was calculated as: $SRI = 1/\sum p_i^2$, where p_i is the proportional numerical abundance of each species i .

The lowermost sample analyzed (72.7 m blf; MIS 6) contains abundant planktic diatoms (65%), mainly *Stephanodiscus medius*, suggestive of relatively high lake level and nutrient-rich conditions (Bradbury, 1997). However, samples from below this level will need to be analyzed to determine whether this is a long-term trend. Samples from 71.1 to 63.8 m blf (late MIS 6) contain few to no diatoms. The near absence of diatoms throughout this interval indicates poor preservation or a lack of diatoms living in Bear Lake. An absence or near absence of diatoms in lake sediments deposited during glacial periods has been observed at other sites, particularly deep lakes, and has been explained by increased dissolution (MacKay, 2007). Because there is no evidence of dissolution in the few diatoms observed in this interval, an absence of diatoms in the lake is favored. Conditions were probably cold, with an associated increase in ice coverage and turbidity, which would have lowered light conditions and prevented diatoms from inhabiting the lake (Bradbury et al., 1994; Bradshaw et al., 2000; Karabanov et al., 2004).

Samples from 63.8 to 60.5 m blf (MIS 5e) contain a mixture of well-preserved diatoms and broken diatoms, some with signs of dissolution. The broken pieces are typically from large pennate diatoms that live in the littoral zone of lakes, including *Epithemia* and *Cymbella*. The sample from 63.1 m blf contains well-preserved small, benthic/tychoplanktic fragilarioid species (>90%), mainly *Pseudostaurosira brevistriata*, indicative of a shallow lake (Bradbury, 1988). Unlike the previous interval, these data suggest that the lack of diatom valves is due to poor preservation. This interval contains aragonite-rich sediment, and the poor preservation of diatoms is probably caused by alkaline water, especially Mg-rich waters (Flower, 1993). The broken

diatoms are consistent with low lake level, and may have been eroded and re-deposited as lake level fell. Alternatively, increased bioturbation due to shallower water and increased oxygen could result in broken diatoms.

From 60.5 to 39.6 m blf (MIS 5d–5a) the diatom assemblages include relatively low percentages of planktic taxa (average = 20%) and are dominated (typically >50%) by small, benthic/tychoplanktic fragilaroid species—mainly *Staurosirella pinnata* and *Pseudostaurosira brevistriata*, which are suggestive of shallow water (Bradbury, 1988). The main planktic diatoms, *Stephanodiscus medius* and *Cyclotella meneghiniana*, indicate high nutrient availability, and *Cyclotella meneghiniana* suggests rapidly fluctuating salinities. This interval is characterized by high diversity (average = 4.1) with assemblages composed of numerous planktic and benthic species. These results suggest an open-water lake with a significant littoral zone and a large macrophyte population, and warmer water than during MIS 6.

In contrast, samples from 36.6 to 20.0 m blf (MIS 4 and MIS 3) are dominated by planktic taxa (average = 78%), mainly *Stephanodiscus medius*, and low diversity (average = 1.8). *Stephanodiscus medius* requires enhanced phosphorus and is typically found in mesotrophic to eutrophic waters (Bradbury, 1997). The decrease in diversity occurred in both planktic and benthic species. These changes suggest an increase in open water and nutrients, indicative of a deeper lake. A deeper lake would increase stratification and increase nutrients during spring and fall overturn (Bradbury, 1997). A loss of macrophytes, perhaps due to lake transgression, could have also led to an increase in nutrient delivery to open water (e.g., Karst and Smol, 2000). More Bear River input during this period would also have increased nutrient delivery to the lake.

Samples from 20 to 10.1 m blf (late MIS 3 and early MIS 2) are characterized by an absence of diatoms. As in to MIS 6 and the lower part of zone 1 in BL96-2, the absence of diatoms is likely due to cold, turbid water (Moser and Kimball, this volume).

The interval from 10.1 to 1.1 m blf (late MIS 2 and MIS 1) is typified by assemblages with low percentages (average = 17.5%) of planktic diatoms and high species diversity (average = 3.3). Samples are dominated (average = 68%) by small, benthic *Staurosirella pinnata* and *Pseudostaurosira brevistriata*, suggestive of shallow water (Bradbury, 1988). The only planktic diatom with an abundance >1% is *Cyclotella meneghiniana*, which suggests more variable salinity than during MIS 3 or 4. These results indicate a warm and dry period. The uppermost sample, 0.5 m blf, is similar to the upper part of cores BL96-1 and 96-2, and is characterized by numerous, large broken pennate diatoms (Moser and Kimball, this volume). The cause of the broken diatoms is unclear, but is suggestive of drying carbonate sediments (Flower, 1993) or a high-energy environment.

In summary, the absence of diatoms in sediment deposited during glacial periods (MIS 6 and MIS 3/2) indicates low-light conditions associated with increased ice cover and increased turbidity, which limited the growing season and diatom population. Diatom assemblages of interglacial periods (MIS 5 and 1) indicate low lake levels and more saline conditions. The MIS 3 assemblage

is distinct from MIS 5 and 1, and suggests that lake level was higher during this period than during the full interglacials.

DISCUSSION

Synthesis of Evidence for Paleoenvironmental Change

The data from BL00-1 document orbital- to millennial-scale fluctuations in the hydrology of Bear Lake and climate-related environmental changes in the catchment during the last quarter-million years. The broad-scale fluctuations (10^4 yr) in mineralogy, isotopes, and pollen generally coincide with summer insolation in the Northern Hemisphere driven by orbital variations, and with global ice volume. Suborbital variability (10^3 yr) in these indicators is also evident. Jiménez-Moreno et al. (2007) suggested that changes in the pollen spectra from BL00-1 coincide with ice-rafting (Heinrich) events in the North Atlantic, but Heil et al. (this volume) note that the timing of major peaks in hematite content (a proxy for glacial rock flour from the Uinta Mountains) does not. The uncertainty in the age model for BL00-1 is too high to determine whether the timing of any millennial-scale fluctuation coincides with a particular shift reported from other paleoclimate records. The chronology is sufficient to conclude only that the frequency of the variability in BL00-1 indicators is similar to stadial-interstadial cycles recognized in well-known records from other lacustrine (e.g., Benson et al., 2003) and marine (e.g., Hendy and Kennett, 1999) basins, and to Dansgaard-Oeschger oscillations exhibited in the isotope record from Greenland ice (Stuiver and Grootes, 2000). Unlike most terrestrial paleoclimate records, BL00-1 extends continuously through the penultimate glacial-interglacial cycle and reveals millennial-scale fluctuations throughout.

Not all of the variability can be attributed to climatic changes, however. Rearrangements of the confluence of Bear River and Bear Lake also affected the paleoenvironmental indicators (Fig. 10). The two end-member paleohydrogeographic configurations are topographically closed, and fluvially dominated; intermediate configurations involve various degrees of hydrologic exchange between the lake and the distributaries of Bear River where the river debouches onto the flat floor of the northern Bear Lake Valley. Presently, the wetland area separating the lake and the main channel moderates the influence of Bear River on the lake. In addition, some of the variability in BL00-1 reflects processes within the lake (as well as tectonic processes) that control the delivery of allogenic sediment to the core site, and the biogeochemical processes that influence the endogenic components.

The rearrangements of the Bear Lake drainage area are reflected in shifts in mineral assemblages, magnetic properties, and isotope ratios of O and Sr. Most of our isotope analyses are on bulk-sediment carbonate, which is confounded by a variable and unknown proportion of allogenic carbonate. Because the bedrock of the region is dominated by carbonate rocks, allogenic carbonate was probably always present in the lake sediment. The extent to which allogenic carbonate dominated the bulk sediment

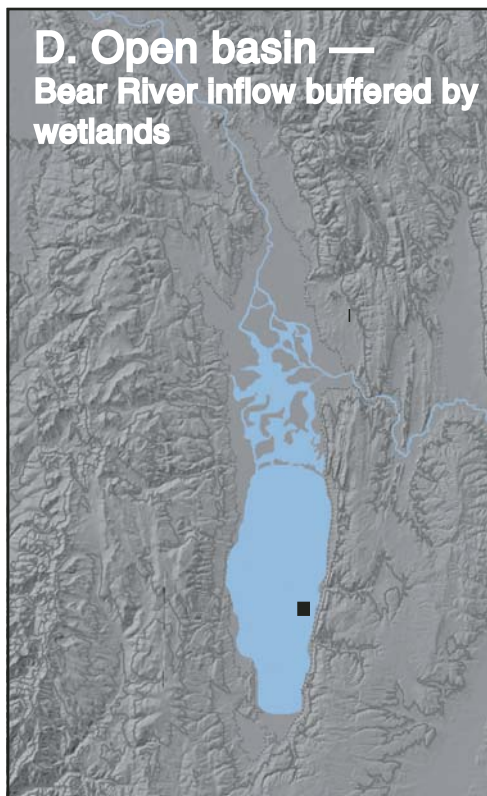
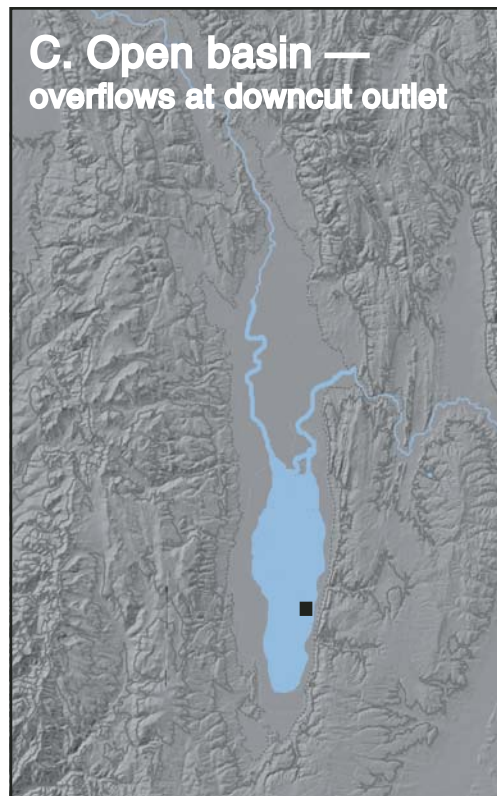
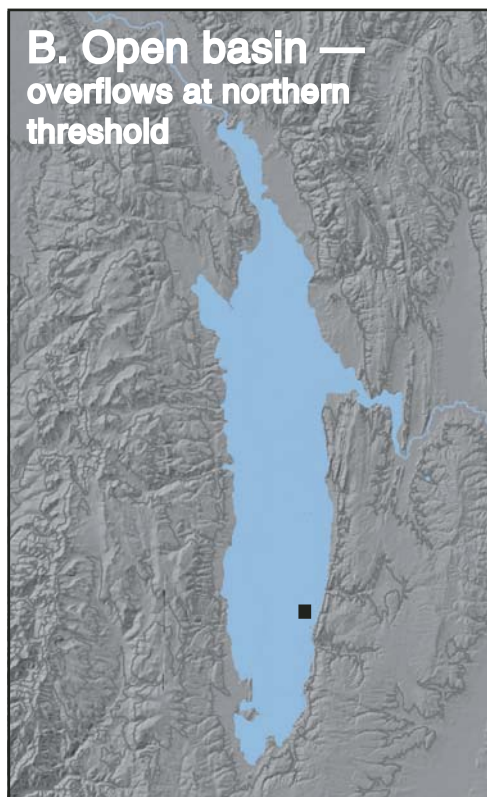
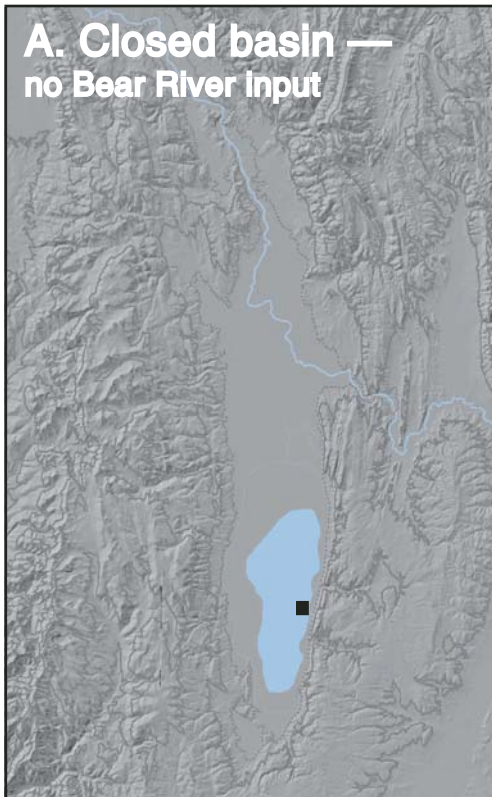


Figure 10. Alternative conceptual hydrogeographies for the confluence of Bear River and Bear Lake. Black square—core site BL00-1. (A) Topographically closed-basin configuration with Bear Lake isolated from surface water flow of Bear River. Separation of Bear Lake from Bear River is caused by climatically controlled reduction in effective moisture that occurred during peak interglaciations. (B) Topographically open basin with the shoreline expanded to the basin threshold at ~1845 m asl. Capture of Bear River by Bear Lake is caused by the transgression of the northern shoreline to intercept the river channel, or by avulsion of the channel southward into the lake. (C) Topographically open basin with regressed shoreline. The direct connection with the outflow of Bear River increases delivery of fluvial sediment to the core site; increased outflow from the lake causes down-cutting at the outlet, which lowers lake level. (D) Intermediate configuration with Bear River confluent with Bear Lake via wetlands at the north end. The effect of the river is moderated by wetlands that impend sediment transport and solute exchange with the lake; this hydrogeography might have been the most common during the past quarter-million years.

depends on its proportion relative to the endogenic component, rather than on its absolute flux. At times when the production of endogenic carbonate was low, the isotope composition was more strongly influenced by the allogenic component. Changes in the proportion of allogenic versus endogenic material, and unknown differences in the concentration of Sr in the two components, complicate the interpretation for Sr isotopes measured in the acid-soluble bulk sediment.

Interglacial Intervals

At the broadest scale, the paleoenvironmental data document at least three distinct intervals when the lake retracted into a topographically closed basin, shut off from Bear River inflow. On the basis of the available age control, these coincide with peak global interglacial intervals of MIS 7, 5, and 1. Diatom assemblages indicate low lake levels during MIS 5e and 1, and pollen spectra from these intervals indicate an expansion of salt-tolerant plants in the valley bottoms and a reduction of coniferous forest in the uplands, consistent with the warm and dry conditions that were required for lake level to regress below the inflow of Bear River.

Once the lake regressed, Bear Lake and Bear River became disconnected. Evidence for the absence of Bear River inflow includes (1) production of aragonite, favored by evaporative conditions and Mg to Ca ratio like that of the lake prior to the artificial diversion of Bear River into the lake; (2) $\delta^{18}\text{O}$ values in bulk-sediment and ostracode calcite that are enriched in ^{18}O , with strongly covarying values of $\delta^{13}\text{C}$, indicating evaporation-dominated fractionation; (3) generally increased Sr isotope ratios in the soluble fraction, reflecting endogenic carbonate precipitated from water derived from the local drainage; and (4) decreased ratio of quartz to dolomite, indicating the influence of dolomite-rich, locally derived stream-sediment input. Furthermore, these parameters all reversed their trends in sediment deposited after the ca. 1912 diversion of Bear River into the lake (Dean et al., 2007).

In deep-marine sediment, MIS 7 includes three global ice-volume minima (MIS 7e, 7c, and 7a), of which the younger two and the termination of the oldest are represented in BL00-1. Sediment apparently deposited in Bear Lake during MIS 7c and 7a exhibits maxima in $\delta^{18}\text{O}$ and carbonate content, and both intervals contain aragonite, suggesting that salinity was relatively high. Sediment of the younger substage (MIS 7a) exhibits an increase in $^{87}\text{Sr}/^{86}\text{Sr}$ values, whereas the next older substage (MIS 7c) does not. The aragonite content is higher during MIS 7a than 7c, and the ratio of “warm+dry” to “cold” pollen indicators reaches its maximum value during MIS 7a. Bear River apparently did not discharge into Bear Lake during MIS 7a. During the older substage, however, the evidence for Bear River input is equivocal, although the presence of aragonite indicates that the salinity and Mg to Ca ratio of the lake were relatively high for at least brief intervals.

Sediment deposited during MIS 5 includes a prominent aragonite-rich zone deposited early during the interval, which we correlate with MIS 5e. Like other interglacial intervals, the pollen spectra of MIS 5e are dominated by high-desert shrub taxa, with abundant juniper, indicating warm and dry conditions. The diatom

data are all suggestive of a shallow lake. Dramatic shifts in mineralogy and isotopes occur in the middle of MIS 5e, and almost certainly record the input of the Bear River. We cannot discern whether the re-entry of the river resulted from a non-climatically influenced avulsion, or from a climate-induced lake-level transgression that captured the river. The return of $\delta^{18}\text{O}$ values to their pre-MIS 5 values suggests that effective moisture was high (similar to conditions during glacial intervals) during the excursion. Similar climate reversals during MIS 5e have been noted elsewhere (e.g., Thouveny et al., 1994; Seidenkrantz et al., 1995).

Later during MIS 5, two peaks in CaCO_3 abundance, including one with aragonite, correlate with peaks in the proportion of “warm” and “dry” pollen indicators, and apparently coincide with the interstadials MIS 5c and 5a. During MIS 5c, the ratio of quartz to dolomite and the ratio of “warm+dry” to “cold” pollen indicators both attain values similar to those of MIS 5e, suggesting the return of peak interglacial conditions, with an increase in locally derived, dolomite-rich fluvial sediment input relative to dolomite-poor Bear River sediment input. During the intervening stadial intervals, $\delta^{18}\text{O}$ and $^{87}\text{Sr}/^{86}\text{Sr}$ in bulk sediment attain values that are among the lowest in the core. We interpret the isotopic data from these stadial deposits as indicating high effective moisture, probably resulting from a combination of higher precipitation and lower temperature.

During the Holocene (MIS 1), $\delta^{18}\text{O}$ and $^{87}\text{Sr}/^{86}\text{Sr}$ attain maximum values similar to those during MIS 5e. CaCO_3 abundance (almost all aragonite) is the highest of the entire quarter-million-year sequence. In contrast, the ratio of “warm+dry” to “cold” pollen indicators is of an intermediate value for interglacial periods. Our sample interval is too coarse to capture centennial-scale climate changes during the last glacial-interglacial transition. A prominent reversal to calcite deposition during the early Holocene is well studied in shorter cores and has been interpreted as the re-entry of Bear River into Bear Lake (Dean et al., 2006; Dean, this volume), perhaps coinciding with the transgression to the Willis Ranch shoreline (Laabs and Kaufman, 2003; Reheis et al., this volume). The 1000-year-long freshening event is succeeded in the shorter cores by a coarsening of grain size, indicating lake-level lowering just prior to the return to the aragonite precipitation that dominated the Holocene (Smoot and Rosenbaum, this volume).

Glacial Intervals

With the exception of the three interglacial periods represented by the prominent aragonitic zones, we infer that the Bear River flowed into Bear Lake, either directly via a channel or indirectly via a wetland, throughout most of the last quarter-million years. The extent to which water and sediment input from Bear River influenced the sedimentation at the core site depended on both climatic and non-climatic factors. Consequently, the manifestations of the glacial intervals were markedly different from one another.

During the penultimate glacial period (MIS 6) the ratio of “warm+dry” to “cold” pollen indicators is lower overall than during the last glacial cycle (MIS 4–2). Values of $\delta^{18}\text{O}$ in bulk-sediment carbonate became progressively higher (gray dashed line

in Fig. 5C), and the proportion of quartz increased. These trends are interpreted as an increase in allogenic input. The correlation between quartz abundance and $^{87}\text{Sr}/^{86}\text{Sr}$ values is consistent with the influence of allogenic carbonate, particularly the proportion of stream sediment from the Bear River, relative to endogenic carbonate. The lowest $\delta^{18}\text{O}$ values in ostracodes were registered during this interval, also indicative of increased meltwater input. We interpret these trends as the progressive buildup of glacial sediment and meltwater from the Uinta Mountains. Although the analyses of $^{87}\text{Sr}/^{86}\text{Sr}$ in the acid-insoluble (residue) fraction are sparse, the high $^{87}\text{Sr}/^{86}\text{Sr}$ values in MIS 6 indicate a strong meltwater signal from the Uinta Mountains. Magnetic properties are equivocal as to the source of the allogenic material, probably because Fe-oxide minerals have been altered in sediments older than MIS 3 (Heil et al., this volume). Quartz content reached its maximum value immediately prior to the rapid regression that led to the sudden precipitation of endogenic carbonate, mostly aragonite. The low $\delta^{18}\text{O}$ values and high quartz values might represent an increase in Bear River sediment over endogenic carbonate and might coincide with the high lake level that occurred late during the Bear Hollow phase of Bear Lake (Laabs and Kaufman, 2003). The age constraints on the shoreline deposits are broad (200–100 ka) and permissive of a range of possible correlations to events in BL00-1.

During the last glacial cycle, the 110,000-year period extending from MIS 5d through MIS 2, $\delta^{18}\text{O}$ values in bulk sediment exhibit four relatively evenly spaced minima ca. 100, 80, 55, and 15 ka (gray dashed lines in Fig. 5C). These minima terminate periods of decreasing $\delta^{18}\text{O}$ values in bulk sediment and are followed by rapid increases in $\delta^{18}\text{O}$, resulting in saw-toothed patterns reminiscent of those exhibited by $\delta^{18}\text{O}$ in Greenland ice (e.g., Stuiver and Grootes, 2000). These abrupt increases in $\delta^{18}\text{O}$ might relate to rapid warming following the peak periods of cold/wet climate and attendant mountain glaciation in the Bear Lake catchment. The penultimate minimum in bulk-sediment $\delta^{18}\text{O}$ values at 29 m blf (ca. 55 ka), unlike the preceding two minima, does not show a parallel decrease in ostracode $\delta^{18}\text{O}$ values (Fig. 5). Instead, $\delta^{18}\text{O}$ values in ostracode valves exhibit two prominent minima at 24 and 19 m blf (ca. 45 and 35 ka). These minima occur following the Laschamp excursion in BL00-1, and their approximated ages are probably somewhat too old. Nonetheless, they coincide broadly with the Jensen Spring highstand of Bear Lake, which is dated to 47–39 ka by ^{14}C and amino acid geochronology (Laabs and Kaufman, 2003). During the Jensen Spring phase, lake level rose by 11 m, producing well-developed spits and other shoreline features in northern Bear Lake Valley. The proportion of quartz is also high during this interval, consistent with enhanced discharge from the Bear River.

Between late MIS 3 and early MIS 2, the absence of diatoms suggests that cold conditions persisted. The proportion of pollen from conifers and other cold-tolerant taxa is high, further suggesting cold conditions. Magnetic properties, trace-element geochemistry, mineralogy, and grain size in core BL96-3 indicate that the amount of sediment derived from the Uinta Mountains varied during this interval (Rosenbaum et al., this volume). On the basis of hematite abundance (HIRM) in BL00-1, and following the inter-

pretation of HIRM in shorter piston cores (Rosenbaum and Heil, this volume), the delivery of glacial flour from the Uinta Mountains to Bear Lake increased dramatically late during MIS 3. In addition, this interval contains the only distinctively red sediment in BL00-1 (unit 6, Fig. 4), reflecting an increase in the proportion of Uinta-derived sediment transported to the core site or the preservation of Fe oxides, or most likely both. Lake level was stable near the present level when the red sediment was deposited (Smoot and Rosenbaum, this volume). We surmise that the overflow threshold of the lake was eroded to near its present elevation, and that the Bear River entered and exited the lake without the shoreline transgressing the wetlands north of the lake (Fig. 10).

MIS 2 was an unremarkable interval in the sedimentary record of Bear Lake, other than the preservation of a prominent red, siliclastic unit. The absence of a peak in the proportion of quartz at the close of the glacial period is difficult to reconcile with the major transgression in the terminal Bonneville Basin. In contrast to Lake Bonneville, no highstand deposits dating to the last glacial maximum have yet been discovered in the Bear Lake Valley, although this might reflect the geomorphic controls on the threshold elevation rather than the hydrologic balance of the lake. As in the shorter piston cores (Rosenbaum and Heil, this volume), the timing of the most recent peak in HIRM in BL00-1 agrees with the cosmogenic exposure ages on moraines formed during the local last glacial maximum in the headwaters of the Bear River in the Uinta Mountains, which have been dated to ca. 19–17 ka (Laabs et al., 2007). This interval also contains high $^{87}\text{Sr}/^{86}\text{Sr}$ values in the residue fraction. The last $\delta^{18}\text{O}$ minimum took place ca. 15 ka, when the level of Bear Lake rose by 8 m and formed shoreline deposits ascribed to the Raspberry Square phase (Laabs and Kaufman, 2003). Sedimentologic evidence from a shallower core also indicates a sharp lake-level rise at this time (Smoot and Rosenbaum, this volume).

Comparison with the Great Salt Lake Subbasin

Site BL00-1 was drilled as part of the same Global Lakes Drilling (GLAD) operation that recovered cores from Great Salt Lake (Dean et al., 2002). Great Salt Lake is the terminus of the Bear River drainage, and it occupies the largest subbasin of the Bonneville drainage basin. At times during the Pleistocene, the Great Salt Lake was isolated from the upper part of the Bear River drainage (Bouchard et al., 1998). The magnitude of lake-level fluctuations in the Great Salt Lake (i.e., Lake Bonneville and its predecessors) was much greater than in Bear Lake because of differences in their topographic confinement. Bear Lake never entirely dried out during the last 220,000 years or longer. During arid intervals, it generated abundant carbonate, but it never evaporated enough to precipitate evaporite minerals (e.g., gypsum and halite). In contrast, salts precipitated and wetland deposits accumulated in the Great Salt Lake during arid intervals (e.g., Oviatt et al., 1999). Although their sedimentary records are distinct, the first-order changes at both lakes are influenced primarily by lake level, driven by periodic changes in the delivery

of Pacific moisture. At Bear Lake, lake level dictated whether the Bear River was in or out of the lake; at Great Salt Lake, lake level determined whether a core site was submerged or subaerial. The two lakes both responded to climate changes, but differed in their response times. The drainage area of Great Salt Lake is much larger than that of Bear Lake, and its hydrologic budget is influenced more strongly by lake-effect precipitation, implying some inherent stability (Hostetler et al., 1994; Laabs et al., 2006). When comparing the sedimentary sequences at Bear Lake and Great Salt Lake, we therefore expect broad-scale similarities in sedimentary features driven by climate, along with secondary differences related to differences in local hydrology.

Recently, Balch et al. (2005) described the sedimentary sequence and analyzed the ostracode fauna in a 120-m-long, ~280,000-year core from Great Salt Lake (GSL00-4). Their data indicate that the environment at the core site, located 9.3 m below present-day lake level, mainly alternated between a saline/hypersaline lake and a saline marsh. In addition, on the basis of their coarse sampling interval (1 m spacing = 2000 yr), they identified four intervals of freshwater marsh deposits and paleosols formed when the site was above lake level, and two intervals when the site was below a deep, freshwater lake. We focus our comparison of the GLAD cores from Bear Lake and Great Salt Lake on these more extreme events, starting with the two deep-water lakes.

The penultimate deep-lake cycle in the Bonneville Basin is represented by the Little Valley shoreline, which has been dated to ca. 150 ka by amino acid geochronology and other evidence (Scott et al., 1983). Using the currently accepted age model for GSL00-4 in the Great Salt Lake, however, Balch et al. (2005) inferred an older age of 170 ± 20 ka for the penultimate deep-water lake. At Bear Lake, the quartz maximum and CaCO_3 minimum located just a few meters below the MIS 5e aragonite might correlate with the Little Valley shoreline in the Bonneville Basin. If the age of the Little Valley shoreline is closer to 170 ka, as suggested by Balch et al. (2005), then we find no extraordinary features around this time in BL00-1 to mark the event, other than the low $\delta^{18}\text{O}$ value in ostracodes at 88 m blf (ca. 165 ka), although an equally low value occurs again at 78 m blf (ca. 145 ka). Nor do we find evidence for extreme aridity in BL00-1 that might coincide with the prominent lower salt layer in GSL00-4 that formed sometime between 170 and 140 ka, immediately following that deep-lake event (Balch et al., 2005).

The Lake Bonneville deep-lake phase occurred between ca. 25 and 15 ka (Oviatt et al., 1992). The last 5000 years of this interval corresponds to the $\delta^{18}\text{O}$ minimum of the most recent 25,000-year “saw tooth” in BL00-1. The decreasing quartz content after 25 ka during MIS 2 is difficult to reconcile with the evidence of extremely high lake levels downstream in Lake Bonneville. It points to intra-regional heterogeneity in climate change and its hydrologic response.

In addition to deep lakes during MIS 6 and MIS 2, lake level in the Great Salt Lake subbasin was high early during MIS 3, ca. 60 ka, as indicated by high flood-plain deposits of Bear River near Great Salt Lake (Kaufman et al., 2001), and by freshening of lake water at site GSL00-4 at about the same time

(Balch et al., 2005). A correlative of this event might be represented by the minimum in $\delta^{18}\text{O}$ values in bulk-sediment carbonate and “warm+dry” to “cold” pollen indicators around 30 m blf (ca. 55 ka) in BL00-1. The $\delta^{18}\text{O}$ values in ostracode calcite do not exhibit minima until ~25 and 19 m blf (45 and 35 ka), however, and these ages are probably too old considering their superposition relative to the assumed Laschamp excursion.

The intervals of exceptionally low lake level identified in GSL00-4 (Balch et al., 2005) appear to correlate with evidence of aridity in BL00-1, at least in three of the four cases. According to the current age model for GSL00-4, these occurred at 215, 130, 105, and 45 ka. The oldest three correspond roughly to prominent $\delta^{18}\text{O}$ maxima and aragonite formation in BL00-1 during MIS 7c, 5e, and 5c (Fig. 5). The lower-than-present lake level in the Great Salt Lake basin ca. 45 ka might correspond to the maximum in bulk-sediment $\delta^{18}\text{O}$ value that occurred immediately following the presumed Laschamp excursion in BL00-1. On the other hand, ostracodes from the same level have $\delta^{18}\text{O}$ values that are among the lowest in the core, and low $^{87}\text{Sr}/^{86}\text{Sr}$ values indicate input from the Bear River. Furthermore, this interval coincides with the Jensen Spring highstand deposits of Bear Lake (47–39 ka; Laabs and Kaufman, 2003). Reconciling these apparently conflicting observations will require further analyses and an improved geochronology.

SUMMARY AND CONCLUSIONS

Core BL00-1 provides a continuous sedimentary record of hydrologic and paleoenvironmental changes in the Bear Lake catchment during the last quarter-million years. The sedimentary sequence from near the depocenter of the lake exhibits major changes in all of the mineralogical, geochemical, isotopic, and paleontological indicators that we analyzed. These variations reflect changes in the water and sediment discharged from the glaciated headwaters of the dominant tributary, Bear River, and the processes that influenced sediment delivery to the core site, including lake-level changes. The first-order fluctuations coincide with orbital cycles and global ice volume. Millennial-scale fluctuations are pervasive throughout the last two glacial cycles and might correspond to stadial-interstadial cycles recognized in other well-known paleoclimate records, but the age control for BL00-1 is presently too uncertain.

In addition to climatic controls, the hydrogeography of the Bear River also influenced the paleoenvironmental indicators in BL00-1, and the two probably worked in concert. Isolation of the lake from the Bear River likely could have been maintained only when effective moisture was low. During most of the last quarter-million years, the Bear River discharged into Bear Lake, although the connection might have been attenuated by wetlands that separated the lake and the main channel. Our data indicate that Bear Lake retracted into a topographically closed basin during portions of global interglaciations (MIS 7c, 7a, 5e, 5c, and 1). During these intervals, the lake generated abundant endogenic carbonate with aragonite and high values of $\delta^{18}\text{O}$ and $^{87}\text{Sr}/^{86}\text{Sr}$. The ratio of “warm+dry” to “cold” pollen indicators was highest

during MIS 7a, 5e, and 5a; the present interglaciation (MIS 1) exhibits intermediate values. During these interglacial intervals, low ratios of quartz to dolomite (allogenic component) indicate the dominance of locally derived stream sediment over Bear River sediment. Both MIS 5e and MIS 1 intervals include excursions of the Bear River into the lake. The excursion during MIS 1 might correspond to global climate changes during the last glacial-interglacial transition; whether the excursion during MIS 5e was induced climatically remains to be determined, although the low $\delta^{18}\text{O}$ values suggests that it was.

Sediment deposited during the penultimate glacial period (MIS 6) contrasts with sediment deposited during the last glacial cycle (MIS 4–2), although diatom data suggest that the termination of both events was characterized by particularly harsh conditions. The ratio of “warm+dry” to “cold” pollen indicators is lower overall during MIS 6, and the sediment exhibits a progressive increase in values of $\delta^{18}\text{O}$ and $^{87}\text{Sr}/^{86}\text{Sr}$, with parallel increases in quartz content. We interpret these changes as the progressive increase in the proportion of clastic sediment derived from the Uinta Mountains, reflecting the increased influence of glacial erosional products. The 100,000-year period following the last interglaciation (i.e., MIS 5d through MIS 2) comprises four relatively evenly spaced intervals of slowly decreasing $\delta^{18}\text{O}$ values, followed by an abrupt increase. The cause of these saw-toothed cycles is not clear, but the last two terminate about the time of high lake stands in Bear Lake Valley, and at least the youngest one coincides with the end of a deep-lake cycle downstream in the Bonneville Basin. The youngest one is characterized by the only red mud with preserved Fe-oxide minerals in the core, indicative of a fluvially dominated, through-flowing lake connected to Bear River.

ACKNOWLEDGMENTS

We thank Dennis Nielson and the DOSECC drilling crew for their essential role in obtaining the Bear Lake GLAD800 cores, and D. Schnurrenberger, B. Haskell, B. Valero-Garcés, and others who worked on the drilling barge and performed much of the initial core description. G. Skipp and D. Thornbury performed the X-ray diffraction and carbon analyses. A. Cohen, R. Reynolds, S. Starratt, and J. Stone provided valuable reviews of this chapter.

ARCHIVED DATA

Archived data for this chapter can be obtained from the NOAA World Data Center for Paleoclimatology at <http://www.ncdc.noaa.gov/paleo/pubs/gsa2009bearlake/>.

REFERENCES CITED

Balch, D.P., Cohen, A.S., Schnurrenberger, D.W., Haskell, B.J., Valero-Garcés, B.L., Beck, J.W., Cheng, H., and Edwards, R.L., 2005, Ecosystem and paleohydrological response to Quaternary climate change in the Bonneville Basin, Utah: *Palaeogeography, Palaeoclimatology, Palaeoecology*, v. 221, p. 99–122, doi: 10.1016/j.palaeo.2005.01.013.

Benson, L., Lund, S., Negrini, R., Linsley, B., and Zic, M., 2003, Response of North American Great Basin lakes to Dansgaard-Oeschger oscillations: *Quaternary*

Science Reviews, v. 22, p. 2239–2251, doi: 10.1016/S0277-3791(03)00210-5.

Bouchard, D.P., Kaufman, D.S., Hochberg, A., and Quade, J., 1998, Quaternary history of the Thatcher Basin, Idaho, reconstructed from the $^{87}\text{Sr}/^{86}\text{Sr}$ and amino acid composition of lacustrine fossils—Implications for the diversion of the Bear River into the Bonneville basin: *Palaeogeography, Palaeoclimatology, Palaeoecology*, v. 141, p. 95–114, doi: 10.1016/S0031-0182(98)00005-4.

Bradbury, J.P., 1988, Diatom biostratigraphy and the paleolimnology of Clear Lake County, California, *in* Sims, J.D., ed., Late Quaternary climate, tectonism and sedimentation in Clear Lake, northern California Coast Ranges: Geological Society of America Special Paper 214, p. 97–129.

Bradbury, J.P., 1997, A diatom record of climate and hydrology for the past 200 ka from Owens Lake, California with comparison to other great basin records: *Quaternary Science Reviews*, v. 16, p. 203–219, doi: 10.1016/S0277-3791(96)00054-6.

Bradbury, J.P., and Forester, R.M., 2002, Environment and paleolimnology of Owens Lake, California: A record of climate and hydrology for the last 50,000 years, *in* Hershler, R., Madsen, D.B., and Currey, D.R., eds., Great Basin aquatic systems history: Washington D.C., Smithsonian Institution Press, p. 145–173.

Bradbury, J.P., Bezrukova, Ye. E., Chernyaeva, G.P., Colman, S.M., Khursevich, G., King, J.W., and Likoshway, Ye. V., 1994, A synthesis of post-glacial diatom records from Lake Baikal: *Journal of Paleolimnology*, v. 10, p. 213–252, doi: 10.1007/BF00684034.

Bradshaw, E.G., Jones, V.J., Birks, H.J.B., and Birks, H.H., 2000, Diatom responses to late-glacial and early-Holocene environmental changes at Krakenes, western Norway: *Journal of Paleolimnology*, v. 23, p. 21–34, doi: 10.1023/A:1008021016027.

Bright, J., 2009, this volume, Chapter 4, Isotope and major-ion chemistry of groundwater in Bear Lake Valley, Utah and Idaho, with emphasis on the Bear River Range, *in* Rosenbaum, J.G., and Kaufman, D.S., eds., Paleoenvironments of Bear Lake, Utah and Idaho, and its catchment: Geological Society of America Special Paper 450, doi: 10.1130/2009.2450(04).

Bright, J., 2009, this volume, Chapter 8, Ostracode endemism in Bear Lake, Utah and Idaho, *in* Rosenbaum, J.G., and Kaufman, D.S., eds., Paleoenvironments of Bear Lake, Utah and Idaho, and its catchment: Geological Society of America Special Paper 450, doi: 10.1130/2009.2450(08).

Bright, J., Forester, R., and Kaufman, D., 2005, Ostracode analysis for cores BL96-1 and BL96-2 from Bear Lake, Utah and Idaho: U.S. Geological Survey Open-File Report 2005-1227, <http://pubs.usgs.gov/of/2005/1227/>.

Bright, J., Kaufman, D.S., Forester, R.M., and Dean, W.E., 2006, A continuous 250,000 yr record of oxygen and carbon isotopes in ostracode and bulk-sediment carbonate from Bear Lake, Utah-Idaho: *Quaternary Science Reviews*, v. 25, no. 17–18, p. 2258–2270, doi: 10.1016/j.quascirev.2005.12.011.

Colman, S.M., 2006, Acoustic stratigraphy of Bear Lake, Utah-Idaho—Late Quaternary sedimentation in a simple half-graben: *Sedimentary Geology*, v. 185, p. 113–125, doi: 10.1016/j.sedgeo.2005.11.022.

Colman, S.M., Kaufman, D.S., Bright, J., Heil, C., King, J.W., Dean, W.E., Rosenbaum, J.G., Forester, R.M., Bischoff, J.L., Perkins, M., and McGeehin, J.P., 2006, Age models for a continuous 250-kyr Quaternary lacustrine record from Bear Lake, Utah-Idaho: *Quaternary Science Reviews*, v. 25, p. 2271–2282, doi: 10.1016/j.quascirev.2005.10.015.

Colman, S.M., Rosenbaum, J.G., Kaufman, D.S., Dean, W.E., and McGeehin, J.P., 2009, this volume, Radiocarbon ages and age models for the last 30,000 years in Bear Lake, Utah and Idaho, *in* Rosenbaum, J.G., and Kaufman, D.S., eds., Paleoenvironments of Bear Lake, Utah and Idaho, and its catchment: Geological Society of America Special Paper 450, doi: 10.1130/2009.2450(05).

Dean, W.E., 2009, this volume, Endogenic carbonate sedimentation in Bear Lake, Utah and Idaho, over the last two glacial-interglacial cycles, *in* Rosenbaum, J.G., and Kaufman, D.S., eds., Paleoenvironments of Bear Lake, Utah and Idaho, and its catchment: Geological Society of America Special Paper 450, doi: 10.1130/2009.2450(07).

Dean, W., Rosenbaum, J., Haskell, B., Kelts, K., Schnurrenberger, D., Valero-Garcés, B., Cohen, A., Davis, O., Dinter, D., and Nielson, D., 2002, Progress in global lake drilling holds potential for global change research: *Eos (Transactions, American Geophysical Union)*, v. 83, p. 85, 90–91.

Dean, W., Rosenbaum, J., Skipp, G., Colman, S., Forester, R., Simmons, K., Liu, A., and Bischoff, J., 2006, Unusual Holocene and late Pleistocene carbonate sedimentation in Bear Lake, Utah and Idaho, USA: *Sedimentary Geology*, v. 185, p. 93–112, doi: 10.1016/j.sedgeo.2005.11.016.

Dean, W.E., Forester, R.M., Bright, J., and Anderson, R.Y., 2007, Influence of the diversion of the Bear River into Bear Lake (Utah and Idaho) on the environment of deposition of carbonate minerals: *Limnology and Oceanography*, v. 53, p. 1094–1111.

Dean, W.E., Wurtsbaugh, W.A., and Lamarra, V.A., 2009, this volume, Climatic

- and limnologic setting of Bear Lake, Utah and Idaho, in Rosenbaum, J.G., and Kaufman, D.S., eds., *Paleoenvironments of Bear Lake, Utah and Idaho, and its catchment*: Geological Society of America Special Paper 450, doi: 10.1130/2009.2450(01).
- Denny, J.F., and Colman, S.M., 2003, Geophysical surveys of Bear Lake, Utah-Idaho, September 2002: U.S. Geological Survey Open-File Report 03-150.
- Doner, L.A., 2009, this volume, A 19,000-year vegetation and climate record for Bear Lake, Utah and Idaho, in Rosenbaum, J.G., and Kaufman, D.S., eds., *Paleoenvironments of Bear Lake, Utah and Idaho, and its catchment*: Geological Society of America Special Paper 450, doi: 10.1130/2009.2450(09).
- Douglas, M.S.V., Smol, J.P., and Blake, W., Jr., 1994, Marked post-18th century environmental change in high-Arctic ecosystems: *Science*, v. 266, p. 416–419, doi: 10.1126/science.266.5184.416.
- Engleman, E.E., Jackson, L.L., Norton, D.R., and Fischer, A.G., 1985, Determination of carbonate carbon in geological materials by coulometric titration: *Chemical Geology*, v. 53, p. 125–128, doi: 10.1016/0009-2541(85)90025-7.
- Evans, J.P., Martindale, D.C., and Kendrick, R.D., Jr., 2003, Geologic setting of the 1884 Bear Lake, Idaho, earthquake: Rupture in the hanging wall of a basin and range normal fault revealed by historical and geological analyses: *Bulletin of the Seismological Society of America*, v. 93, p. 1621–1632, doi: 10.1785/0120020159.
- Flower, R.J., 1993, Diatom preservation—Experiments and observations on dissolution and breakage in modern and fossil material: *Hydrobiologia*, v. 269–270, p. 473–484, doi: 10.1007/BF00028045.
- Heil, C.W., Jr., King, J.W., Rosenbaum, J.G., Reynolds, R.L., and Colman, S.M., 2009, this volume, Paleomagnetism and environmental magnetism of GLAD800 sediment cores from Bear Lake, Utah and Idaho, in Rosenbaum, J.G., and Kaufman, D.S., eds., *Paleoenvironments of Bear Lake, Utah and Idaho, and its catchment*: Geological Society of America Special Paper 450, doi: 10.1130/2009.2450(13).
- Hendy, I.L., and Kennett, J.P., 1999, Latest Quaternary North Pacific surface water responses imply atmosphere-driven climate instability: *Geology*, v. 27, p. 291–294, doi: 10.1130/0091-7613(1999)027<0291:LQNPSW>2.3.CO;2.
- Hostetler, S.W., Giorgi, F., Bates, G.T., and Bartlein, P.J., 1994, Lake-atmosphere feedbacks associated with paleolakes Bonneville and Lahontan: *Science*, v. 263, p. 665–668, doi: 10.1126/science.263.5147.665.
- Jiménez-Moreno, G., Anderson, R.S., and Fawcett, P.J., 2007, Orbital- and millennial-scale vegetation and climate changes of the past 225 ka from Bear Lake, Utah-Idaho (USA): *Quaternary Science Reviews*, v. 26, p. 1713–1724, doi: 10.1016/j.quascirev.2007.05.001.
- Karabanov, E., Williams, D., Kuzmin, M., Sideleva, V., Khursevich, G., and Prokopenko, A.A., 2004, Ecological collapse of Lake Baikal and Lake Hovsgal, ecosystems during the last glacial and consequences for aquatic species diversity: *Palaeogeography, Palaeoclimatology, Palaeoecology*, v. 209, p. 227–243, doi: 10.1016/j.palaeo.2004.02.017.
- Karst, T.L., and Smol, J.P., 2000, Paleolimnological evidence of limnetic nutrient concentration equilibrium in a shallow, macrophyte-dominated lake: *Aquatic Sciences*, v. 62, p. 20–38, doi: 10.1007/s000270050073.
- Kaufman, D.S., Forman, S.L., and Bright, J., 2001, Age of the Cutler Dam Alloformation (late Pleistocene), Bonneville basin, Utah: *Quaternary Research*, v. 56, p. 322–334, doi: 10.1006/qres.2001.2275.
- Krammer, K., and Lange-Bertalot, H., 1986–1991, Süßwasserflora von Mitteleuropa, Bacillariophyceae Band 2/1–4: Gustav Fischer Verlag, Stuttgart, Germany.
- Laabs, B.J., and Kaufman, D.S., 2003, Quaternary highstands in Bear Lake Valley, Utah and Idaho: *Geological Society of America Bulletin*, v. 115, p. 463–478, doi: 10.1130/0016-7606(2003)115<0463:QHIBLV>2.0.CO;2.
- Laabs, B.J.C., Plummer, M.A., and Mickelson, D.M., 2006, Climate during the last glacial maximum in the Wasatch and southern Uinta Mountains inferred from glacier modeling: *Geomorphology*, v. 75, p. 300–317, doi: 10.1016/j.geomorph.2005.07.026.
- Laabs, B.J.C., Munroe, J.S., Rosenbaum, J.G., Refsnider, K.A., Mickelson, D.M., Singer, B.S., and Chafee, M.W., 2007, Chronology of the last glacial maximum in the upper Bear River Basin, Utah: Arctic, Antarctic, and Alpine Research, v. 39, p. 537–548, doi: 10.1657/1523-0430(06-089)[LAABS]2.0.CO;2.
- Lamarra, V., Liff, C., and Carter, J., 1986, Hydrology of Bear Lake basin and its impact on the trophic state of Bear Lake, Utah-Idaho: *The Great Basin Naturalist*, v. 46, p. 690–705.
- MacKay, A.W., 2007, The paleoclimatology of Lake Baikal: A diatom synthesis and prospectus: *Earth-Science Reviews*, v. 82, p. 181–215, doi: 10.1016/j.earscirev.2007.03.002.
- McConnell, W.J., Clark, W.J., and Sigler, W.F., 1957, Bear Lake: Its fish and fishing: Utah State Department of Fish and Game, Idaho Department of Fish and Game, Wildlife Management Department of Utah State Agricultural College, 76 p.
- Moore, D.M., and Reynolds, R.C., Jr., 1989, X-ray diffraction and identification and analysis of clay minerals: Oxford, UK, Oxford University Press, 332 p.
- Moser, K.A., and Kimball, J.P., 2009, this volume, A 19,000-year record of hydrologic and climatic change inferred from diatoms from Bear Lake, Utah and Idaho, in Rosenbaum, J.G., and Kaufman, D.S., eds., *Paleoenvironments of Bear Lake, Utah and Idaho, and its catchment*: Geological Society of America Special Paper 450, doi: 10.1130/2009.2450(10).
- Oviatt, C.G., Currey, D.R., and Sack, D., 1992, Radiocarbon chronology of Lake Bonneville, eastern Great Basin, USA: *Palaeogeography, Palaeoclimatology, Palaeoecology*, v. 99, p. 225–241, doi: 10.1016/0031-0182(92)90017-Y.
- Oviatt, C.G., Thompson, R.S., Kaufman, D.S., Bright, J., and Forester, R.M., 1999, Reinterpretation of the Burmester core, Bonneville basin, Utah: *Quaternary Research*, v. 52, p. 180–184, doi: 10.1006/qres.1999.2058.
- Reheis, M.C., Laabs, B.J.C., and Kaufman, D.S., 2009, this volume, Geology and geomorphology of Bear Lake Valley and upper Bear River, Utah and Idaho, in Rosenbaum, J.G., and Kaufman, D.S., eds., *Paleoenvironments of Bear Lake, Utah and Idaho, and its catchment*: Geological Society of America Special Paper 450, doi: 10.1130/2009.2450(02).
- Reynolds, R.L., and Rosenbaum, J.G., 2005, Magnetic mineralogy of sediments in Bear Lake and its watershed: Support for paleomagnetic and paleoenvironmental interpretations: U.S. Geological Survey Open-File Report 2005-1406, <http://pubs.usgs.gov/of/2005/1406/>.
- Rosenbaum, J.G., and Heil, C.W., Jr., 2009, this volume, The glacial/deglacial history of sedimentation in Bear Lake, Utah and Idaho, in Rosenbaum, J.G., and Kaufman, D.S., eds., *Paleoenvironments of Bear Lake, Utah and Idaho, and its catchment*: Geological Society of America Special Paper 450, doi: 10.1130/2009.2450(11).
- Rosenbaum, J.G., and Kaufman, D.S., 2009, this volume, Introduction to *Paleoenvironments of Bear Lake, Utah and Idaho, and its catchment*, in Rosenbaum, J.G., and Kaufman, D.S., eds., *Paleoenvironments of Bear Lake, Utah and Idaho, and its catchment*: Geological Society of America Special Paper 450, doi: 10.1130/2009.2450(00).
- Rosenbaum, J.G., Dean, W.E., Reynolds, R.L., and Reheis, M.C., 2009, this volume, Allogenic sedimentary components of Bear Lake, Utah and Idaho, in Rosenbaum, J.G., and Kaufman, D.S., eds., *Paleoenvironments of Bear Lake, Utah and Idaho, and its catchment*: Geological Society of America Special Paper 450, doi: 10.1130/2009.2450(06).
- Scott, W.E., McCoy, W.D., Shroba, R.R., and Rubin, M., 1983, Reinterpretation of the exposed record of the last two cycles of Lake Bonneville, western United States: *Quaternary Research*, v. 20, p. 261–285, doi: 10.1016/0033-5894(83)90013-3.
- Seidenkrantz, P., Kristensen, P., and Knudsen, K.L., 1995, Marine evidence for climatic instability during the last interglacial in shelf records from northwest Europe: *Journal of Quaternary Science*, v. 10, p. 77–82, doi: 10.1002/jqs.3390100108.
- Simpson, E.H., 1949, Measurement of diversity: *Nature*, v. 163, p. 688, doi: 10.1038/163688a0.
- Smoot, J.P., and Rosenbaum, J.G., 2009, this volume, Sedimentary constraints on late Quaternary lake-level fluctuations at Bear Lake, Utah and Idaho, in Rosenbaum, J.G., and Kaufman, D.S., eds., *Paleoenvironments of Bear Lake, Utah and Idaho, and its catchment*: Geological Society of America Special Paper 450, doi: 10.1130/2009.2450(12).
- Stuiver, M., and Grootes, P.M., 2000, GISP2 oxygen isotope ratios: *Quaternary Research*, v. 53, p. 277–284, doi: 10.1006/qres.2000.2127.
- Thouveny, N., de Beaulieu, J.-L., Bonifay, E., Creer, K.M., Guiot, J., Icole, M., Johnsen, S., Jouzel, J., Reille, M., Williams, T., and Williamson, D., 1994, Climate variations in Europe over the last 140 kyr deduced from rock magnetism: *Nature*, v. 371, p. 503–506, doi: 10.1038/371503a0.
- von Grafenstien, U., Erlernkeuser, H., and Trimborn, P., 1999, Oxygen and carbon isotopes in modern fresh-water ostracode valves: Assessing the vital offsets and autecological effects of interest for palaeoclimatic studies: *Palaeogeography, Palaeoclimatology, Palaeoecology*, v. 148, p. 133–152, doi: 10.1016/S0031-0182(98)00180-1.
- Winograd, I.J., Copen, T.B., Landwehr, J.M., Riggs, A.C., Ludwig, K.R., Szabo, B.J., Kolesar, P.T., and Revesz, K.M., 1992, Continuous 500,000-year climate record from vein calcite in Devils Hole, Nevada: *Science*, v. 258, p. 255–260, doi: 10.1126/science.258.5080.255.
- Wolin, J.A., and Duthie, H.C., 1999, Diatoms as indicators of water level change in freshwater lakes, in Stoermer, E.F., and Smol, J.P., eds., *The diatoms: Applications for the environmental and earth sciences*: Cambridge, UK, Cambridge University Press, p. 183–226.

APPENDIX A. MINERALOGY, INORGANIC, AND ORGANIC CARBON CONTENT, BL00-1

Sample #	Depth (m blf)	Quartz (%)	Plag. (%)	Arag. (%)	Dolo. (%)	Calcite (%)	CaCO ₃ (%)	Organic carbon (%)
1h1 5	0.45	27.9	4.9	48.8	5.3	13.1	60.9	1.9
1h1 89.9	1.29	29.4	5.3	50.4	4.4	10.4	66.9	2.2
1h1 110.2	1.50	21.3	0.0	63.5	4.8	10.4	58.8	3.9
1E-1h	2.15	15.8	0.0	63.8	9.5	10.9	75.6	1.7
1h2 60	2.51	22.6	0.1	62.9	4.6	9.9	72.3	1.8
1h2 90	2.81	18.1	0.1	66.8	4.8	10.3	76.8	1.1
1h2 106	2.97	22.9	0.1	63.9	3.8	9.4	76.7	1.2
1D-1h	3.40	17.4	6.2	64.6	4.4	7.4	79.3	1.0
2h1 70	4.10	17.5	3.6	68.5	3.6	6.9	76.3	1.4
1E-2h	5.15	14.8	0.0	69.0	5.0	11.2	78.4	1.1
2h2 60	5.51	18.5	4.1	61.4	5.3	10.8	75.8	1.3
2h2 85	5.76	21.1	4.1	58.4	5.4	11.1	68.9	1.8
1D-2h	6.40	18.2	3.5	63.1	4.4	10.8	75.8	1.1
3h2 109.6	7.57	27.0	0.2	45.1	5.9	21.8	62.6	2.3
3h2 117	7.64	35.8	7.1	35.1	5.4	16.7	51.0	3.9
3h2 125.4	7.72	22.6	4.1	58.0	4.5	10.8	74.1	1.3
3h2 148.5	7.96	22.2	0.2	61.3	4.5	11.7	74.7	1.8
1E-3h	8.15	18.1	4.0	60.5	6.7	10.8	74.5	2.4
3h3 40	8.39	24.6	5.7	47.0	6.2	16.5	67.8	1.6
3h3 90	8.89	19.8	2.7	0.0	3.4	74.1	63.6	1.6
1D-3h	9.40	65.3	7.4	0.0	6.3	21.0	10.4	1.0
4h1 63	10.03	45.6	4.0	0.0	6.2	44.2	27.9	1.8
4h1 84	10.24	68.2	6.5	0.0	10.1	15.2	13.9	1.7
4h1 140	10.80	66.5	4.5	0.0	7.0	22.0	14.2	0.6
1E-4h	11.15	67.2	5.0	0.0	7.9	20.0	15.2	0.4
4h2 30	11.20	69.5	4.3	0.0	6.6	19.6	12.5	0.7
4h2 57.4	11.47	65.7	7.7	0.0	7.5	19.2	15.9	0.2
1D-4h	12.40	72.8	6.7	0.0	6.5	14.0	13.4	0.4
5h1 54	12.94	70.7	5.3	0.0	7.8	16.3	14.3	0.3
5h2 20	14.10	71.5	5.0	0.0	9.9	13.6	14.5	0.2
1E-5h	14.15	77.1	3.9	0.0	7.6	11.4	11.3	0.5
5h2 110	15.00	63.3	11.9	0.0	5.7	19.1	12.3	0.6
1D-5h	15.40	67.5	6.7	0.0	6.3	19.5	17.3	0.3
6h1 30	15.70	66.7	5.1	0.0	9.4	18.9	19.8	
6h1 110	16.50	66.5	4.9	0.0	7.3	21.3	15.9	0.3
6h1 123	16.63	66.2	6.2	0.0	7.5	20.0	14.2	0.3
6h1 146	16.86	71.5	9.5	0.0	9.0	10.0	14.0	0.4
6h1 147.5	16.87	68.8	8.2	0.0	10.8	12.3	11.3	0.7
1E-6h	17.15	65.4	12.3	0.0	10.5	11.8	13.3	0.7
6h2 42	17.33	68.3	7.3	0.0	11.7	12.7		
6h2 80	17.71	74.9	8.4	0.0	6.1	10.7	8.2	0.9
1D-6h	18.40	75.1	6.4	0.0	5.8	12.8	10.6	0.7
7h1 40	18.80	70.0	6.0	0.0	6.9	17.1	13.4	0.4
7h1 80	19.20	66.2	6.1	0.0	6.8	21.0	22.8	0.4
7h1 126	19.66	75.5	7.2	0.0	8.2	9.1	5.6	1.3
1E-7h	20.15	73.0	10.6	0.0	9.4	7.0	6.4	1.5
7h2 42	20.33	77.3	6.6	0.0	5.5	10.6	14.0	0.2
7h2 67	20.58	68.0	6.2	0.0	5.9	19.9	18.5	0.6
7h2 130	21.21	64.8	7.5	0.0	9.0	18.7	13.1	1.8
1D-7h	21.40	59.1	13.9	0.0	7.4	19.7	14.0	1.5
8h1 74	22.14	63.6	4.8	0.0	7.3	24.3	15.2	0.5
8h2 20.5	23.10	60.4	6.0	0.0	6.9	26.7	19.0	0.8
1E-8h	23.15	57.6	4.6	0.0	7.9	29.8	16.4	1.2
8h2 120.3	24.10	52.9	5.3	0.0	6.5	35.2	19.0	2.2
1D-8h	24.40	64.4	6.0	0.0	7.4	22.2	11.8	1.4
9h2 26	26.15	66.6	6.0	0.0	7.9	19.5	13.0	0.8
1E-9h	26.15	66.3	6.5	0.0	8.5	18.7	12.6	0.7
9h2 128.2	27.16	77.5	6.3	0.0	7.7	8.5	3.6	3.7
1D-9h	27.40	78.4	7.1	0.0	8.7	5.8	5.5	2.6
10h1 36	27.76	78.3	10.1	0.0	11.6	0.0	14.3	2.2
10h1 57	27.97	75.6	9.7	0.0	11.4	3.3	9.8	3.3
10h1 120	28.60	67.7	9.8	0.0	6.1	16.4	20.8	
1E-10h	29.15	68.7	5.4	0.0	9.1	16.7	10.5	2.3
10h2 60	29.51	50.4	5.3	0.0	4.6	39.7	21.2	2.5
10h2 129.7	30.20	54.5	6.0	0.0	5.2	34.3	21.1	2.6
1D-10h	30.40	59.0	6.9	0.0	8.9	25.3	13.8	2.3
11h1 69.9	31.09	58.9	7.6	0.0	7.3	26.2	14.2	1.7
11h1 131.7	31.71	73.0	8.6	0.0	9.5	9.0	7.1	3.2
1E-11h	32.15	45.8	5.1	0.0	6.2	42.8	30.8	1.9
1D-11h	33.40	62.5	8.1	0.0	7.6	21.8	13.4	1.6
1E-12h	35.15	61.7	7.9	0.0	9.9	20.6	14.1	1.0

(continued)

APPENDIX A. MINERALOGY, INORGANIC, AND ORGANIC CARBON CONTENT, BL00-1 (continued)

Sample #	Depth (m blf)	Quartz (%)	Plag. (%)	Arag. (%)	Dolo. (%)	Calcite (%)	CaCO ₃ (%)	Organic carbon (%)
12h2 33.1	35.24	61.4	6.4	0.0	8.6	23.7	17.5	1.0
12h2 79.2	35.70	63.8	7.1	0.0	8.5	20.6	10.0	1.5
1D-12h	36.40	66.0	6.8	0.0	6.3	20.9	14.6	0.8
13h1 66	37.02	71.1	7.9	0.0	5.6	15.4	9.9	2.0
1E-13h	38.15	61.6	16.3	0.0	5.5	16.6	10.0	0.9
13h2 83.8	38.63	48.9	6.1	0.0	4.8	40.2	26.6	1.9
13h2 101.7	38.80	47.5	7.1	0.0	4.2	41.1	24.8	1.9
14h1 9.8	39.49	69.0	7.2	0.0	5.9	17.9	9.2	0.9
14h1 99.6	40.39	44.4	5.8	0.0	5.5	44.3	23.2	1.2
1E-14h	41.15	34.0	5.6	0.0	4.6	55.9	41.8	1.5
14h2 100	41.91	43.3	5.1	0.0	6.0	45.7	43.8	1.5
14h2 134	42.25	36.3	4.4	0.0	4.6	54.7	27.8	0.8
1D-14h	42.40	39.1	4.8	0.0	5.0	51.1	25.8	0.7
15h1 50	42.90	51.6	6.2	0.0	6.7	35.4	16.8	0.6
15h1 139.5	43.79	51.8	7.2	0.0	7.1	33.9	18.3	0.5
1E-15h	44.15	56.7	4.3	0.0	6.9	32.1	20.9	0.3
15h2 87.5	44.77	53.1	5.3	0.0	5.7	35.9	20.3	0.9
1D-15h	45.40	50.8	5.5	0.0	6.2	37.5	24.0	1.3
16a1 75	46.11	58.5	5.6	0.0	7.0	28.9	18.0	0.5
1E-16h	47.15	40.2	3.9	0.0	6.1	49.8	31.5	1.5
16a2 50	47.30	42.9	4.8	0.0	5.1	47.2	22.2	2.7
16a2 107.5	47.87	57.4	6.1	0.0	7.4	29.2	22.1	0.7
1D-16a	48.36	55.9	6.2	0.0	7.4	30.5	20.2	0.8
17a1 59.3	48.94	59.5	5.6	0.0	7.8	27.1	19.7	0.1
17a1 109.3	49.42	59.8	5.0	0.0	6.0	29.1	18.8	0.5
17a1 139.2	49.71	47.2	8.1	0.0	5.3	39.4	33.4	0.4
1E-17e	50.15	42.8	7.1	0.0	6.7	43.4	21.7	1.6
17a2 52	50.33	39.3	32.3	0.0	0.0	28.4	3.2	0.3
17a2 99.2	50.78	49.3	5.6	0.0	5.0	40.1	20.4	1.6
18a2 11.5	50.82	31.0	8.6	0.0	7.7	52.7	26.8	0.8
1D-17a	51.36	40.1	5.6	0.0	7.3	46.9	27.3	2.1
18a2 21.5	51.91	36.0	33.1	0.0	0.0	30.9	1.6	
18a2 21.5	51.91						1.3	
18a2 90	52.52	27.8	4.4	0.0	4.9	62.9	49.0	1.1
1E-18e	53.15	30.5	7.2	0.0	8.1	54.2	25.9	0.7
18a3 133	54.22	42.6	4.7	0.0	4.0	48.8	19.0	2.3
1D-18a	54.36	44.7	4.5	0.0	5.3	45.5	28.0	0.9
1D-19A-2-5	54.48	43.7	4.0	0.0	5.1	47.2	23.5	1.3
1D-19A-2-26	54.68	53.4	0.0	0.0	6.1	40.6	23.8	0.6
19a2 35.5	54.76	50.5	4.7	0.0	5.2	39.6	22.5	0.7
1D-19A-2-45	54.86	47.9	4.6	0.0	5.7	41.9	24.9	1.0
1D-19A-2-65	55.06	41.6	3.9	0.0	5.0	49.5	30.4	1.6
1D-19A-2-85	55.25	38.5	4.6	9.5	6.8	40.6	36.6	1.7
1D-19A-2-105	55.44	42.7	0.0	31.6	7.9	17.9	45.6	1.7
1D-19A-2-125	55.63	41.0	5.0	31.8	6.0	16.3	49.0	1.7
1E-19e	55.65	42.9	5.1	29.2	5.7	17.2	48.3	1.6
1D-19A-2-145	55.82	50.2	6.0	27.7	9.7	6.4	41.8	2.1
1D-19A-3-5	55.92	39.0	5.9	0.0	6.1	49.1	44.3	1.5
1D-19A-3-25	56.11	49.2	0.0	0.0	5.6	45.2	25.1	0.7
1D-19A-3-45	56.30	40.5	0.0	0.0	4.8	54.7	32.1	0.8
1D-19A-3-65	56.50	78.8	11.4	0.0	9.8	0.0	48.8	2.0
19a3 79.3	56.62	77.6	9.6	0.0	12.8	0.0	49.6	1.5
1D-19A-3-105	56.88	48.6	4.5	0.0	5.8	41.0	28.5	1.8
1D-19A-3-125	57.07	48.6	5.3	0.0	6.2	40.0	25.3	1.7
1D-19A-3-145	57.26	57.6	5.8	0.0	6.3	30.4	20.5	1.4
1D-19a	57.36	59.0	4.9	0.0	6.4	29.7	19.9	1.0
1E-20e	58.15	55.2	3.4	0.0	5.9	35.5	23.1	0.7
20a2 24.3	59.04	48.9	5.6	0.0	5.4	40.2	29.7	2.9
20a2 55.7	59.35	53.0	5.6	0.0	5.7	35.7	23.5	0.6
20a2 62.5	59.42	51.2	6.7	0.0	5.6	36.5	25.6	1.2
20a2 92.6	59.71	46.9	12.7	0.0	5.2	35.2	24.8	0.8
1D-20a	60.36	43.5	5.8	0.0	5.2	45.5	33.9	2.7
1D-21A-1-5	60.41	58.0	0.0	0.0	7.0	35.1	20.2	2.7
1D-21A-1-25	60.60	62.8	0.0	5.9	5.5	25.9	22.9	2.4
1E-21e	60.65	53.9	5.2	0.0	8.0	32.9	21.9	1.4
1D-21A-1-45	60.80	52.9	4.3	0.0	4.9	38.0	24.5	1.7
21a1 67.5	61.00	50.6	5.8	4.0	4.8	34.8	22.7	2.2
1D-21A-1-85	61.19	48.9	6.3	21.5	5.5	17.8	38.5	1.6
21a1 113	61.44	37.3	6.3	34.7	4.8	16.9	54.6	1.0

(continued)

APPENDIX A. MINERALOGY, INORGANIC, AND ORGANIC CARBON CONTENT, BL00-1 (continued)

Sample #	Depth (m blf)	Quartz (%)	Plag. (%)	Arag. (%)	Dolo. (%)	Calcite (%)	CaCO ₃ (%)	Organic carbon (%)
1D-21A-1-125	61.57	38.1	0.0	39.3	6.2	16.3	56.4	1.3
1D-21A-1-145	61.77	31.7	8.5	37.7	6.4	15.7	60.8	1.2
21a2 24.8	62.08	28.8	1.8	50.7	5.1	13.7	68.9	1.4
21a2 79.8	62.60	16.7	1.1	3.2	2.6	76.4	67.6	0.8
21a2 104.7	62.84	27.5	5.1	50.6	4.9	12.0	70.0	1.7
21a2 133.8	63.12	30.6	1.7	46.5	4.5	16.6	73.3	0.6
1E-22e	63.15	29.0	3.3	45.8	7.3	14.5	71.6	1.2
1D-21a	63.36	33.0	5.9	34.0	4.4	22.7	62.8	1.2
22a1 70.9	64.06	37.3	5.4	35.0	9.0	13.3	46.2	0.9
22a1 143.5	64.78	26.3	8.4	43.4	9.6	12.3	53.3	3.1
1D-22A-2-5	64.90	35.3	4.7	42.8	6.9	10.4	66.4	1.3
1D-22A-2-25	65.10	32.1	5.3	38.8	7.7	16.1	60.3	1.4
1D-22A-2-45	65.30	29.1	4.5	42.9	7.8	15.8	64.2	1.0
22a2 68.5	65.53	32.2	1.7	42.3	6.9	17.0	63.4	1.1
1E-23e	65.65	35.6	5.0	34.9	9.0	15.5	55.4	1.3
1D-22A-2-95	65.79	32.8	0.0	38.5	10.5	18.2	59.3	1.6
22a2 126.5	66.10	41.7	5.7	29.6	6.8	16.2	53.2	1.2
22a2 126.5	66.10						51.7	
1D-22A-2-145	66.29	30.6	11.6	32.2	7.6	18.0	54.2	1.2
1D-22a	66.36	37.8	5.5	30.7	8.4	17.5	54.3	1.8
1D-23A-1-5	66.40	34.4	4.7	37.2	7.1	16.7	58.0	1.2
1D-23A-1-25	66.58	35.9	5.4	33.2	6.3	19.2	54.4	1.3
1D-23A-1-45	66.75	35.5	5.3	34.7	8.8	15.7	51.7	1.3
1D-23A-1-65	66.93	43.6	0.0	37.9	6.1	12.4	58.1	1.4
23a1 87	67.12	29.2	6.9	43.1	5.1	15.7	65.0	1.7
23a1 117	67.38	30.7	5.2	10.6	5.3	48.2	46.4	
23a1 117	67.38						45.0	2.8
1D-23A-1-145	67.62	43.7	4.2	0.0	4.7	47.4	28.3	2.8
1D-23A-2-5	67.71	54.6	4.6	0.0	7.7	33.1	21.8	2.4
1D-23A-2-25	67.89	69.6	5.5	0.0	10.7	14.2	10.6	2.6
1D-23A-2-45	68.06	76.5	5.0	0.0	13.0	5.5	6.9	2.2
1E-24e	68.15	70.1	11.9	0.0	10.1	7.9	9.8	2.0
23a2 57.5	68.17	76.8	6.1	0.0	10.5	6.6	10.2	1.6
23a2 57.5	68.17						9.1	
1D-23A-2-85	68.41	74.7	9.1	0.0	10.6	5.6	5.8	1.4
23a2 110	68.63	65.0	7.9	0.0	8.2	18.8	24.8	0.5
23a2 110	68.63						23.0	0.8
1D-23a	68.86	63.1	9.2	0.0	8.2	19.5	13.8	0.3
24e2 14.3	69.08	63.6	8.2	0.0	8.0	20.2	12.3	0.3
24e2 14.3	69.08						10.8	0.5
24e2 62.7	69.47	70.1	6.7	0.0	9.8	13.4	11.7	
24e2 62.7	69.47						10.3	0.9
24e3 2.5	70.16	65.8	8.5	0.0	7.0	18.8	6.5	1.3
24e3 58.7	70.61	60.3	6.9	0.0	8.9	23.9	21.1	1.0
1E-25e	70.65	64.4	4.5	0.0	8.4	22.8	15.1	0.3
24e3 112.8	71.03	63.2	6.5	0.0	7.7	22.5	21.0	0.5
24e3 133.4	71.19	71.9	8.2	0.0	10.0	10.0	10.4	0.7
1D-24e	71.37	71.2	7.1	0.0	9.0	12.7	12.9	1.2
25e2 132.5	72.50	65.6	8.6	0.0	8.2	17.6	15.3	1.8
1E-26e	73.15	66.8	6.0	0.0	8.9	18.4	13.8	1.1
25e3 77	73.24	63.2	6.4	0.0	8.4	22.0	13.9	0.9
1D-25e	73.87	70.1	8.8	0.0	8.1	13.0	21.8	1.1
26e2 95.3	74.75	59.0	5.5	0.0	7.0	28.5	24.0	0.9
26e2 132.7	75.04	59.7	5.4	0.0	9.1	25.8	19.4	0.5
26e3 39	75.47	58.9	6.7	0.0	8.6	25.8	23.2	0.4
1E-27e	75.65	61.2	3.7	0.0	7.8	27.2	22.0	0.4
26e3 109	76.01	55.9	6.7	0.0	7.9	29.5	15.8	1.7
1D-26e	76.37	59.2	5.4	0.0	7.8	27.5	19.4	0.4
27e1 38	76.66	60.8	5.1	0.0	7.6	26.5	18.2	0.4
1D-27e	76.97	60.3	5.6	0.0	7.2	26.9	15.7	0.8
28e2 77.8	77.77	60.7	5.5	0.0	7.5	26.3	19.7	0.4
1E-28e	78.15	60.1	4.3	0.0	6.5	29.1	19.0	0.5
28e2 147	78.29	56.9	5.8	0.0	7.3	30.0	20.5	0.3
28e3 16.4	78.43	56.2	5.4	0.0	8.7	29.7	22.8	0.7
28e3 60.2	78.75	59.1	7.1	0.0	8.0	25.8	13.3	1.8
28e3 93.4	79.00	57.2	6.2	0.0	7.5	29.1	20.2	1.0
28e3 140.3	79.35	57.5	5.8	0.0	6.6	30.1	22.3	1.0
1D-28e	79.47	54.0	7.0	0.0	9.6	29.4	23.5	0.9
29e3 58.3	80.41	67.0	5.7	0.0	8.3	19.1	9.9	1.7
1E-29e	80.65	53.5	6.4	0.0	9.7	30.4	22.2	1.4

(continued)

APPENDIX A. MINERALOGY, INORGANIC, AND ORGANIC CARBON CONTENT, BL00-1 (continued)

Sample #	Depth (m blf)	Quartz (%)	Plag. (%)	Arag. (%)	Dolo. (%)	Calcite (%)	CaCO ₃ (%)	Organic carbon (%)
29e2 110.3	81.18	75.4	6.8	0.0	9.3	8.6	16.8	0.3
1D-29e	81.97	62.7	5.5	0.0	8.2	23.7	16.4	0.5
30e2 38	82.49	58.2	5.9	0.0	10.6	25.3	23.6	0.2
29e3 136	82.80	60.9	6.6	0.0	7.9	24.6	20.1	0.2
1E-30e	82.90	57.0	4.2	0.0	5.8	33.0	27.5	0.4
30e3 26.4	83.51	59.1	5.3	0.0	8.8	26.9	18.9	1.6
30e3 73.7	83.86	59.9	8.4	0.0	8.4	23.3	40.0	0.7
30e3 96.2	84.02	71.8	7.7	0.0	7.2	13.3	9.5	0.7
1D-30e	84.47	65.6	7.9	0.0	8.0	18.5	10.3	1.0
31e1 60.5	84.94	64.3	11.7	0.0	6.3	17.6	11.3	0.7
31e1 81.8	85.10	57.0	9.2	0.0	6.2	27.6	9.7	0.9
1E-31e	85.15	68.6	6.2	0.0	7.8	17.5	12.3	1.2
31e2 16.8	85.75	61.6	6.4	0.0	7.0	25.0	24.4	0.5
31e2 66.6	86.14	60.1	6.0	0.0	6.5	27.4	18.2	1.1
1D-31e	86.47	55.4	6.2	0.0	6.4	32.0	20.2	0.7
32e1 59.3	86.90	58.2	6.8	0.0	7.0	28.0	14.7	0.4
32e1 123	87.35	50.3	7.0	0.0	6.1	36.5	30.9	0.6
1E-32e	87.40	54.1	3.8	0.0	6.3	35.8	29.0	0.7
32e2 59.9	87.99	54.6	6.2	0.0	7.5	31.6	17.9	0.6
1D-32e	88.47	58.6	5.7	0.0	6.7	29.1	17.3	0.6
33e1 35.9	88.75	53.3	7.8	0.0	6.5	32.5	23.4	0.6
33e1 141.8	89.60	38.4	5.4	0.0	7.1	49.2	36.8	1.5
1E-33e	89.65	38.7	3.6	0.0	5.7	52.0	38.6	1.3
33e2 43.6	90.02	53.0	8.4	0.0	7.0	31.6	24.8	0.7
33e2 91.2	90.40	39.7	4.8	0.0	6.0	49.6	26.9	1.2
1D-33e	90.47	48.2	5.9	0.0	6.7	39.2	25.0	1.2
34e1 119.8	91.33	49.9	6.0	0.0	7.5	36.6	27.0	1.3
34e2 47.1	91.90	41.7	4.9	0.0	6.9	46.5	33.8	1.1
1E-34e	91.90	36.7	5.5	0.0	5.5	52.4	35.3	1.3
34e2 111	92.36	53.0	15.2	0.0	7.4	24.4	14.6	1.6
1D-34e	92.47	62.8	6.2	0.0	7.3	23.8	15.4	1.0
35e1 82.2	93.07	60.2	5.9	0.0	7.6	26.4	19.1	0.3
1E-35e	94.15	57.4	4.4	0.0	7.0	31.3	18.8	0.8
35e2 86.6	94.19	56.2	10.9	0.0	6.5	26.3	16.8	1.4
36e1 51.5	94.83	66.8	6.7	0.0	7.7	18.8	15.7	0.8
36e2 19.1	95.65	60.6	9.3	0.0	7.0	23.1	30.3	0.2
1E-36e	95.90	62.4	5.6	0.0	10.1	21.9	11.4	0.3
36e2 92.6	96.16	68.7	8.2	0.0	7.9	15.2	9.8	0.8
36e2 109.5	96.28	61.8	7.4	0.0	6.6	24.3	14.7	0.4
1D-36e	96.47	58.4	11.7	0.0	6.8	23.2	14.8	0.3
37e2 45.4	97.98	53.0	7.7	0.0	5.6	33.7	22.8	1.3
1E-37e	98.15	59.5	5.1	0.0	7.1	28.3	17.2	1.1
37e2 92	98.34	60.5	7.9	0.0	5.3	26.3	16.8	0.9
37e2 94.1	98.35	70.7	9.6	0.0	6.9	12.8	9.3	0.7
38e2 52.8	99.95	32.9	10.8	0.0	7.2	49.1	18.1	0.7
38e2 75.8	100.11	28.1	1.6	0.0	5.4	65.0	40.3	2.3
1E-38e	100.40	28.6	3.4	0.0	5.4	62.6	45.9	1.6
1D-38e	100.47	45.8	6.3	0.0	7.6	40.3	20.5	1.4
1E-39E-2-9	100.59	31.6	3.2	0.0	4.9	60.3	42.1	1.7
1E-39E-2-25	100.71	49.1	4.8	0.0	7.2	39.0	20.3	1.5
1E-39E-2-45	100.85	48.7	0.0	0.0	6.9	44.5	24.0	1.4
39E-2-53.6-54.9	100.91	47.5	4.6	0.0	5.7	42.2	24.9	1.4
1E-39E-2-65	101.05	45.9	5.2	0.0	6.0	42.9	23.8	1.5
1E-39E-2-85	101.13	49.5	4.4	0.0	5.6	40.5	24.6	1.1
1E-39E-2-105	101.27	37.1	4.2	0.0	5.1	53.6	36.5	1.3
1E-39E-2-125	101.42	27.9	4.0	0.0	7.3	60.8	47.2	1.1
39E-2-144.9-145.7	101.56	37.8	8.3	9.9	7.1	36.9	42.7	1.2
1E-39E-3-5	101.64	40.4	6.5	23.5	7.8	21.9	45.8	1.1
1E-39E-3-25	101.78	29.9	3.8	45.8	7.1	13.4	58.7	1.1
1E-39E-3-45	101.92	37.2	4.3	38.0	6.5	14.0	57.4	1.0
39E-3-59.4-60	102.02	36.4	5.2	34.6	7.7	16.1	51.7	0.9
1E-39E-3-85	102.20	44.1	0.0	31.6	10.9	13.4	55.8	1.0
39E-3-96.6	102.29	36.6	4.1	35.4	9.1	14.8	50.1	0.9
39E-3-119.5	102.45	36.9	4.1	37.1	7.6	14.4	54.7	1.1
1E-39E-3-140	102.59	36.5	0.0	39.6	7.5	16.4	53.2	1.1
39E	102.65	35.2	4.7	38.4	6.4	15.3	53.6	1.2
1E-40E-1-5	102.69	32.0	5.0	39.1	8.2	15.7	55.8	0.9
1E-40E-1-25	102.84	38.8	0.0	34.1	7.7	19.5	51.2	1.1
1E-40E-1-45	102.99	54.4	0.0	0.0	10.5	35.2	53.0	1.0

(continued)

APPENDIX A. MINERALOGY, INORGANIC, AND ORGANIC CARBON CONTENT, BL00-1 (continued)

Sample #	Depth (m blf)	Quartz (%)	Plag. (%)	Arag. (%)	Dolo. (%)	Calcite (%)	CaCO ₃ (%)	Organic carbon (%)
40E-1-59.8-61	103.10	35.1	0.0	40.0	7.5	17.4	39.5	2.9
1E-40E-1-85	103.29	52.2	6.7	0.0	10.4	30.7	54.9	1.3
1E-40E-1-105	103.45	31.1	0.0	0.0	4.1	64.8	49.1	1.5
40E-1-130-130.8	103.63	33.1	3.8	0.0	3.8	59.3	29.2	2.8
1E-40E-1-145	103.75	36.3	3.9	0.0	5.4	54.4	35.4	1.4
40E-2-32	104.03	43.6	4.0	0.0	5.5	46.9	25.3	1.7
40E-2-45.1	104.13	39.7	3.5	0.0	4.7	52.1	30.1	1.5
40E	104.90	53.3	4.8	0.0	6.5	35.4	22.1	0.6
41E-2-79.6	105.62	56.6	4.5	0.0	6.4	32.5	22.4	0.4
41E-2-129	105.95	37.4	4.9	0.0	5.0	52.7	19.6	3.0
41E-3-111.9	106.84	39.7	4.1	0.0	4.7	51.4	17.2	2.6
41E	107.15	41.4	3.5	0.0	4.6	50.5	30.5	1.3
42E-1-33-34	107.40	46.1	4.3	0.0	5.4	44.1	25.2	1.0
42E-2-99.4-100.5	107.90	41.1	3.7	0.0	4.9	50.3	21.7	0.8
1E-42E-2-5	108.32	45.1	0.0	0.0	5.2	49.6	24.7	1.2
1E-42E-2-25	108.47	51.5	4.8	0.0	6.3	37.4	19.1	0.8
42E-2-52.8	108.68	32.6	3.6	0.0	3.5	60.3	24.6	3.5
1E-42E-2-70	108.81	33.7	4.0	0.0	3.7	58.6	35.6	1.4
1E-42E-2-100	109.04	23.1	3.4	0.0	5.6	67.9	50.0	1.4
42E-2-122.9	109.21	35.2	3.4	0.0	3.5	57.9	26.0	2.8
1E-42E-2-141	109.35	31.2	10.0	0.0	3.4	55.3	40.3	0.7
42E	109.40	29.1	3.9	0.0	4.7	62.3	48.4	1.2
1E-43E-1-4	109.43	47.2	0.0	0.0	6.9	45.9	24.5	1.2
1E-43E-1-24	109.58	28.0	3.2	0.0	3.7	65.2	53.8	1.6
1E-43E-1-45	109.73	31.5	0.0	0.0	3.6	64.9	39.5	1.2
1E-43E-1-65	109.87	24.5	0.0	0.0	4.0	71.6	47.1	1.1
1E-43E-1-85	110.02	30.5	3.4	0.0	3.8	62.2	37.4	1.1
1E-43E-1-104	110.16	31.6	0.0	0.0	3.9	64.6	38.2	1.5
1E-43E-1-124	110.31	72.2		15.3	12.5	0.0	57.0	1.4
1E-43E-1-145	110.46	19.0	0.0	3.6	3.2	74.2	62.0	1.6
1E-43E-2-4	110.53	83.4	0.0	0.0	16.7	0.0	63.3	1.2
1E-43E-2-24	110.68	25.7	0.0	0.0	3.4	70.9	47.9	0.8
1E-43E-2-44	110.82	25.8	0.0	0.0	3.2	71.0	50.8	0.9
43E-2-49.2-49.9	110.86	21.5	2.5	0.0	3.2	72.8	54.9	1.0
1E-43E-2-64	110.97	17.4	0.0	5.0	3.4	74.2	65.1	1.1
1E-43E-2-84	111.11	16.6	3.3	0.0	3.5	76.6	65.9	1.1
1E-43E-2-104	111.26	18.6	0.0	0.0	3.9	77.5	65.3	1.1
1E-43E-2-124	111.41	71.1	13.7	0.0	15.3	0.0	64.0	1.3
1E-43E-2-144	111.55	19.5		0.0	4.8	75.7	61.8	1.3
43E	111.65	25.3	2.3	0.0	3.1	69.3	60.3	1.4
42E-2-59.9	113.20	38.1	5.5	0.0	6.2	50.3	35.0	1.1
44E	113.90	38.9	3.8	0.0	6.4	50.9	36.6	1.1
45E-2-69.5-70.4	114.54	37.2	3.6	0.0	4.5	54.8	37.6	1.4
45E-2-129-130.2	114.94	43.1	4.7	0.0	6.3	46.0	30.3	2.0
45E-3-3.1	115.11	54.7	6.2	0.0	10.5	28.6	18.7	1.5
45E-3-32.8	115.31	61.2	7.1	0.0	11.2	20.6	13.5	0.7
45E-3-132.8	115.99	57.1	5.3	0.0	7.2	30.4	18.1	3.6
45E	116.15	66.4	10.5	0.0	7.8	15.3	18.3	1.0
46E-1-81.2-82.1	116.76	59.5	9.1	0.0	8.3	23.1	13.8	
46E-1-140.8-141.3	117.21	81.5	18.5	0.0	0.0	0.0		
46E-2-91.1	117.97	56.7	4.8	0.0	6.5	32.0	19.3	2.4
46E	118.40	52.8	4.8	0.0	6.2	36.3	21.3	1.0
47E-2-29.5-30.6	118.74	51.0	4.6	0.0	5.6	38.9	7.3	1.7
47E-2-64.8-65.8	118.98	57.1	4.0	0.0	7.3	31.5	18.3	1.1
47E-3-80	120.12	40.3	3.9	0.0	4.5	51.3	27.7	1.6
47E-3-144.9	120.57	29.5	3.9	0.0	3.7	62.9	35.8	0.8
47E	120.65	32.1	3.1	0.0	4.4	60.4	40.3	0.9

Note: Mineralogic composition based on X-ray diffraction peak intensities and are approximations only. Organic and inorganic carbon contents are based on coulometry.

APPENDIX B. OXYGEN, CARBON, AND STRONTIUM ISOTOPIC RATIOS OF BULK SEDIMENT AND OSTROCODES, BL00-1

Bulk-sediment carbonate											
Depth (m bif)	$\delta^{18}\text{O}$ (‰VPDB)	$\delta^{13}\text{C}$ (‰VPDB)	Depth (m bif)	$\delta^{18}\text{O}$ (‰VPDB)	$\delta^{13}\text{C}$ (‰VPDB)	Depth (m bif)	$\delta^{18}\text{O}$ (‰VPDB)	$\delta^{13}\text{C}$ (‰VPDB)	Depth (m bif)	$\delta^{18}\text{O}$ (‰VPDB)	$\delta^{13}\text{C}$ (‰VPDB)
0.20	-4.0	3.2	29.10	-9.7	-0.5	43.76	-11.1	-3.2	58.20	-10.6	-2.2
0.50	-3.6	3.3	29.50	-11.5	-0.2	44.20	-10.7	-2.7	58.55	-10.8	-2.0
0.80	-3.9	2.9	29.90	-11.4	0.2	44.90	-10.3	-0.1	58.80	-11.0	-1.2
1.20	-3.9	3.1	30.20	-10.9	0.4	45.20	-10.3	-0.7	59.00	-8.7	1.6
1.47	-4.4	3.2	30.40	-10.1	0.3	45.40	-10.0	-1.0	59.36	-8.7	1.9
2.20	-4.4	2.9	30.80	-10.4	-0.3	45.80	-10.4	-2.1	59.70	-11.1	-2.1
2.50	-4.8	2.7	31.20	-10.6	-0.2	46.10	-9.9	-3.5	60.00	-9.0	1.5
2.85	-5.5	2.4	31.50	-11.0	1.2	46.35	-8.7	1.4	60.19	-9.4	-0.4
3.20	-5.6	2.5	31.80	-10.7	1.0	46.70	-8.5	1.6	60.40	-9.6	-1.6
3.40	-5.4	2.6	32.20	-10.6	0.2	47.00	-8.7	1.2	60.70	-8.9	0.4
3.70	-5.2	2.7	32.50	-10.5	0.3	47.20	-9.4	0.6	61.08	-10.5	-1.3
3.97	-5.6	2.7	32.80	-10.4	0.9	47.62	-9.8	-1.4	61.40	-5.7	2.4
4.40	-5.9	2.4	33.20	-10.3	0.1	47.90	-9.8	-0.9	61.70	-5.1	2.9
5.20	-5.3	2.5	33.60	-9.8	-0.3	48.30	-8.9	0.6	61.95	-4.5	3.3
5.50	-5.2	2.7	34.00	-9.6	0.5	48.55	-9.1	0.5	62.40	-4.5	3.6
5.90	-5.6	2.4	34.30	-10.0	-0.6	48.90	-9.7	-3.6	62.84	-4.5	3.6
6.15	-5.5	2.4	34.60	-9.5	-1.2	49.20	-9.0	0.3	63.10	-6.0	2.4
6.60	-6.3	2.0	34.90	-8.6	2.6	49.47	-9.7	-2.7	63.40	-6.9	1.8
6.90	-7.8	1.3	35.20	-9.3	0.3	49.80	-9.1	0.9	63.72	-11.5	-1.6
7.15	-8.4	0.4	35.50	-9.9	1.0	50.20	-9.6	0.3	64.10	-7.9	1.3
7.60	-7.5	2.2	35.70	-9.5	-0.8	50.50	-10.3	0.0	64.40	-4.5	7.4
8.00	-5.1	2.7	36.10	-9.5	-0.1	50.80	-10.4	0.5	64.55	-3.7	3.8
8.25	-6.2	2.2	36.45	-9.6	-0.3	51.20	-9.8	0.8	65.00	-4.5	3.1
8.60	-7.5	1.0	36.80	-9.7	1.8	51.45	-9.3	1.3	65.37	-4.7	3.1
8.90	-7.6	1.1	37.10	-7.7	5.9	51.90	-7.4	0.9	65.70	-5.3	2.5
9.25	-11.0	-1.0	37.54	-10.1	-0.8	52.20	-8.6	0.9	66.00	-5.3	3.1
9.70	-11.3	-1.1	37.90	-9.8	-2.2	52.45	-8.8	0.9	66.21	-4.5	3.5
10.00	-10.8	-0.7	38.20	-9.0	0.8	52.80	-7.8	1.0	66.50	-4.8	3.4
10.26	-8.7	-2.2	38.50	-8.5	2.4	53.20	-8.8	0.5	66.70	-4.3	3.7
10.60	-9.7	-1.7	38.65	-8.7	2.1	53.55	-9.7	-0.1	67.07	-3.8	3.8
10.80	-8.6	-2.2	39.00	-9.7	-2.1	53.80	-10.3	-0.7	67.40	-6.7	3.4
11.20	-9.3	-3.1	39.30	-9.9	-2.7	54.00	-11.4	-1.3	67.60	-8.7	0.4
11.45	-9.3	-2.1	39.60	-10.1	-2.5	54.36	-12.5	-2.2	67.92	-9.0	-0.2
11.80	-9.4	-2.9	40.00	-9.3	-0.1	54.80	-12.5	-3.5	68.20	-6.8	1.8
12.10	-9.5	-2.5	40.40	-9.2	-0.2	55.20	-10.9	-0.8	68.50	-7.8	-1.5
12.45	-10.1	-2.2	40.60	-9.0	0.4	55.50	-8.2	1.9	68.74	-6.6	4.4
12.70	-10.1	-2.5	41.00	-8.9	0.3	55.70	-9.3	0.6	69.10	-7.0	-0.3
13.00	-8.5	-1.9	41.50	-8.4	0.4	56.10	-9.6	-0.5	69.48	-8.8	-1.9
13.20	-9.6	-2.7	41.75	-8.0	0.2	56.30	-11.5	-2.3	69.90	-7.2	3.1
13.50	-9.4	-2.8	42.30	-12.7	-3.2	56.60	-7.2	1.2	70.22	-6.8	-1.7
13.80	-9.6	-2.9	42.60	-12.9	-3.3	56.86	-9.8	0.6	70.60	-7.4	4.7
14.10	-9.7	-2.6	42.76	-12.6	-3.1	57.20	-9.7	-0.5	71.06	-9.2	-0.3
14.40	-9.6	-2.5	43.10	-11.5	-3.7	57.40	-9.4	-1.3	71.40	-9.5	-0.3
14.70	-9.6	-2.5	43.50	-10.7	-3.1	57.72	-10.4	-1.3	71.70	-9.2	0.9

(continued)

APPENDIX B. OXYGEN, CARBON, AND STRONTIUM ISOTOPIIC RATIOS OF BULK SEDIMENT AND OSTRACODES, BL00-1 (continued)

Bulk-sediment carbonate										Cytherissa		
Depth (m blf)	$\delta^{18}\text{O}$ (‰VPDB)	$\delta^{13}\text{C}$ (‰VPDB)	Depth (m blf)	$\delta^{18}\text{O}$ (‰VPDB)	$\delta^{13}\text{C}$ (‰VPDB)	Depth (m blf)	$\delta^{18}\text{O}$ (‰VPDB)	$\delta^{13}\text{C}$ (‰VPDB)	Depth (m blf)	$\delta^{18}\text{O}$ (‰VPDB)	$\delta^{13}\text{C}$ (‰VPDB)	
71.87	-9.7	-0.1	85.68	-9.8	-1.1	99.70	-10.2	-3.2	113.42	-10.6	0.0	
72.30	-9.2	0.2	86.10	-10.1	-1.8	100.04	-10.7	-0.1	113.70	-10.3	0.0	
72.72	-9.7	-0.9	86.45	-10.4	-1.6	100.40	-10.0	-0.8	113.90	-10.0	0.7	
73.00	-9.8	-1.1	86.70	-10.5	-0.1	100.80	-11.8	-0.8	114.21	-10.3	0.2	
73.20	-10.1	-1.1	86.90	-9.4	-2.9	101.20	-11.0	-1.5	114.50	-10.1	0.9	
73.48	-9.5	-1.1	87.22	-10.4	-2.4	101.52	-9.8	0.6	114.89	-9.1	2.4	
73.90	-9.0	0.1	87.99	-9.5	-2.6	101.80	-7.9	2.6	115.10	-9.5	0.4	
74.24	-9.3	-1.2	88.40	-9.5	-3.0	102.23	-7.8	2.2	115.30	-9.9	-0.8	
74.50	-9.6	-1.6	88.73	-11.3	-1.8	102.70	-7.4	2.3	115.56	-8.7	2.8	
74.80	-8.4	1.1	89.10	-10.0	-2.9	103.03	-8.3	0.4	116.00	-9.6	0.6	
74.99	-9.4	-1.5	89.47	-10.5	-0.8	103.30	-8.0	0.4	116.30	-10.0	-1.4	
75.30	-9.2	-1.4	89.70	-9.8	-1.8	103.74	-11.7	-0.8	116.60	-10.5	-2.9	
75.50	-8.9	-0.1	90.00	-10.3	-1.1	104.00	-12.0	-1.1	117.05	-9.6	-1.9	
75.80	-9.2	-2.3	90.27	-11.0	-1.4	104.20	-11.4	-0.9	117.81	-8.7	1.2	
76.10	-8.1	2.1	90.50	-10.3	-0.3	104.54	-11.2	-1.1	118.10	-8.9	-0.5	
76.54	-9.2	-2.4	90.80	-10.7	-1.4	104.90	-10.0	-2.5	118.40	-9.5	-1.3	
76.70	-9.3	-2.7	91.03	-10.2	-0.6	105.29	-10.4	-1.9	118.61	-9.5	-0.8	
77.00	-9.4	-2.4	91.30	-10.7	-0.9	105.60	-10.6	-1.4	119.00	-10.1	-2.7	
77.29	-9.1	-1.8	91.60	-10.6	-0.9	105.96	-9.4	0.7	119.30	-11.0	-2.6	
77.50	-9.1	-2.2	91.84	-10.2	-0.5	106.30	-11.0	-0.2	119.70	-11.9	-2.9	
77.80	-9.1	-1.8	92.10	-9.9	-0.1	106.63	-12.0	-1.6	119.98	-13.0	-2.7	
78.04	-8.8	-2.0	92.40	-9.9	-1.2	106.90	-10.0	0.2	120.30	-13.2	-3.0	
78.40	-9.6	-1.1	92.57	-9.9	-2.4	107.20	-11.6	-0.6	120.59	-12.8	-1.7	
78.83	-8.8	-0.1	92.80	-9.3	-1.8	107.36	-11.7	-1.3				
79.20	-10.0	-0.4	93.10	-9.3	-2.6	107.70	-11.8	-1.4				
79.57	-9.7	0.8	93.27	-9.5	-2.0	107.90	-12.2	-2.3				
80.00	-9.8	-0.1	93.60	-9.4	-1.8	108.12	-12.0	-1.5				
80.31	-9.5	1.5	93.96	-9.3	-0.7	108.40	-11.6	-2.0				
80.70	-9.8	2.0	94.20	-9.7	-0.7	108.74	-11.0	-1.1				
81.10	-10.3	2.1	94.50	-9.1	0.2	109.10	-10.0	0.5				
81.50	-9.7	-0.8	94.74	-9.9	-1.4	109.40	-10.9	-0.8				
81.87	-9.2	-1.0	95.00	-9.5	-1.0	109.69	-11.8	-0.9				
82.20	-9.5	-1.7	95.20	-9.3	0.3	110.00	-12.1	-1.5				
82.62	-10.2	-1.5	95.49	-10.1	-2.8	110.42	-8.2	1.3				
82.90	-9.6	0.3	96.27	-9.2	-2.1	110.70	-8.9	0.6				
83.00	-9.5	-1.9	96.70	-10.1	-3.9	110.90	-9.6	-0.1				
83.41	-9.2	-1.2	96.99	-9.5	-2.0	111.16	-8.3	0.6				
83.70	-10.3	-0.1	97.30	-9.4	-2.1	111.50	-9.1	0.3				
83.90	-7.5	5.9	97.73	-10.0	0.0	111.70	-8.8	0.4				
84.14	-9.8	-1.2	98.00	-9.9	1.6	111.94	-8.5	0.8				
84.50	-9.9	-2.0	98.20	-10.7	2.2	112.30	-12.1	-1.4				
84.87	-10.5	-1.8	98.54	-10.0	-0.5	112.67	-11.8	-0.5				
85.20	-9.8	-1.4	98.90	-10.1	-0.7	113.00	-10.4	0.4				
85.50	-10.0	-2.2	99.31	-9.9	-0.1	113.20	-10.8	0.2				

(continued)

APPENDIX B. OXYGEN, CARBON, AND STRONTIUM ISOTOPIC RATIOS OF BULK SEDIMENT AND OSTROCODES, BL00-1 (continued)

Candona				Soluble Sr isotopes				Residue Sr isotopes	
Depth (m bif)	$\delta^{18}\text{O}$ (‰VPDB)	$\delta^{13}\text{C}$ (‰VPDB)	Depth (m bif)	$\delta^{18}\text{O}$ (‰VPDB)	$\delta^{13}\text{C}$ (‰VPDB)	Depth (m bif)	$^{87}\text{Sr}/^{86}\text{Sr}$	Depth (m bif)	$^{87}\text{Sr}/^{86}\text{Sr}$
0.5	-2.2	-5.2	52.5	-3.7	-1.7	1.20	0.71039	113.20	0.70950
1.5	-2.5	-5.2	53.6	-3.0	-2.5	3.40	0.71030	115.31	0.70990
2.9	-2.0	-3.1	54.4	-8.5	-5.9	5.51	0.71024	117.21	0.70970
4.0	-2.4	-3.8	55.2	-6.9	-5.0	6.40	0.71010	118.10	0.70965
4.0	-1.7	-4.7	56.1	-2.5	-3.5	7.20	0.70943	118.98	0.70950
6.2	-2.0	-5.4	56.9	-6.1	-2.7	7.96	0.70995		
7.2	-2.5	-4.3	59.4	-4.3	-1.4	8.30	0.71017	63.7	0.71095
8.3	-1.1	-4.9	61.1	-7.8	-3.4	9.40	0.71000	62.4	0.71124
9.3	-6.3	-5.4	62.8	-3.5	-9.2	10.80	0.71004	8.3	0.71149
10.3	-8.4	-5.2	65.4	-1.9	-5.5	11.50	0.70994	95.5	0.71169
12.5	-9.8	-4.8	66.2	-4.8	-0.4	12.40	0.71000	65.7	0.71189
16.7	-9.7	-4.7	67.1	-1.1	-5.4	12.50	0.71013	118.0	0.71431
17.9	-8.7	-3.3	67.9	-6.2	-4.3	13.80	0.71016	102.7	0.71566
19.0	-12.5	-6.2	70.2	-8.6	-2.2	14.10	0.71019	71.9	0.71621
20.0	-9.4	-3.4	71.1	-8.4	-2.6	14.70	0.71018	12.5	0.71829
21.0	-7.1	-3.1	72.7	-6.3	-1.6	15.40	0.70990	78.8	0.71847
22.0	-8.8	-6.3	78.0	-12.7	-7.4	16.86	0.71016	108.1	0.71920
23.0	-6.4	-2.5	81.1	-5.7	-0.2	18.40	0.71000	13.8	0.71932
24.1	-6.6	-3.5	83.4	-8.0	-1.2	19.66	0.71003	14.7	0.72055
25.1	-12.3	-6.5	84.9	-8.3	-2.1	21.40	0.70990	11.5	0.72944
26.0	-10.0	-5.0	85.7	-6.7	-2.2	23.10	0.70962	68.7	0.73443
27.0	-7.1	-1.7	88.0	-13.2	-6.8	24.40	0.70960		
28.0	-6.5	-4.0	88.0	-13.8	-5.6	26.15	0.70965	76.97	0.70960
29.1	-7.2	-4.7	97.7	-5.7	-1.5	27.40	0.70990	77.77	0.70969
30.2	-7.1	-4.9	101.5	-4.4	-2.1	28.60	0.70984	78.80	0.70972
31.2	-7.7	-4.4	102.2	-1.3	-4.5	30.40	0.70980	79.47	0.70990
32.2	-7.7	-4.7	103.0	-2.1	-2.2	31.71	0.70976	80.41	0.71002
33.2	-7.1	-2.7	105.3	-8.9	-3.7	33.40	0.70990	81.97	0.70980
34.3	-6.8	-3.8	107.4	-8.8	-4.5	35.24	0.71000	84.47	0.70990
35.5	-6.0	-2.0	108.1	-8.4	-3.6	36.40	0.71000	86.47	0.70950
36.5	-6.3	-2.0	110.4	-2.3	-1.4	38.63	0.70996	88.47	0.70960
37.5	-8.5	-3.7	111.2	-3.1	-1.7	42.40	0.70940	88.70	0.70941
38.7	-3.3	-1.7	111.9	-2.6	-1.8	42.90	0.70956	90.47	0.70970
39.6	-4.9	-3.7	117.1	-5.9	-1.4	43.79	0.70958	92.47	0.70990
40.6	-7.6	-2.6	117.8	-4.6	-0.7	45.40	0.70990	94.83	0.70996
41.8	-2.4	-3.8	119.3	-10.5	-5.5	47.30	0.71000	95.50	0.70988
42.8	-9.1	-6.8				48.36	0.70977	96.47	0.70980
43.8	-12.0	-8.3				49.71	0.70984	100.47	0.70960
44.9	-5.8	-2.5				51.36	0.71000	102.29	0.70970
45.8	-7.5	-3.7				52.52	0.71005	102.70	0.70995
46.4	-7.8	-4.0				54.36	0.70950	104.03	0.70940
47.6	-3.9	-2.1				54.50	0.70943	105.62	0.70970
48.6	-5.7	-3.3				55.60	0.71018	108.10	0.70932
49.5	-9.7	-5.3				57.36	0.70990	108.68	0.70970
								110.86	0.70920

Note: m bif—meters below lake floor; VPDB—Vienna Pee Dee Belemnite.

APPENDIX C. OSTRACODE FAUNA FROM BL00-1

Depth (m blf)	Wt (g)	C sp. 1 (vpg)	C sp. 2 (vpg)	C sp. 3 (vpg)	C sp. 4 (vpg)	C sp. 5 (vpg)	C sp. 7 (vpg)	Cyth lac (vpg)	Unk sp (vpg)	Limno 1 (vpg)	Total (vpg)	Juvenile Limno	Juvenile Cyth
0.5	9.1	2.1	6.4	3.0	0.2	0.7	0.2	0.0	1.4	0.4	14.4	x	
1.5	9.7	2.5	9.3	0.8	0.4	0.0	0.3	0.0	0.0	0.2	13.5		
2.9	8.2	1.1	0.0	0.0	1.1	0.0	0.1	0.0	0.1	0.5	2.9		
4.0	12.0	2.1	0.1	0.1	0.8	0.0	0.0	0.0	0.0	0.0	3.1	x	
6.2	13.4	1.3	0.8	0.1	0.6	0.0	0.2	0.0	0.0	0.1	3.2		
7.2	14.6	2.1	0.3	0.1	0.0	0.0	0.1	0.0	0.0	0.0	2.5		
8.3	18.9	1.7	1.6	0.1	0.1	0.0	0.1	0.0	0.0	0.1	3.6	x	
9.3	26.7	2.2	0.0	0.0	0.0	0.0	0.0	0.0	0.0	0.0	2.2		
10.3	38.8	0.4	0.0	0.0	0.0	0.0	0.0	0.0	0.0	0.0	0.4		
11.5	62.8	0.0	0.0	0.0	0.0	0.0	0.0	0.0	0.0	0.0	0.0		
12.5	62.3	0.3	0.0	0.0	0.0	0.0	0.0	0.0	0.0	0.0	0.4		
13.5	69.5	0.1	0.0	0.0	0.0	0.0	0.0	0.0	0.0	0.0	0.1		
14.7	61.0	0.0	0.0	0.0	0.0	0.0	0.0	0.0	0.0	0.0	0.0		
15.7	57.4	0.0	0.0	0.0	0.0	0.0	0.0	0.0	0.0	0.0	0.0		
16.7	66.8	0.4	0.1	0.0	0.0	0.2	0.0	0.0	0.0	0.0	0.8		
17.9	60.6	0.5	0.0	0.0	0.0	0.0	0.0	0.0	0.0	0.0	0.5		
19.0	64.9	0.2	0.1	0.0	0.0	0.0	0.0	0.1	0.0	0.0	0.4		
20.0	50.5	1.0	0.0	0.2	0.0	0.0	0.0	0.0	0.0	0.0	1.2		
21.0	54.4	1.0	0.0	0.3	0.0	0.0	0.0	0.0	0.0	0.0	1.3		
22.0	65.3	0.5	0.0	0.0	0.0	0.0	0.0	0.1	0.0	0.0	0.6		
23.0	49.7	1.3	0.0	0.2	0.0	0.7	0.0	0.0	0.0	0.0	1.4		x
24.1	49.2	1.7	0.0	0.2	0.0	0.0	0.0	0.0	0.0	0.0	1.9		
25.1	71.5	0.6	0.0	0.0	0.0	0.0	0.0	0.0	0.0	0.0	0.7		
26.0	59.9	0.4	0.0	0.0	0.0	0.0	0.0	0.0	0.0	0.0	0.4		
27.0	50.1	0.2	0.0	0.0	0.0	0.0	0.0	0.0	0.0	0.0	0.2		
28.0	48.7	0.9	0.0	0.0	0.0	0.0	0.0	0.0	0.0	0.0	0.9		
29.1	45.2	0.2	0.0	0.0	0.0	0.0	0.0	0.0	0.0	0.0	0.2		
30.2	56.4	1.8	0.0	0.1	0.0	0.0	0.0	0.0	0.0	0.0	1.8		
31.2	58.1	1.7	0.0	0.1	0.0	0.0	0.0	0.0	0.0	0.0	1.7		
32.2	50.8	0.4	0.0	0.1	0.0	0.0	0.0	0.0	0.0	0.0	0.5		
33.2	51.2	0.8	0.0	0.2	0.0	0.0	0.0	0.0	0.0	0.0	1.0		
34.3	56.0	0.4	0.0	0.0	0.0	0.0	0.0	0.0	0.0	0.0	0.4		
35.5	51.5	0.4	0.0	0.1	0.0	0.0	0.0	0.0	0.0	0.0	0.4		
36.5	51.3	0.9	0.0	0.1	0.0	0.0	0.0	0.0	0.0	0.0	1.1		
37.5	65.2	0.4	0.0	0.2	0.0	0.0	0.0	0.0	0.0	0.0	0.6		
38.7	47.1	0.7	0.0	0.0	0.0	0.0	0.0	0.0	0.0	0.0	0.7	x	
39.6	48.4	0.5	0.0	0.1	0.0	0.0	0.0	0.0	0.0	0.0	0.6		
40.6	48.9	0.9	0.0	0.1	0.0	0.0	0.0	0.0	0.0	0.0	1.1		
41.8	60.1	1.3	0.0	0.4	0.0	0.0	0.0	0.0	0.0	0.0	1.7	x	
42.8	49.0	0.1	0.0	0.1	0.0	0.0	0.0	0.0	0.1	0.0	0.3		
43.8	64.2	0.4	0.0	0.0	0.0	0.0	0.0	0.0	0.0	0.0	0.5		
44.9	57.8	0.7	0.0	0.0	0.0	0.0	0.0	0.0	0.0	0.0	0.8	x	
45.8	55.5	0.2	0.0	0.1	0.0	0.0	0.0	0.0	0.0	0.0	0.3	x	
46.4	52.4	0.9	0.0	0.0	0.0	0.0	0.0	0.0	0.0	0.0	0.9		
47.6	61.0	0.4	0.0	0.0	0.0	0.0	0.0	0.0	0.0	0.0	0.4		
48.6	54.6	0.3	0.0	0.0	0.0	0.0	0.0	0.0	0.0	0.0	0.3		
49.5	62.4	0.0	0.0	0.0	0.0	0.0	0.0	0.0	0.0	0.0	0.0	x	
50.5	50.9	0.1	0.0	0.0	0.0	0.0	0.0	0.0	0.0	0.0	0.1		
51.5	43.7	0.0	0.0	0.0	0.0	0.0	0.0	0.0	0.0	0.0	0.0		
52.5	57.7	0.3	0.0	0.0	0.0	0.0	0.0	0.0	0.0	0.0	0.3	x	
53.6	57.4	1.0	0.0	0.0	0.0	0.0	0.0	0.0	0.0	0.0	1.0	x	
54.4	48.5	0.1	0.0	0.0	0.0	0.0	0.0	0.0	0.0	0.0	0.2		
55.2	55.8	0.3	0.0	0.0	0.0	0.0	0.0	0.0	0.0	0.0	0.3	x	
56.1	64.0	0.8	0.0	0.0	0.0	0.0	0.0	0.0	0.0	0.0	0.8	x	
56.9	57.2	0.3	0.0	0.0	0.0	0.0	0.0	0.1	0.0	0.0	0.4	x	
57.7	53.5	0.0	0.0	0.0	0.0	0.0	0.0	0.0	0.0	0.0	0.0	x	
58.6	48.3	0.0	0.0	0.0	0.0	0.0	0.0	0.0	0.0	0.0	0.0		
59.4	45.0	0.2	0.0	0.0	0.0	0.0	0.0	0.2	0.0	0.0	0.4	x	
60.2	48.3	0.0	0.0	0.0	0.0	0.0	0.0	0.0	0.0	0.0	0.0	x	
61.1	55.2	0.1	0.0	0.0	0.0	0.0	0.0	0.0	0.0	0.0	0.1		
62.0	53.8	0.0	0.0	0.0	0.0	0.0	0.0	0.0	0.0	0.0	0.0	x	
62.8	49.6	0.1	0.0	0.0	0.0	0.0	0.0	0.0	0.0	0.0	0.1	x	
63.7	61.8	0.0	0.0	0.0	0.0	0.0	0.0	0.0	0.0	0.0	0.0	x	
64.6	57.0	0.0	0.4	0.0	0.0	0.0	0.0	0.0	0.0	0.0	0.4	x	
65.4	52.8	0.1	0.0	0.0	0.0	0.0	0.0	0.0	0.0	0.0	0.1	x	
66.2	47.6	0.0	0.0	0.0	0.0	0.0	0.0	0.0	0.0	0.0	0.0	x	
67.1	49.6	0.0	0.0	0.0	0.0	0.0	0.0	0.0	0.0	0.0	0.1	x	
67.9	49.3	0.0	0.0	0.0	0.0	0.0	0.0	0.0	0.0	0.0	0.0	x	
68.7	71.2	0.0	0.0	0.0	0.0	0.0	0.0	0.0	0.0	0.0	0.0	x	
69.5	53.9	0.0	0.0	0.0	0.0	0.0	0.0	0.0	0.0	0.0	0.0		x
70.2	62.4	0.0	0.0	0.0	0.0	0.0	0.0	0.0	0.0	0.0	0.1		

(continued)

APPENDIX C. OSTRACODE FAUNA FROM BL00-1 (continued)

Depth (m blf)	Wt (g)	C sp. 1 (vpg)	C sp. 2 (vpg)	C sp. 3 (vpg)	C sp. 4 (vpg)	C sp. 5 (vpg)	C sp. 7 (vpg)	Cyth lac (vpg)	Unk sp (vpg)	Limno 1 (vpg)	Total (vpg)	Juvenile Limno	Juvenile Cyth
71.1	61.9	0.0	0.0	0.0	0.0	0.0	0.0	0.0	0.0	0.0	0.0		
71.9	38.1	0.0	0.0	0.0	0.0	0.0	0.0	0.0	0.0	0.0	0.0		
72.7	60.5	0.0	0.0	0.0	0.0	0.0	0.0	0.0	0.0	0.0	0.0		
73.5	39.8	0.0	0.0	0.0	0.0	0.0	0.0	0.0	0.0	0.0	0.0		
74.2	59.5	0.0	0.0	0.0	0.0	0.0	0.0	0.0	0.0	0.0	0.0		
75.0	79.4	0.0	0.0	0.0	0.0	0.0	0.0	0.0	0.0	0.0	0.0		
75.8	62.0	0.0	0.0	0.0	0.0	0.0	0.0	0.0	0.0	0.0	0.0	x	x
76.5	67.3	0.0	0.0	0.0	0.0	0.0	0.0	0.0	0.0	0.0	0.0	x	
77.3	64.8	0.0	0.0	0.0	0.0	0.0	0.0	0.0	0.0	0.0	0.0		x
78.0	72.5	0.0	0.0	0.0	0.0	0.0	0.0	0.0	0.0	0.0	0.0		
78.8	69.5	0.0	0.0	0.0	0.0	0.0	0.0	0.0	0.0	0.0	0.0		
79.6	64.1	0.0	0.0	0.0	0.0	0.0	0.0	0.0	0.0	0.0	0.0		
80.3	64.6	0.0	0.0	0.0	0.0	0.0	0.0	0.0	0.0	0.0	0.0		
81.1	63.7	0.0	0.0	0.0	0.0	0.0	0.0	0.0	0.0	0.0	0.0	x	
81.9	71.8	0.0	0.0	0.0	0.0	0.0	0.0	0.0	0.0	0.0	0.0		
82.6	75.3	0.0	0.0	0.0	0.0	0.0	0.0	0.0	0.0	0.0	0.0		x
83.4	61.5	0.0	0.0	0.0	0.0	0.0	0.0	0.0	0.0	0.0	0.1		
84.1	59.5	0.0	0.0	0.0	0.0	0.0	0.0	0.0	0.0	0.0	0.0		
84.9	64.0	0.0	0.0	0.0	0.0	0.0	0.0	0.0	0.0	0.0	0.0		
85.7	55.3	0.0	0.0	0.0	0.0	0.0	0.0	0.0	0.0	0.0	0.0	x	x
86.5	49.9	0.0	0.0	0.0	0.0	0.0	0.0	0.0	0.0	0.0	0.0	x	
87.2	61.3	0.0	0.0	0.0	0.0	0.0	0.0	0.0	0.0	0.0	0.0		x
88.0	65.1	0.0	0.0	0.0	0.0	0.0	0.0	0.0	0.0	0.0	0.0	x	
88.7	55.2	0.0	0.0	0.0	0.0	0.0	0.0	0.0	0.0	0.0	0.0		
89.5	56.4	0.0	0.0	0.0	0.0	0.0	0.0	0.0	0.0	0.0	0.0		
90.3	63.5	0.0	0.0	0.0	0.0	0.0	0.0	0.0	0.0	0.0	0.0		
91.0	58.6	0.0	0.0	0.0	0.0	0.0	0.0	0.0	0.0	0.0	0.0		
91.8	57.4	0.0	0.0	0.0	0.0	0.0	0.0	0.0	0.0	0.0	0.0		
92.6	61.6	0.0	0.0	0.0	0.0	0.0	0.0	0.0	0.0	0.0	0.0		
93.3	60.5	0.0	0.0	0.0	0.0	0.0	0.0	0.0	0.0	0.0	0.0		x
94.0	69.8	0.0	0.0	0.0	0.0	0.0	0.0	0.0	0.0	0.0	0.0		x
94.7	68.7	0.0	0.0	0.0	0.0	0.0	0.0	0.0	0.0	0.0	0.0		
95.5	58.8	0.0	0.0	0.0	0.0	0.0	0.0	0.0	0.0	0.0	0.0		
96.3	66.7	0.0	0.0	0.0	0.0	0.0	0.0	0.0	0.0	0.0	0.0		
97.0	53.3	0.0	0.0	0.0	0.0	0.0	0.0	0.0	0.0	0.0	0.0		
97.7	55.3	0.0	0.0	0.0	0.0	0.0	0.0	0.0	0.0	0.0	0.0	x	
98.5	74.6	0.0	0.0	0.0	0.0	0.0	0.0	0.0	0.0	0.0	0.0		x
99.3	69.2	0.0	0.0	0.0	0.0	0.0	0.0	0.4	0.0	0.0	0.4		
100.0	47.3	0.0	0.0	0.0	0.0	0.0	0.0	0.0	0.0	0.0	0.0		
100.8	55.2	0.0	0.0	0.0	0.0	0.0	0.0	0.0	0.0	0.0	0.0		
101.5	64.9	0.0	0.0	0.0	0.0	0.0	0.0	0.0	0.0	0.0	0.0		
102.2	66.2	0.1	0.0	0.0	0.0	0.0	0.0	0.0	0.0	0.0	0.1	x	
103.0	56.4	0.0	0.0	0.0	0.0	0.0	0.0	0.0	0.0	0.0	0.0	x	
103.7	66.4	0.0	0.0	0.0	0.0	0.0	0.0	0.0	0.0	0.0	0.0		
104.5	49.5	0.0	0.0	0.0	0.0	0.0	0.0	0.0	0.0	0.0	0.0		
105.3	63.6	0.0	0.0	0.0	0.0	0.0	0.0	0.0	0.0	0.0	0.0	x	
106.0	43.5	0.0	0.0	0.0	0.0	0.0	0.0	0.0	0.0	0.0	0.0		
106.6	60.8	0.0	0.0	0.0	0.0	0.0	0.0	0.0	0.0	0.0	0.0		
107.4	55.6	0.0	0.0	0.0	0.0	0.0	0.0	0.0	0.0	0.0	0.0		
108.1	56.1	0.0	0.0	0.0	0.0	0.0	0.0	0.0	0.0	0.0	0.0		
108.7	64.1	0.0	0.0	0.0	0.0	0.0	0.0	0.0	0.0	0.0	0.0		x
109.7	68.5	0.0	0.0	0.0	0.0	0.0	0.0	0.0	0.0	0.0	0.0		x
110.4	40.0	0.0	0.0	0.0	0.0	0.0	0.0	0.6	0.0	0.0	0.7	x	
111.2	57.4	0.0	0.0	0.0	0.0	0.0	0.0	0.4	0.0	0.0	0.5	x	
111.9	55.5	0.0	0.0	0.0	0.0	0.0	0.0	0.0	0.0	0.0	0.0	x	x
112.7	38.7	0.0	0.0	0.0	0.0	0.0	0.0	0.0	0.0	0.0	0.0		x
113.4	49.7	0.0	0.0	0.0	0.0	0.0	0.0	0.0	0.0	0.0	0.0		x
114.2	46.4	0.0	0.0	0.0	0.0	0.0	0.0	0.0	0.0	0.0	0.0		
114.9	37.2	0.0	0.0	0.0	0.0	0.0	0.0	0.1	0.0	0.0	0.1		
115.6	37.6	0.0	0.0	0.0	0.0	0.0	0.0	0.0	0.0	0.0	0.0		
116.3	46.3	0.0	0.0	0.0	0.0	0.0	0.0	0.0	0.0	0.0	0.0		x
117.1	45.0	0.0	0.0	0.0	0.0	0.0	0.0	0.2	0.0	0.0	0.2		
117.8	31.9	0.0	0.0	0.0	0.0	0.0	0.0	0.0	0.0	0.0	0.0		
118.6	48.2	0.0	0.0	0.0	0.0	0.0	0.0	0.0	0.0	0.0	0.0		
119.3	43.3	0.0	0.0	0.0	0.0	0.0	0.0	0.0	0.0	0.0	0.0	x	
120.0	56.0	0.0	0.0	0.0	0.0	0.0	0.0	0.0	0.0	0.0	0.0		
120.6	45.6	0.0	0.0	0.0	0.0	0.0	0.0	0.0	0.0	0.0	0.0		x

Note: C—*Candona*; Cyth lac—*Cytherissa lacustris*; Unk—unknown; vpg—valves per gram of sediment; x—present. Photo documentation of endemic species in Bright et al. (2005).

APPENDIX D. DIATOM FLORA FROM BL00-1

				Benthic Taxa			
Sample ID	Depth	Comments	No. of diatoms counted	No. of spp. not including unid	Simpson reciprocal index	<i>Achnanthes curtissima</i>	
<i>Core catcher samples</i>							
1E-26E	1.72		498	22	1.0	0.0	
1E-27E	4.97		634	45	4.9	0.5	
1E-28E	8.02		541	25	1.1	0.0	
1E-29E	11.01	no visible diatoms or pieces	1	0	0.0	0.0	
1E-30E	14.03	no visible diatoms or pieces	1	0	0.0	0.0	
1E-31E	17.04	no visible diatoms or pieces	1	0	0.0	0.0	
1E-32E	20.09		372	12	1.3	0.0	
1E-33E	23.07		563	19	2.9	0.0	
1E-34E	26.10		680	6	1.1	0.0	
1E-35E	29.09		619	19	1.5	0.0	
1E-36E	32.09		622	25	2.3	0.0	
1E-37E	35.09		570	18	1.7	0.5	
1E-38E	38.08	few diatoms	1	0	0.0	0.0	
1E-39E	41.09		610	33	4.6	0.3	
1E-40E	43.90	no visible diatoms or pieces	1	0	0.0	0.0	
1E-41E	47.10		558	25	4.2	0.4	
1E-42E	50.09		571	29	4.2	0.0	
1E-43E	52.99		595	41	5.4	1.0	
1E-44E	55.60		536	38	7.1	0.4	
1E-45E	58.10	no visible diatoms or pieces	1	0	0.0	0.0	
1E-46E	60.60		527	37	3.4	0.4	
1E-22E	63.10	dissolution of some cells present, mostly on broken diatoms	417	15	0.8	0.0	
1E-23E	65.60	no visible diatoms or pieces	1	0	0.0	0.0	
1E-24E	68.10	very small pieces, some dissolution evident	1	0	0.0	0.0	
1E-25E	70.61	no visible diatoms or pieces	1	0	0.0	0.0	
1E-26E	76.32	very few diatoms, mostly <i>Stephanodiscus</i> and small fragilaroid, some dissolution	NA				
1E-27E	76.90	no diatoms, no pieces	NA				
1E-28E	79.43	no diatoms, no pieces	NA				
1E-29E	81.91	some diatoms, mostly small fragilaroid and <i>Stephanodiscus</i> , lots of cysts	NA				
1E-30E	84.42	very sparse, mostly small fragilaroid	NA				
1E-31E	86.42	very few diatoms, mostly <i>Stephanodiscus</i> and small fragilaroid, some dissolution	NA				
1E-32E	88.43	very sparse, centrics and pennates, mostly broken, some dissolution	NA				
1E-33E	90.42	abundant diatoms, both centrics and pennates, very diverse	NA				
1E-34E	92.43	abundant diatoms, both centrics and pennates, very diverse	NA				
1E-35E	94.43	abundant diatoms, mostly planktonic, dissolution and breakage present	NA				
1E-36E	96.43	sparse diatoms	NA				
1E-37E	98.42	sparse diatoms, mostly small fragilaroid, dissolution present	NA				
1E-38E	100.43	abundant diatoms and cysts, many <i>Stephanodiscus</i> and <i>Aulacoseira (granulata?)</i>	NA				
1E-39E	102.20	abundant <i>Stephanodiscus</i>	NA				
1E-40E	104.50	abundant <i>Stephanodiscus</i>	NA				
1E-41E	106.00	abundant <i>Stephanodiscus</i>	NA				
1E-42E	108.10	abundant diatoms, mostly small fragilaroid, few centrics	NA				
1E-43E	110.40	abundant diatoms, both pennates and centrics, very diverse	NA				
1E-44E	113.40	abundant diatoms, both <i>Fragilaria</i> and a few centrics	NA				
1E-45E	114.90	no diatoms, no pieces	NA				
1E-46E	117.80	abundant diatoms, many big centrics and <i>Aulacoseira</i>	NA				
<i>Non-core catcher</i>							
1H-1 50-54	0.50	many broken pieces, mostly <i>Navicula oblonga</i> , <i>Pinnularia viridis</i> , and <i>Cymbella</i> , very few others	0	0	0.0	0.0	
2H-1 80-84	2.85	1/2 transect	723	44	4.2	0.3	
2H-2 28-30	3.97	1/2 transect	622	38	3.0	0.6	
3H-2 50-52	7.15	1/2 transect	683	35	5.4	0.0	
4H-1 110-112	9.25	2 transects	645	28	3.7	0.2	
5H-1 30-32	11.45	no diatoms, no pieces, no cysts, plenty of sediment	0	0	0.0	0.0	
5H-2 80-83	13.50	no diatoms, no pieces, no cysts, plenty of sediment	0	0	0.0	0.0	
6H-2 0-3	15.70	no diatoms, no pieces, no cysts, plenty of sediment	0	0	0.0	0.0	
7H-1 70-73	19.00	mostly broken <i>Stephanodiscus</i> , very little dissolution visible	0	0	0.0	0.0	
16E-2 60-63	44.90	15 transects	577	28	5.8	0.3	
18E-1 30-33	50.50	1 transect	754	27	4.1	0.0	
18E-2 80-83	52.45	1/2 transect	603	31	2.3	0.0	
20E-1 50-53	56.10	1 transect	629	30	4.2	0.0	
20E-2 100-103	57.72	4 transects	539	16	1.3	0.0	
21E-1 150-153	59.36	3 transects, lots of pieces	615	41	6.7	0.0	
21E-2 120-123	60.39	2 transects	614	26	3.9	0.0	
22E-1 50-53	61.08	many well-preserved periphytic diatoms, but dissolution of some planktic diatoms	0	0	0.0	0.0	
22E-2 100-103	62.84	many whole and well-preserved diatoms, including <i>Amphora</i> , <i>Aulacoseira</i> and small benthic/tychoplanktic fragilaroid species, but also many broken and dissolved large <i>Cymbella</i> and <i>Epithemia</i> diatoms	0	0	0.0	0.0	
23E-2 20-23	64.55	no diatoms, no pieces, no cysts, plenty of sediment	0	0	0.0	0.0	
24E-1 67-70	66.21	diatoms are rare, no evidence of dissolution	0	0	0.0	0.0	
24E-2 120-123	67.92	no diatoms, no pieces, no cysts, plenty of sediment	0	0	0.0	0.0	
25E-2 30-33	69.48	no diatoms, no pieces, no cysts, plenty of sediment	0	0	0.0	0.0	
26E-2 50-53	71.06	few diatoms observed, some breakage, but no evidence of dissolution	0	0	0.0	0.0	
26E-2 100-103	72.72	no dissolution evidenced	802	25	2.7	0.0	

Benthic Taxa

Sample ID	Depth	<i>A. lanceolata</i>	<i>A. saccula</i>	<i>Amphora inariensis</i>	<i>A. ovalis</i>	<i>A. pediculus</i>	<i>Caloneis schumanniana</i>	<i>Caloneis</i> sp. BL1	<i>Cocconeis placentula</i>	<i>C. placentula</i> var. <i>lineata</i>
<i>Core catcher samples</i>										
1E-26E	1.72	0.2	0.4	1.4	0.4	0.0	0.0	1.4	0.0	0.0
1E-27E	4.97	0.6	1.9	1.4	0.3	5.8	0.0	0.9	0.3	0.3
1E-28E	8.02	0.0	0.0	0.7	6.8	2.0	2.0	0.9	0.0	2.6
1E-29E	11.01	0.0	0.0	0.0	0.0	0.0	0.0	0.0	0.0	0.0
1E-30E	14.03	0.0	0.0	0.0	0.0	0.0	0.0	0.0	0.0	0.0
1E-31E	17.04	0.0	0.0	0.0	0.0	0.0	0.0	0.0	0.0	0.0
1E-32E	20.09	0.0	0.0	0.3	0.0	0.0	0.0	0.0	0.0	2.2
1E-33E	23.07	0.2	1.2	1.8	0.0	0.7	0.0	0.0	0.0	0.5
1E-34E	26.10	0.0	0.1	0.0	0.0	0.0	0.0	0.0	0.0	0.0
1E-35E	29.09	0.0	0.3	0.6	0.2	0.0	0.0	0.0	0.0	0.3
1E-36E	32.09	1.3	0.6	1.3	0.0	0.8	0.0	0.0	0.0	1.1
1E-37E	35.09	0.5	0.5	0.5	0.0	0.5	0.0	0.0	0.0	0.7
1E-38E	38.08	0.0	0.0	0.0	0.0	0.0	0.0	0.0	0.0	0.0
1E-39E	41.09	0.5	0.5	2.1	0.0	0.8	0.2	0.3	0.2	0.0
1E-40E	43.90	0.0	0.0	0.0	0.0	0.0	0.0	0.0	0.0	0.0
1E-41E	47.10	1.1	0.0	0.7	0.0	1.8	0.0	0.0	0.0	0.4
1E-42E	50.09	1.1	0.4	0.4	0.0	1.1	0.0	0.0	0.0	0.0
1E-43E	52.99	0.7	0.8	0.8	0.7	1.2	0.0	0.0	0.2	0.2
1E-44E	55.60	1.1	0.7	2.6	0.9	0.9	0.2	0.0	1.1	0.7
1E-45E	58.10	0.0	0.0	0.0	0.0	0.0	0.0	0.0	0.0	0.0
1E-46E	60.60	0.4	0.0	1.5	0.0	6.6	0.0	0.4	1.9	0.6
1E-22E	63.10	0.0	0.0	0.0	0.2	0.0	0.0	0.0	0.0	0.0
1E-23E	65.60	0.0	0.0	0.0	0.0	0.0	0.0	0.0	0.0	0.0
1E-24E	68.10	0.0	0.0	0.0	0.0	0.0	0.0	0.0	0.0	0.0
1E-25E	70.61	0.0	0.0	0.0	0.0	0.0	0.0	0.0	0.0	0.0
1E-26E	76.32									
1E-27E	76.90									
1E-28E	79.43									
1E-29E	81.91									
1E-30E	84.42									
1E-31E	86.42									
1E-32E	88.43									
1E-33E	90.42									
1E-34E	92.43									
1E-35E	94.43									
1E-36E	96.43									
1E-37E	98.42									
1E-38E	100.43									
1E-39E	102.20									
1E-40E	104.50									
1E-41E	106.00									
1E-42E	108.10									
1E-43E	110.40									
1E-44E	113.40									
1E-45E	114.90									
1E-46E	117.80									
<i>Non-core catcher</i>										
1H-1 50-54	0.50	0.0	0.0	0.0	0.0	0.0	0.0	0.0	0.0	0.0
2H-1 80-84	2.85	0.1	0.4	1.0	1.8	4.1	0.4	1.7	0.0	0.1
2H-2 28-30	3.97	0.2	0.8	0.2	1.0	2.6	0.5	0.3	0.0	0.2
3H-2 50-52	7.15	0.3	0.0	0.1	0.4	1.0	0.3	0.0	0.0	0.0
4H-1 110-112	9.25	0.0	0.2	0.9	0.3	1.2	0.0	0.0	0.0	0.2
5H-1 30-32	11.45	0.0	0.0	0.0	0.0	0.0	0.0	0.0	0.0	0.0
5H-2 80-83	13.50	0.0	0.0	0.0	0.0	0.0	0.0	0.0	0.0	0.0
6H-2 0-3	15.70	0.0	0.0	0.0	0.0	0.0	0.0	0.0	0.0	0.0
7H-1 70-73	19.00	0.0	0.0	0.0	0.0	0.0	0.0	0.0	0.0	0.0
16E-2 60-63	44.90	0.0	0.0	0.3	0.2	0.9	0.0	0.0	0.2	0.3
18E-1 30-33	50.50	0.1	0.0	0.0	0.1	0.5	0.0	0.0	0.0	0.0
18E-2 80-83	52.45	0.5	0.3	0.0	0.5	0.3	0.0	0.0	0.0	0.2
20E-1 50-53	56.10	0.0	0.0	0.0	0.0	0.0	0.0	0.0	0.0	0.0
20E-2 100-103	57.72	0.0	0.0	0.2	0.0	0.6	0.0	0.0	0.0	0.0
21E-1 150-153	59.36	0.2	0.0	1.0	0.0	2.6	0.0	0.0	0.0	2.9
21E-2 120-123	60.39	0.3	0.3	0.7	0.0	0.3	0.0	0.0	0.0	0.3
22E-1 50-53	61.08	0.0	0.0	0.0	0.0	0.0	0.0	0.0	0.0	0.0
22E-2 100-103	62.84	0.0	0.0	0.0	0.0	0.0	0.0	0.0	0.0	0.0
23E-2 20-23	64.55	0.0	0.0	0.0	0.0	0.0	0.0	0.0	0.0	0.0
24E-1 67-70	66.21	0.0	0.0	0.0	0.0	0.0	0.0	0.0	0.0	0.0
24E-2 120-123	67.92	0.0	0.0	0.0	0.0	0.0	0.0	0.0	0.0	0.0
25E-2 30-33	69.48	0.0	0.0	0.0	0.0	0.0	0.0	0.0	0.0	0.0
26E-2 50-53	71.06	0.0	0.0	0.0	0.0	0.0	0.0	0.0	0.0	0.0
26E-2 100-103	72.72	0.0	0.1	0.2	0.0	0.0	0.1	0.0	0.2	0.0

(continued)

APPENDIX D. DIATOM FLORA FROM BL00-1 (continued)

Benthic Taxa						
Sample ID	Depth	Comments	<i>Cymbella mesiana</i>	<i>Diatoma tenuis</i> var. <i>elongatum</i>	<i>Diploneis elliptica</i>	<i>Epithemia adnata</i>
<i>Core catcher samples</i>						
1E-26E	1.72		0.0	0.0	0.6	0.0
1E-27E	4.97		1.1	1.1	0.6	0.0
1E-28E	8.02		0.0	0.0	2.4	0.0
1E-29E	11.01	no visible diatoms or pieces	0.0	0.0	0.0	0.0
1E-30E	14.03	no visible diatoms or pieces	0.0	0.0	0.0	0.0
1E-31E	17.04	no visible diatoms or pieces	0.0	0.0	0.0	0.0
1E-32E	20.09		0.0	0.0	0.3	0.3
1E-33E	23.07		0.0	0.0	0.0	0.0
1E-34E	26.10		0.0	0.0	0.0	0.0
1E-35E	29.09		0.0	0.0	0.0	0.0
1E-36E	32.09		0.0	0.0	0.0	0.0
1E-37E	35.09		0.0	0.0	0.0	0.0
1E-38E	38.08	few diatoms	0.0	0.0	0.0	0.0
1E-39E	41.09		0.0	0.0	0.0	0.0
1E-40E	43.90	no visible diatoms or pieces	0.0	0.0	0.0	0.0
1E-41E	47.10		0.0	0.0	0.0	0.5
1E-42E	50.09		0.0	0.0	0.0	0.7
1E-43E	52.99		0.0	0.0	0.3	0.3
1E-44E	55.60		0.0	0.0	0.0	0.0
1E-45E	58.10	no visible diatoms or pieces	0.0	0.0	0.0	0.0
1E-46E	60.60		0.0	0.0	0.0	3.4
1E-22E	63.10	dissolution of some cells present, mostly on broken diatoms	0.0	0.0	0.0	0.7
1E-23E	65.60	no visible diatoms or pieces	0.0	0.0	0.0	0.0
1E-24E	68.10	very small pieces, some dissolution evident	0.0	0.0	0.0	0.0
1E-25E	70.61	no visible diatoms or pieces	0.0	0.0	0.0	0.0
1E-26E	76.32	very few diatoms, mostly <i>Stephanodiscus</i> and small fragilaroid, some dissolution	0.0	0.0	0.0	0.0
1E-27E	76.90	no diatoms, no pieces				
1E-28E	79.43	no diatoms, no pieces				
1E-29E	81.91	some diatoms, mostly small fragilaroid and <i>Stephanodiscus</i> , lots of cysts				
1E-30E	84.42	very sparse, mostly small fragilaroid				
1E-31E	86.42	very few diatoms, mostly <i>Stephanodiscus</i> and small fragilaroid, some dissolution				
1E-32E	88.43	very sparse, centrics and pennates, mostly broken, some dissolution				
1E-33E	90.42	abundant diatoms, both centrics and pennates, very diverse				
1E-34E	92.43	abundant diatoms, both centrics and pennates, very diverse				
1E-35E	94.43	abundant diatoms, mostly planktonic, dissolution and breakage present				
1E-36E	96.43	sparse diatoms				
1E-37E	98.42	sparse diatoms, mostly small fragilaroid, dissolution present				
1E-38E	100.43	abundant diatoms and cysts, many <i>Stephanodiscus</i> and <i>Aulacoseira (granulata?)</i>				
1E-39E	102.20	abundant <i>Stephanodiscus</i>				
1E-40E	104.50	abundant <i>Stephanodiscus</i>				
1E-41E	106.00	abundant <i>Stephanodiscus</i>				
1E-42E	108.10	abundant diatoms, mostly small fragilaroid, few centrics				
1E-43E	110.40	abundant diatoms, both pennates and centrics, very diverse				
1E-44E	113.40	abundant diatoms, both <i>Fragilaria</i> and a few centrics				
1E-45E	114.90	no diatoms, no pieces				
1E-46E	117.80	abundant diatoms, many big centrics and <i>Aulacoseira</i>				
<i>Non-core catcher</i>						
1H-1 50-54	0.50	many broken pieces, mostly <i>Navicula oblonga</i> , <i>Pinnularia viridis</i> , and <i>Cymbella</i> , very few others	0.0	0.0	0.0	0.0
2H-1 80-84	2.85	1/2 transect	0.1	0.1	2.8	0.6
2H-2 28-30	3.97	1/2 transect	0.0	0.0	1.8	0.0
3H-2 50-52	7.15	1/2 transect	0.1	0.1	0.0	0.0
4H-1 110-112	9.25	2 transects	0.0	0.0	0.0	0.0
5H-1 30-32	11.45	no diatoms, no pieces, no cysts, plenty of sediment	0.0	0.0	0.0	0.0
5H-2 80-83	13.50	no diatoms, no pieces, no cysts, plenty of sediment	0.0	0.0	0.0	0.0
6H-2 0-3	15.70	no diatoms, no pieces, no cysts, plenty of sediment	0.0	0.0	0.0	0.0
7H-1 70-73	19.00	mostly broken <i>Stephanodiscus</i> , very little dissolution visible	0.0	0.0	0.0	0.0
16E-2 60-63	44.90	15 transects	0.0	0.0	0.0	0.2
18E-1 30-33	50.50	1 transect	0.0	0.0	0.1	0.0
18E-2 80-83	52.45	1/2 transect	0.0	0.0	0.0	0.2
20E-1 50-53	56.10	1 transect	0.0	0.0	0.0	0.0
20E-2 100-103	57.72	4 transects	0.0	0.0	0.0	0.0
21E-1 150-153	59.36	3 transects, lots of pieces	0.0	0.0	0.2	0.7
21E-2 120-123	60.39	2 transects	0.0	0.0	0.0	0.0
22E-1 50-53	61.08	many well-preserved periphytic diatoms, but dissolution of some planktic diatoms	0.0	0.0	0.0	0.0
22E-2 100-103	62.84	many whole and well-preserved diatoms, including <i>Amphora</i> , <i>Aulacoseira</i> and small benthic/tychoplanktic fragilaroid species, but also many broken and dissolved large <i>Cymbella</i> and <i>Epithemia</i> diatoms	0.0	0.0	0.0	0.0
23E-2 20-23	64.55	no diatoms, no pieces, no cysts, plenty of sediment	0.0	0.0	0.0	0.0
24E-1 67-70	66.21	diatoms are rare, no evidence of dissolution	0.0	0.0	0.0	0.0
24E-2 120-123	67.92	no diatoms, no pieces, no cysts, plenty of sediment	0.0	0.0	0.0	0.0
25E-2 30-33	69.48	no diatoms, no pieces, no cysts, plenty of sediment	0.0	0.0	0.0	0.0
26E-2 50-53	71.06	few diatoms observed, some breakage, but no evidence of dissolution	0.0	0.0	0.0	0.0
26E-2 100-103	72.72	no dissolution evidenced	0.0	0.0	0.2	0.0

Benthic Taxa										
Sample ID	Depth	<i>E. frickeii</i>	<i>Pseudostaurosira brevistriata</i> total	<i>P. brevistriata</i>	<i>P. brevistriata</i> (rhombic)	<i>P. brevistriata</i> (oval)	<i>Ulnaria biceps</i>	<i>Fragilariforma constricta</i>	<i>Staurosira construens</i>	<i>S. construens</i> var. <i>venter</i>
<i>Core catcher samples</i>										
1E-26E	1.72	0.2	83.1	45.0	33.5	4.6	0.0	0.0	0.0	0.0
1E-27E	4.97	0.0	33.1	12.1	14.4	6.6	0.0	0.0	0.5	0.0
1E-28E	8.02	2.8	63.4	54.5	7.9	0.9	0.0	0.6	0.0	0.0
1E-29E	11.01	0.0	0.0	0.0	0.0	0.0	0.0	0.0	0.0	0.0
1E-30E	14.03	0.0	0.0	0.0	0.0	0.0	0.0	0.0	0.0	0.0
1E-31E	17.04	0.0	0.0	0.0	0.0	0.0	0.0	0.0	0.0	0.0
1E-32E	20.09	0.5	2.4	2.4	0.0	0.0	0.0	0.0	0.0	0.8
1E-33E	23.07	0.0	17.4	16.0	0.5	0.9	0.0	0.5	0.7	0.4
1E-34E	26.10	0.0	0.0	0.0	0.0	0.0	0.0	0.0	0.0	0.0
1E-35E	29.09	0.0	6.6	2.3	3.7	0.6	0.0	0.0	0.6	0.2
1E-36E	32.09	0.0	13.2	8.4	4.0	0.8	0.0	0.2	1.8	0.6
1E-37E	35.09	0.0	0.9	0.9	0.0	0.0	0.0	0.0	0.2	0.0
1E-38E	38.08	0.0	0.0	0.0	0.0	0.0	0.0	0.0	0.0	0.0
1E-39E	41.09	0.0	27.7	12.8	12.3	2.6	0.0	0.5	4.6	3.8
1E-40E	43.90	0.0	0.0	0.0	0.0	0.0	0.0	0.0	0.0	0.0
1E-41E	47.10	0.0	26.9	15.1	9.5	2.3	0.7	0.4	0.0	2.9
1E-42E	50.09	0.0	32.6	17.2	14.5	0.9	5.6	0.4	1.8	8.1
1E-43E	52.99	0.0	18.3	5.9	7.9	4.5	0.5	0.5	2.0	1.0
1E-44E	55.60	0.0	22.6	7.1	12.9	2.6	9.1	0.0	1.5	1.9
1E-45E	58.10	0.0	0.0	0.0	0.0	0.0	0.0	0.0	0.0	0.0
1E-46E	60.60	0.0	43.8	17.5	20.9	5.5	0.9	0.9	2.7	1.9
1E-22E	63.10	1.7	91.6	54.7	31.4	5.5	0.0	0.0	0.0	0.0
1E-23E	65.60	0.0	0.0	0.0	0.0	0.0	0.0	0.0	0.0	0.0
1E-24E	68.10	0.0	0.0	0.0	0.0	0.0	0.0	0.0	0.0	0.0
1E-25E	70.61	0.0	0.0	0.0	0.0	0.0	0.0	0.0	0.0	0.0
1E-26E	76.32									
1E-27E	76.90									
1E-28E	79.43									
1E-29E	81.91									
1E-30E	84.42									
1E-31E	86.42									
1E-32E	88.43									
1E-33E	90.42									
1E-34E	92.43									
1E-35E	94.43									
1E-36E	96.43									
1E-37E	98.42									
1E-38E	100.43									
1E-39E	102.20									
1E-40E	104.50									
1E-41E	106.00									
1E-42E	108.10									
1E-43E	110.40									
1E-44E	113.40									
1E-45E	114.90									
1E-46E	117.80									
<i>Non-core catcher</i>										
1H-1 50-54	0.50	0.0	0.0	0.0	0.0	0.0	0.0	0.0	0.0	0.0
2H-1 80-84	2.85	0.0	36.4	21.0	8.7	6.6	0.0	0.1	0.0	0.0
2H-2 28-30	3.97	0.0	44.7	22.2	12.5	10.0	0.0	0.0	0.3	0.0
3H-2 50-52	7.15	0.0	20.8	3.7	8.8	8.3	0.0	0.0	1.0	1.8
4H-1 110-112	9.25	0.0	28.2	14.9	10.9	2.5	0.0	0.0	1.7	2.2
5H-1 30-32	11.45	0.0	0.0	0.0	0.0	0.0	0.0	0.0	0.0	0.0
5H-2 80-83	13.50	0.0	0.0	0.0	0.0	0.0	0.0	0.0	0.0	0.0
6H-2 0-3	15.70	0.0	0.0	0.0	0.0	0.0	0.0	0.0	0.0	0.0
7H-1 70-73	19.00	0.0	0.0	0.0	0.0	0.0	0.0	0.0	0.0	0.0
16E-2 60-63	44.90	0.0	18.9	5.9	10.4	2.6	0.2	0.7	0.9	3.1
18E-1 30-33	50.50	0.0	34.1	16.8	11.7	5.6	0.5	2.1	3.2	2.0
18E-2 80-83	52.45	0.0	51.9	30.7	16.3	5.0	0.7	0.0	3.2	1.5
20E-1 50-53	56.10	0.0	0.0	0.0	0.0	0.0	0.0	0.0	0.0	0.0
20E-2 100-103	57.72	0.0	2.8	0.2	2.0	0.6	0.0	0.0	0.0	0.0
21E-1 150-153	59.36	0.2	26.8	8.6	13.7	4.6	3.1	0.7	0.2	0.7
21E-2 120-123	60.39	0.0	35.5	14.0	10.9	10.6	0.0	1.8	4.1	6.7
22E-1 50-53	61.08	0.0	0.0	0.0	0.0	0.0	0.0	0.0	0.0	0.0
22E-2 100-103	62.84	0.0	0.0	0.0	0.0	0.0	0.0	0.0	0.0	0.0
23E-2 20-23	64.55	0.0	0.0	0.0	0.0	0.0	0.0	0.0	0.0	0.0
24E-1 67-70	66.21	0.0	0.0	0.0	0.0	0.0	0.0	0.0	0.0	0.0
24E-2 120-123	67.92	0.0	0.0	0.0	0.0	0.0	0.0	0.0	0.0	0.0
25E-2 30-33	69.48	0.0	0.0	0.0	0.0	0.0	0.0	0.0	0.0	0.0
26E-2 50-53	71.06	0.0	0.0	0.0	0.0	0.0	0.0	0.0	0.0	0.0
26E-2 100-103	72.72	0.4	15.0	7.2	5.4	2.4	0.0	0.0	0.7	2.2

(continued)

APPENDIX D. DIATOM FLORA FROM BL00-1 (continued)

Sample ID	Depth	Comments	Benthic Taxa			
			<i>Staurosirella leptostauron</i>	<i>S. pinnata</i>	<i>S. pinnata</i> var. <i>accuminata</i>	<i>Fragilaria tenera</i>
<i>Core catcher samples</i>						
1E-26E	1.72		0.0	4.0	0.6	0.0
1E-27E	4.97		0.0	19.2	1.9	0.9
1E-28E	8.02		0.0	0.6	0.0	0.0
1E-29E	11.01	no visible diatoms or pieces	0.0	0.0	0.0	0.0
1E-30E	14.03	no visible diatoms or pieces	0.0	0.0	0.0	0.0
1E-31E	17.04	no visible diatoms or pieces	0.0	0.0	0.0	0.0
1E-32E	20.09		0.0	1.3	1.1	0.0
1E-33E	23.07		0.0	28.8	0.9	0.0
1E-34E	26.10		0.0	0.0	0.0	0.0
1E-35E	29.09		0.0	4.0	0.6	0.0
1E-36E	32.09		0.0	5.5	0.3	0.0
1E-37E	35.09		0.0	0.4	1.1	0.0
1E-38E	38.08	few diatoms	0.0	0.0	0.0	0.0
1E-39E	41.09		0.0	18.0	1.6	0.0
1E-40E	43.90	no visible diatoms or pieces	0.0	0.0	0.0	0.0
1E-41E	47.10		0.0	31.7	3.0	0.0
1E-42E	50.09		0.0	10.9	2.1	0.0
1E-43E	52.99		0.2	33.9	1.5	0.0
1E-44E	55.60		0.0	12.1	0.7	0.0
1E-45E	58.10	no visible diatoms or pieces	0.0	0.0	0.0	0.0
1E-46E	60.60		0.0	12.1	1.1	1.3
1E-22E	63.10	dissolution of some cells present, mostly on broken diatoms	0.0	2.9	0.2	0.0
1E-23E	65.60	no visible diatoms or pieces	0.0	0.0	0.0	0.0
1E-24E	68.10	very small pieces, some dissolution evident	0.0	0.0	0.0	0.0
1E-25E	70.61	no visible diatoms or pieces	0.0	0.0	0.0	0.0
1E-26E	76.32	very few diatoms, mostly <i>Stephanodiscus</i> and small fragilaroid, some dissolution				
1E-27E	76.90	no diatoms, no pieces				
1E-28E	79.43	no diatoms, no pieces				
1E-29E	81.91	some diatoms, mostly small fragilaroid and <i>Stephanodiscus</i> , lots of cysts				
1E-30E	84.42	very sparse, mostly small fragilaroid				
1E-31E	86.42	very few diatoms, mostly <i>Stephanodiscus</i> and small fragilaroid, some dissolution				
1E-32E	88.43	very sparse, centrics and pennates, mostly broken, some dissolution				
1E-33E	90.42	abundant diatoms, both centrics and pennates, very diverse				
1E-34E	92.43	abundant diatoms, both centrics and pennates, very diverse				
1E-35E	94.43	abundant diatoms, mostly planktonic, dissolution and breakage present				
1E-36E	96.43	sparse diatoms				
1E-37E	98.42	sparse diatoms, mostly small fragilaroid, dissolution present				
1E-38E	100.43	abundant diatoms and cysts, many <i>Stephanodiscus</i> and <i>Aulacoseira (granulata?)</i>				
1E-39E	102.20	abundant <i>Stephanodiscus</i>				
1E-40E	104.50	abundant <i>Stephanodiscus</i>				
1E-41E	106.00	abundant <i>Stephanodiscus</i>				
1E-42E	108.10	abundant diatoms, mostly small fragilaroid, few centrics				
1E-43E	110.40	abundant diatoms, both pennates and centrics, very diverse				
1E-44E	113.40	abundant diatoms, both <i>Fragilaria</i> and a few centrics				
1E-45E	114.90	no diatoms, no pieces				
1E-46E	117.80	abundant diatoms, many big centrics and <i>Aulacoseira</i>				
<i>Non-core catcher</i>						
1H-1 50-54	0.50	many broken pieces, mostly <i>Navicula oblonga</i> , <i>Pinnularia viridis</i> , and <i>Cymbella</i> , very few others	0.0	0.0	0.0	0.0
2H-1 80-84	2.85	1/2 transect	1.2	18.1	1.2	0.0
2H-2 28-30	3.97	1/2 transect	1.4	22.5	1.3	0.0
3H-2 50-52	7.15	1/2 transect	0.0	31.9	1.0	0.1
4H-1 110-112	9.25	2 transects	0.3	15.8	0.3	0.0
5H-1 30-32	11.45	no diatoms, no pieces, no cysts, plenty of sediment	0.0	0.0	0.0	0.0
5H-2 80-83	13.50	no diatoms, no pieces, no cysts, plenty of sediment	0.0	0.0	0.0	0.0
6H-2 0-3	15.70	no diatoms, no pieces, no cysts, plenty of sediment	0.0	0.0	0.0	0.0
7H-1 70-73	19.00	mostly broken <i>Stephanodiscus</i> , very little dissolution visible	0.0	0.0	0.0	0.0
16E-2 60-63	44.90	15 transects	0.2	28.1	1.0	0.0
18E-1 30-33	50.50	1 transect	0.0	25.2	1.2	0.0
18E-2 80-83	52.45	1/2 transect	0.3	8.8	2.2	0.0
20E-1 50-53	56.10	1 transect	0.0	0.0	0.0	0.0
20E-2 100-103	57.72	4 transects	0.0	1.1	0.9	0.4
21E-1 150-153	59.36	3 transects, lots of pieces	0.0	6.5	1.0	0.0
21E-2 120-123	60.39	2 transects	0.0	20.8	3.9	0.0
22E-1 50-53	61.08	many well-preserved periphytic diatoms, but dissolution of some planktic diatoms	0.0	0.0	0.0	0.0
22E-2 100-103	62.84	many whole and well-preserved diatoms, including <i>Amphora</i> , <i>Aulacoseira</i> and small benthic/tychoplanktic fragilaroid species, but also many broken and dissolved large <i>Cymbella</i> and <i>Epithemia</i> diatoms	0.0	0.0	0.0	0.0
23E-2 20-23	64.55	no diatoms, no pieces, no cysts, plenty of sediment	0.0	0.0	0.0	0.0
24E-1 67-70	66.21	diatoms are rare, no evidence of dissolution	0.0	0.0	0.0	0.0
24E-2 120-123	67.92	no diatoms, no pieces, no cysts, plenty of sediment	0.0	0.0	0.0	0.0
25E-2 30-33	69.48	no diatoms, no pieces, no cysts, plenty of sediment	0.0	0.0	0.0	0.0
26E-2 50-53	71.06	few diatoms observed, some breakage, but no evidence of dissolution	0.0	0.0	0.0	0.0
26E-2 100-103	72.72	no dissolution evidenced	0.0	5.5	1.2	0.0

Benthic Taxa											
Sample ID	Depth	<i>F. ulna</i>	<i>F. virescens</i>	<i>Navicula capitata</i> var. <i>lueneburgensis</i>	<i>N. cryptocephala</i>	<i>N. cryptotenella</i>	<i>N. oblonga</i>	<i>N. pupula</i>	<i>N. rhyncocephala</i>	<i>N. tuscula</i>	
<i>Core catcher samples</i>											
1E-26E	1.72	0.0	0.0	0.2	0.0	0.0	0.2	0.0	1.6	0.0	
1E-27E	4.97	0.0	0.0	2.8	0.0	1.1	0.0	0.0	4.1	0.6	
1E-28E	8.02	0.0	0.0	0.0	0.0	0.0	4.1	0.0	0.0	0.0	
1E-29E	11.01	0.0	0.0	0.0	0.0	0.0	0.0	0.0	0.0	0.0	
1E-30E	14.03	0.0	0.0	0.0	0.0	0.0	0.0	0.0	0.0	0.0	
1E-31E	17.04	0.0	0.0	0.0	0.0	0.0	0.0	0.0	0.0	0.0	
1E-32E	20.09	0.0	0.0	0.0	0.0	0.0	0.0	0.0	0.0	0.0	
1E-33E	23.07	0.0	0.0	0.0	0.0	0.0	0.0	0.2	0.0	0.2	
1E-34E	26.10	0.0	0.0	0.0	0.0	0.0	0.0	0.0	0.0	0.0	
1E-35E	29.09	0.0	0.0	0.0	0.0	0.0	0.0	0.0	0.2	0.2	
1E-36E	32.09	0.0	0.0	0.0	0.0	0.0	0.0	0.2	0.0	0.0	
1E-37E	35.09	0.0	0.0	0.0	0.0	0.0	0.0	0.2	0.0	0.0	
1E-38E	38.08	0.0	0.0	0.0	0.0	0.0	0.0	0.0	0.0	0.0	
1E-39E	41.09	0.0	0.0	0.3	0.0	0.2	0.0	0.2	0.7	0.3	
1E-40E	43.90	0.0	0.0	0.0	0.0	0.0	0.0	0.0	0.0	0.0	
1E-41E	47.10	0.0	0.0	0.0	0.0	0.0	0.0	0.0	0.0	0.4	
1E-42E	50.09	0.0	0.0	0.4	0.0	0.0	0.0	0.0	0.0	0.5	
1E-43E	52.99	0.0	0.0	0.8	0.0	0.0	0.0	0.2	0.7	0.7	
1E-44E	55.60	1.9	0.0	1.1	0.0	0.0	0.0	0.2	0.7	0.7	
1E-45E	58.10	0.0	0.0	0.0	0.0	0.0	0.0	0.0	0.0	0.0	
1E-46E	60.60	0.2	0.0	0.0	0.0	0.6	0.0	0.4	0.2	0.0	
1E-22E	63.10	0.0	0.0	0.0	0.0	0.0	0.0	0.0	0.5	0.0	
1E-23E	65.60	0.0	0.0	0.0	0.0	0.0	0.0	0.0	0.0	0.0	
1E-24E	68.10	0.0	0.0	0.0	0.0	0.0	0.0	0.0	0.0	0.0	
1E-25E	70.61	0.0	0.0	0.0	0.0	0.0	0.0	0.0	0.0	0.0	
1E-26E	76.32										
1E-27E	76.90										
1E-28E	79.43										
1E-29E	81.91										
1E-30E	84.42										
1E-31E	86.42										
1E-32E	88.43										
1E-33E	90.42										
1E-34E	92.43										
1E-35E	94.43										
1E-36E	96.43										
1E-37E	98.42										
1E-38E	100.43										
1E-39E	102.20										
1E-40E	104.50										
1E-41E	106.00										
1E-42E	108.10										
1E-43E	110.40										
1E-44E	113.40										
1E-45E	114.90										
1E-46E	117.80										
<i>Non-core catcher</i>											
1H-1 50-54	0.50	0.0	0.0	0.0	0.0	0.0	0.0	0.0	0.0	0.0	
2H-1 80-84	2.85	0.0	0.1	2.1	0.4	0.0	0.0	1.2	1.1	1.1	
2H-2 28-30	3.97	0.0	1.6	1.8	2.1	0.0	0.2	0.0	2.4	0.8	
3H-2 50-52	7.15	0.0	1.2	1.9	0.0	0.0	0.0	0.0	0.1	0.3	
4H-1 110-112	9.25	0.0	0.0	0.3	0.0	0.0	0.0	0.3	0.0	0.0	
5H-1 30-32	11.45	0.0	0.0	0.0	0.0	0.0	0.0	0.0	0.0	0.0	
5H-2 80-83	13.50	0.0	0.0	0.0	0.0	0.0	0.0	0.0	0.0	0.0	
6H-2 0-3	15.70	0.0	0.0	0.0	0.0	0.0	0.0	0.0	0.0	0.0	
7H-1 70-73	19.00	0.0	0.0	0.0	0.0	0.0	0.0	0.0	0.0	0.0	
16E-2 60-63	44.90	3.3	0.0	0.0	0.0	0.0	0.0	0.2	0.0	0.0	
18E-1 30-33	50.50	0.0	0.3	0.0	0.0	0.0	0.0	0.1	0.0	0.0	
18E-2 80-83	52.45	0.0	0.2	0.3	0.0	0.0	0.0	0.2	0.0	0.0	
20E-1 50-53	56.10	0.0	0.0	0.0	0.0	0.0	0.0	0.0	0.0	0.0	
20E-2 100-103	57.72	0.0	0.0	0.0	0.0	0.0	0.0	0.2	0.0	0.0	
21E-1 150-153	59.36	0.0	0.0	0.0	0.0	0.0	0.2	0.2	0.3	0.2	
21E-2 120-123	60.39	0.0	1.1	0.2	0.0	0.0	0.0	0.2	0.0	0.0	
22E-1 50-53	61.08	0.0	0.0	0.0	0.0	0.0	0.0	0.0	0.0	0.0	
22E-2 100-103	62.84	0.0	0.0	0.0	0.0	0.0	0.0	0.0	0.0	0.0	
23E-2 20-23	64.55	0.0	0.0	0.0	0.0	0.0	0.0	0.0	0.0	0.0	
24E-1 67-70	66.21	0.0	0.0	0.0	0.0	0.0	0.0	0.0	0.0	0.0	
24E-2 120-123	67.92	0.0	0.0	0.0	0.0	0.0	0.0	0.0	0.0	0.0	
25E-2 30-33	69.48	0.0	0.0	0.0	0.0	0.0	0.0	0.0	0.0	0.0	
26E-2 50-53	71.06	0.0	0.0	0.0	0.0	0.0	0.0	0.0	0.0	0.0	
26E-2 100-103	72.72	0.0	0.7	0.0	0.0	0.0	0.0	0.2	0.0	0.0	

(continued)

APPENDIX D. DIATOM FLORA FROM BL00-1 (continued)

		Benthic Taxa					
Sample ID	Depth	Comments	<i>Nitzschia fonticola</i>	<i>N. unid</i>	<i>Pinnularia viridis</i>	<i>Rhopalodia gibba</i>	<i>Surirella angusta</i>
<i>Core catcher samples</i>							
1E-26E	1.72		0.8	0.2	0.4	0.0	0.0
1E-27E	4.97		0.5	1.1	0.3	0.0	0.0
1E-28E	8.02		0.0	0.7	1.7	0.0	0.0
1E-29E	11.01	no visible diatoms or pieces	0.0	0.0	0.0	0.0	0.0
1E-30E	14.03	no visible diatoms or pieces	0.0	0.0	0.0	0.0	0.0
1E-31E	17.04	no visible diatoms or pieces	0.0	0.0	0.0	0.0	0.0
1E-32E	20.09		0.0	0.0	0.0	0.0	0.0
1E-33E	23.07		0.0	0.2	0.0	0.0	0.0
1E-34E	26.10		0.0	0.0	0.0	0.0	0.0
1E-35E	29.09		0.0	0.0	0.0	0.0	0.2
1E-36E	32.09		0.0	0.0	0.0	0.0	0.2
1E-37E	35.09		0.0	0.7	0.0	0.0	0.0
1E-38E	38.08	few diatoms	0.0	0.0	0.0	0.0	0.0
1E-39E	41.09		0.3	0.0	0.0	0.0	0.5
1E-40E	43.90	no visible diatoms or pieces	0.0	0.0	0.0	0.0	0.0
1E-41E	47.10		1.1	0.4	0.0	0.0	0.2
1E-42E	50.09		0.0	0.0	0.0	0.0	0.7
1E-43E	52.99		0.5	0.3	0.0	0.0	0.0
1E-44E	55.60		1.1	0.0	0.0	0.0	0.0
1E-45E	58.10	no visible diatoms or pieces	0.0	0.0	0.0	0.0	0.0
1E-46E	60.60		0.4	0.6	0.0	2.5	0.0
1E-22E	63.10	dissolution of some cells present, mostly on broken diatoms	0.2	0.0	0.0	0.0	0.0
1E-23E	65.60	no visible diatoms or pieces	0.0	0.0	0.0	0.0	0.0
1E-24E	68.10	very small pieces, some dissolution evident	0.0	0.0	0.0	0.0	0.0
1E-25E	70.61	no visible diatoms or pieces	0.0	0.0	0.0	0.0	0.0
1E-26E	76.32	very few diatoms, mostly <i>Stephanodiscus</i> and small fragilaroid, some dissolution					
1E-27E	76.90	no diatoms, no pieces					
1E-28E	79.43	no diatoms, no pieces					
1E-29E	81.91	some diatoms, mostly small fragilaroid and <i>Stephanodiscus</i> , lots of cysts					
1E-30E	84.42	very sparse, mostly small fragilaroid					
1E-31E	86.42	very few diatoms, mostly <i>Stephanodiscus</i> and small fragilaroid, some dissolution					
1E-32E	88.43	very sparse, centrics and pennates, mostly broken, some dissolution					
1E-33E	90.42	abundant diatoms, both centrics and pennates, very diverse					
1E-34E	92.43	abundant diatoms, both centrics and pennates, very diverse					
1E-35E	94.43	abundant diatoms, mostly planktonic, dissolution and breakage present					
1E-36E	96.43	sparse diatoms					
1E-37E	98.42	sparse diatoms, mostly small fragilaroid, dissolution present					
1E-38E	100.43	abundant diatoms and cysts, many <i>Stephanodiscus</i> and <i>Aulacoseira (granulata?)</i>					
1E-39E	102.20	abundant <i>Stephanodiscus</i>					
1E-40E	104.50	abundant <i>Stephanodiscus</i>					
1E-41E	106.00	abundant <i>Stephanodiscus</i>					
1E-42E	108.10	abundant diatoms, mostly small fragilaroid, few centrics					
1E-43E	110.40	abundant diatoms, both pennates and centrics, very diverse					
1E-44E	113.40	abundant diatoms, both <i>Fragilaria</i> and a few centrics					
1E-45E	114.90	no diatoms, no pieces					
1E-46E	117.80	abundant diatoms, many big centrics and <i>Aulacoseira</i>					
<i>Non-core catcher</i>							
1H-1 50-54	0.50	many broken pieces, mostly <i>Navicula oblonga</i> , <i>Pinnularia viridis</i> , and <i>Cymbella</i> , very few others	0.0	0.0	0.0	0.0	0.0
2H-1 80-84	2.85	1/2 transect	2.1	0.4	0.0	0.0	0.0
2H-2 28-30	3.97	1/2 transect	1.0	0.3	0.0	0.0	0.0
3H-2 50-52	7.15	1/2 transect	0.0	0.0	0.0	0.0	0.0
4H-1 110-112	9.25	2 transects	0.3	0.0	0.0	0.3	0.0
5H-1 30-32	11.45	no diatoms, no pieces, no cysts, plenty of sediment	0.0	0.0	0.0	0.0	0.0
5H-2 80-83	13.50	no diatoms, no pieces, no cysts, plenty of sediment	0.0	0.0	0.0	0.0	0.0
6H-2 0-3	15.70	no diatoms, no pieces, no cysts, plenty of sediment	0.0	0.0	0.0	0.0	0.0
7H-1 70-73	19.00	mostly broken <i>Stephanodiscus</i> , very little dissolution visible	0.0	0.0	0.0	0.0	0.0
16E-2 60-63	44.90	15 transects	0.0	0.0	0.0	0.0	0.0
18E-1 30-33	50.50	1 transect	0.1	0.0	0.0	0.0	0.0
18E-2 80-83	52.45	1/2 transect	0.3	0.0	0.0	0.0	0.0
20E-1 50-53	56.10	1 transect	0.0	0.0	0.0	0.0	0.0
20E-2 100-103	57.72	4 transects	0.0	0.0	0.0	0.0	0.2
21E-1 150-153	59.36	3 transects, lots of pieces	0.2	0.0	0.0	0.0	1.0
21E-2 120-123	60.39	2 transects	0.0	0.0	0.0	0.0	0.0
22E-1 50-53	61.08	many well-preserved periphytic diatoms, but dissolution of some planktic diatoms	0.0	0.0	0.0	0.0	0.0
22E-2 100-103	62.84	many whole and well-preserved diatoms, including <i>Amphora</i> , <i>Aulacoseira</i> and small benthic/tychoplanktic fragilaroid species, but also many broken and dissolved large <i>Cymbella</i> and <i>Epithemia</i> diatoms	0.0	0.0	0.0	0.0	0.0
23E-2 20-23	64.55	no diatoms, no pieces, no cysts, plenty of sediment	0.0	0.0	0.0	0.0	0.0
24E-1 67-70	66.21	diatoms are rare, no evidence of dissolution	0.0	0.0	0.0	0.0	0.0
24E-2 120-123	67.92	no diatoms, no pieces, no cysts, plenty of sediment	0.0	0.0	0.0	0.0	0.0
25E-2 30-33	69.48	no diatoms, no pieces, no cysts, plenty of sediment	0.0	0.0	0.0	0.0	0.0
26E-2 50-53	71.06	few diatoms observed, some breakage, but no evidence of dissolution	0.0	0.0	0.0	0.0	0.0
26E-2 100-103	72.72	no dissolution evidenced	0.0	0.0	0.0	0.0	0.0

Planktic Taxa									
Sample ID	Depth	<i>Aulacoseira granulata</i>	<i>A. islandica</i>	<i>Cyclotella bodanica</i>	<i>C. glabriuscula</i>	<i>C. meneghiniana</i>	<i>C. michiganiana</i>	<i>C. ocellata</i>	<i>C. planktonica</i>
<i>Core catcher samples</i>									
1E-26E	1.72	0.0	0.0	0.0	0.0	0.0	0.0	0.0	0.0
1E-27E	4.97	0.0	0.0	0.0	0.0	9.9	1.6	0.0	0.0
1E-28E	8.02	0.0	0.0	0.0	0.0	0.4	0.0	0.0	0.0
1E-29E	11.01	0.0	0.0	0.0	0.0	0.0	0.0	0.0	0.0
1E-30E	14.03	0.0	0.0	0.0	0.0	0.0	0.0	0.0	0.0
1E-31E	17.04	0.0	0.0	0.0	0.0	0.0	0.0	0.0	0.0
1E-32E	20.09	0.0	0.0	0.0	0.0	0.0	0.0	0.0	0.0
1E-33E	23.07	0.0	0.0	0.0	0.0	0.0	0.0	0.0	0.0
1E-34E	26.10	0.0	0.0	0.0	0.0	0.0	0.0	0.0	0.0
1E-35E	29.09	0.0	0.0	0.2	0.0	0.0	0.0	0.0	0.0
1E-36E	32.09	0.0	0.0	0.2	0.0	0.2	0.0	2.4	0.0
1E-37E	35.09	0.0	0.0	0.4	0.0	1.1	0.0	0.0	0.0
1E-38E	38.08	0.0	0.0	0.0	0.0	0.0	0.0	0.0	0.0
1E-39E	41.09	0.0	0.0	0.8	0.0	2.3	0.0	3.9	0.0
1E-40E	43.90	0.0	0.0	0.0	0.0	0.0	0.0	0.0	0.0
1E-41E	47.10	0.0	0.0	0.9	0.0	3.0	0.0	2.5	0.0
1E-42E	50.09	24.3	1.9	0.0	0.0	0.7	0.0	0.2	0.0
1E-43E	52.99	4.7	0.0	0.0	2.4	1.5	0.0	0.0	0.0
1E-44E	55.60	0.0	0.0	0.0	0.0	5.2	0.0	2.2	0.0
1E-45E	58.10	0.0	0.0	0.0	0.0	0.0	0.0	0.0	0.0
1E-46E	60.60	0.0	0.0	4.9	0.0	0.2	0.0	0.0	0.0
1E-22E	63.10	0.0	0.0	0.2	0.0	0.0	0.0	0.0	0.0
1E-23E	65.60	0.0	0.0	0.0	0.0	0.0	0.0	0.0	0.0
1E-24E	68.10	0.0	0.0	0.0	0.0	0.0	0.0	0.0	0.0
1E-25E	70.61	0.0	0.0	0.0	0.0	0.0	0.0	0.0	0.0
1E-26E	76.32								
1E-27E	76.90								
1E-28E	79.43								
1E-29E	81.91								
1E-30E	84.42								
1E-31E	86.42								
1E-32E	88.43								
1E-33E	90.42								
1E-34E	92.43								
1E-35E	94.43								
1E-36E	96.43								
1E-37E	98.42								
1E-38E	100.43								
1E-39E	102.20								
1E-40E	104.50								
1E-41E	106.00								
1E-42E	108.10								
1E-43E	110.40								
1E-44E	113.40								
1E-45E	114.90								
1E-46E	117.80								
<i>Non-core catcher</i>									
1H-1 50-54	0.50	0.0	0.0	0.0	0.0	0.0	0.0	0.0	0.0
2H-1 80-84	2.85	0.0	0.0	0.0	0.0	9.4	0.7	0.0	0.0
2H-2 28-30	3.97	0.0	0.0	0.0	0.0	6.6	0.6	0.0	0.0
3H-2 50-52	7.15	0.0	0.0	0.0	0.0	8.1	0.0	1.6	0.3
4H-1 110-112	9.25	0.0	0.0	0.0	0.0	0.5	0.0	0.8	0.0
5H-1 30-32	11.45	0.0	0.0	0.0	0.0	0.0	0.0	0.0	0.0
5H-2 80-83	13.50	0.0	0.0	0.0	0.0	0.0	0.0	0.0	0.0
6H-2 0-3	15.70	0.0	0.0	0.0	0.0	0.0	0.0	0.0	0.0
7H-1 70-73	19.00	0.0	0.0	0.0	0.0	0.0	0.0	0.0	0.0
16E-2 60-63	44.90	0.0	0.0	1.9	0.0	2.4	0.0	0.0	0.0
18E-1 30-33	50.50	8.2	0.7	0.0	0.0	0.3	0.1	0.0	0.0
18E-2 80-83	52.45	19.1	1.0	0.2	0.0	0.3	0.0	0.0	0.0
20E-1 50-53	56.10	0.0	0.0	0.0	0.0	0.0	0.0	0.0	0.0
20E-2 100-103	57.72	0.0	87.8	0.0	0.0	0.4	0.0	0.0	2.0
21E-1 150-153	59.36	0.0	15.6	1.8	0.0	1.1	0.0	0.0	5.4
21E-2 120-123	60.39	0.0	0.0	0.7	0.0	0.5	0.2	0.0	0.0
22E-1 50-53	61.08	0.0	0.0	0.0	0.0	0.0	0.0	0.0	0.0
22E-2 100-103	62.84	0.0	0.0	0.0	0.0	0.0	0.0	0.0	0.0
23E-2 20-23	64.55	0.0	0.0	0.0	0.0	0.0	0.0	0.0	0.0
24E-1 67-70	66.21	0.0	0.0	0.0	0.0	0.0	0.0	0.0	0.0
24E-2 120-123	67.92	0.0	0.0	0.0	0.0	0.0	0.0	0.0	0.0
25E-2 30-33	69.48	0.0	0.0	0.0	0.0	0.0	0.0	0.0	0.0
26E-2 50-53	71.06	0.0	0.0	0.0	0.0	0.0	0.0	0.0	0.0
26E-2 100-103	72.72	0.0	0.0	1.9	0.0	0.7	0.2	0.1	0.0

(continued)

APPENDIX D. DIATOM FLORA FROM BL00-1 (continued)

Sample ID	Depth	Comments	Planktic Taxa		
			<i>Cyclotella rossii</i>	<i>C. unid</i>	<i>Stephanodiscus hantzschii</i>
<i>Core catcher samples</i>					
1E-26E	1.72		0.0	0.0	0.0
1E-27E	4.97		0.0	0.5	0.0
1E-28E	8.02		0.0	0.0	0.0
1E-29E	11.01	no visible diatoms or pieces	0.0	0.0	0.0
1E-30E	14.03	no visible diatoms or pieces	0.0	0.0	0.0
1E-31E	17.04	no visible diatoms or pieces	0.0	0.0	0.0
1E-32E	20.09		0.0	0.0	0.0
1E-33E	23.07		0.0	0.0	0.0
1E-34E	26.10		0.0	0.0	0.0
1E-35E	29.09		2.3	0.0	0.0
1E-36E	32.09		4.8	0.0	0.0
1E-37E	35.09		0.0	0.2	5.1
1E-38E	38.08	few diatoms	0.0	0.0	0.0
1E-39E	41.09		0.3	0.0	0.0
1E-40E	43.90	no visible diatoms or pieces	0.0	0.0	0.0
1E-41E	47.10		0.0	0.0	0.0
1E-42E	50.09		0.0	0.0	3.5
1E-43E	52.99		0.0	0.0	2.5
1E-44E	55.60		0.6	4.1	0.0
1E-45E	58.10	no visible diatoms or pieces	0.0	0.0	0.0
1E-46E	60.60		0.0	0.0	0.0
1E-22E	63.10	dissolution of some cells present, mostly on broken diatoms	0.0	0.5	0.0
1E-23E	65.60	no visible diatoms or pieces	0.0	0.0	0.0
1E-24E	68.10	very small pieces, some dissolution evident	0.0	0.0	0.0
1E-25E	70.61	no visible diatoms or pieces	0.0	0.0	0.0
1E-26E	76.32	very few diatoms, mostly <i>Stephanodiscus</i> and small fragilaroid, some dissolution			
1E-27E	76.90	no diatoms, no pieces			
1E-28E	79.43	no diatoms, no pieces			
1E-29E	81.91	some diatoms, mostly small fragilaroid and <i>Stephanodiscus</i> , lots of cysts			
1E-30E	84.42	very sparse, mostly small fragilaroid			
1E-31E	86.42	very few diatoms, mostly <i>Stephanodiscus</i> and small fragilaroid, some dissolution			
1E-32E	88.43	very sparse, centrics and pennates, mostly broken, some dissolution			
1E-33E	90.42	abundant diatoms, both centrics and pennates, very diverse			
1E-34E	92.43	abundant diatoms, both centrics and pennates, very diverse			
1E-35E	94.43	abundant diatoms, mostly planktonic, dissolution and breakage present			
1E-36E	96.43	sparse diatoms			
1E-37E	98.42	sparse diatoms, mostly small fragilaroid, dissolution present			
1E-38E	100.43	abundant diatoms and cysts, many <i>Stephanodiscus</i> and <i>Aulacoseira (granulata?)</i>			
1E-39E	102.20	abundant <i>Stephanodiscus</i>			
1E-40E	104.50	abundant <i>Stephanodiscus</i>			
1E-41E	106.00	abundant <i>Stephanodiscus</i>			
1E-42E	108.10	abundant diatoms, mostly small fragilaroid, few centrics			
1E-43E	110.40	abundant diatoms, both pennates and centrics, very diverse			
1E-44E	113.40	abundant diatoms, both <i>Fragilaria</i> and a few centrics			
1E-45E	114.90	no diatoms, no pieces			
1E-46E	117.80	abundant diatoms, many big centrics and <i>Aulacoseira</i>			
<i>Non-core catcher</i>					
1H-1 50-54	0.50	many broken pieces, mostly <i>Navicula oblonga</i> , <i>Pinnularia viridis</i> , and <i>Cymbella</i> , very few others	0.0		0.0
2H-1 80-84	2.85	1/2 transect	0.0		0.1
2H-2 28-30	3.97	1/2 transect	0.0		0.0
3H-2 50-52	7.15	1/2 transect	0.0		0.1
4H-1 110-112	9.25	2 transects	0.0		2.0
5H-1 30-32	11.45	no diatoms, no pieces, no cysts, plenty of sediment	0.0		0.0
5H-2 80-83	13.50	no diatoms, no pieces, no cysts, plenty of sediment	0.0		0.0
6H-2 0-3	15.70	no diatoms, no pieces, no cysts, plenty of sediment	0.0		0.0
7H-1 70-73	19.00	mostly broken <i>Stephanodiscus</i> , very little dissolution visible	0.0		0.0
16E-2 60-63	44.90	15 transects	0.0		14.7
18E-1 30-33	50.50	1 transect	0.0		9.3
18E-2 80-83	52.45	1/2 transect	0.0		2.2
20E-1 50-53	56.10	1 transect	0.0		0.0
20E-2 100-103	57.72	4 transects	0.0		0.4
21E-1 150-153	59.36	3 transects, lots of pieces	0.0		3.4
21E-2 120-123	60.39	2 transects	0.0		0.0
22E-1 50-53	61.08	many well-preserved periphytic diatoms, but dissolution of some planktic diatoms	0.0		0.0
22E-2 100-103	62.84	many whole and well-preserved diatoms, including <i>Amphora</i> , <i>Aulacoseira</i> and small benthic/tychoplanktic fragilaroid species, but also many broken and dissolved large <i>Cymbella</i> and <i>Epithemia</i> diatoms	0.0		0.0
23E-2 20-23	64.55	no diatoms, no pieces, no cysts, plenty of sediment	0.0		0.0
24E-1 67-70	66.21	diatoms are rare, no evidence of dissolution	0.0		0.0
24E-2 120-123	67.92	no diatoms, no pieces, no cysts, plenty of sediment	0.0		0.0
25E-2 30-33	69.48	no diatoms, no pieces, no cysts, plenty of sediment	0.0		0.0
26E-2 50-53	71.06	few diatoms observed, some breakage, but no evidence of dissolution	0.0		0.0
26E-2 100-103	72.72	no dissolution evidenced	0.0		0.4

Note: Species are divided into benthic and planktic species. Only taxa that occurred in at least 1 sample in amounts $\geq 1\%$ are included.

		Planktic Taxa								
Sample ID	Depth	<i>S. medius</i>	<i>S. minutulus</i>	<i>S. niagarae</i>	<i>S. neoastreae</i>	<i>S. sp. BL1</i>	<i>S. unid</i>	Unid pennates	Unid centrics	% Planktonics
<i>Core catcher samples</i>										
1E-26E	1.72	0.0	0.0	0.0	0.0	0.0	0.0	2.2	0.0	0.0
1E-27E	4.97	0.0	0.6	0.0	0.0	0.0	0.0	0.9	0.0	12.6
1E-28E	8.02	1.8	0.0	0.0	0.0	0.0	0.0	2.8	0.4	2.6
1E-29E	11.01	0.0	0.0	0.0	0.0	0.0	0.0	0.0	0.0	0.0
1E-30E	14.03	0.0	0.0	0.0	0.0	0.0	0.0	0.0	0.0	0.0
1E-31E	17.04	0.0	0.0	0.0	0.0	0.0	0.0	0.0	0.0	0.0
1E-32E	20.09	89.0	0.5	0.0	0.0	0.0	0.0	1.1	0.0	89.5
1E-33E	23.07	40.1	0.0	3.6	0.0	0.0	0.0	2.1	0.4	44.0
1E-34E	26.10	95.7	2.8	0.1	0.0	0.0	0.0	0.4	0.4	99.1
1E-35E	29.09	81.6	1.0	0.2	0.0	0.0	0.0	0.5	0.0	85.1
1E-36E	32.09	62.7	0.0	0.3	0.0	0.0	0.0	1.6	0.0	70.6
1E-37E	35.09	75.6	8.2	0.0	0.0	0.0	1.2	1.1	0.0	91.8
1E-38E	38.08	0.0	0.0	0.0	0.0	0.0	0.0	0.0	0.0	0.0
1E-39E	41.09	26.2	0.7	0.0	0.0	0.0	0.0	1.3	0.0	34.3
1E-40E	43.90	0.0	0.0	0.0	0.0	0.0	0.0	0.0	0.0	0.0
1E-41E	47.10	16.7	2.9	0.0	0.0	0.0	0.0	1.3	0.0	26.0
1E-42E	50.09	1.4	0.5	0.0	0.0	0.0	0.0	0.0	0.0	32.6
1E-43E	52.99	13.8	2.5	0.0	0.0	0.0	0.0	2.0	0.0	27.4
1E-44E	55.60	19.2	1.3	0.0	0.0	0.0	0.0	1.7	0.0	32.6
1E-45E	58.10	0.0	0.0	0.0	0.0	0.0	0.0	0.0	0.0	0.0
1E-46E	60.60	0.0	0.0	0.0	0.0	0.0	0.0	4.0	0.4	6.1
1E-22E	63.10	0.2	0.0	0.0	0.0	0.0	0.0	0.5	0.0	1.0
1E-23E	65.60	0.0	0.0	0.0	0.0	0.0	0.0	0.0	0.0	0.0
1E-24E	68.10	0.0	0.0	0.0	0.0	0.0	0.0	0.0	0.0	0.0
1E-25E	70.61	0.0	0.0	0.0	0.0	0.0	0.0	0.0	0.0	0.0
1E-26E	76.32									
1E-27E	76.90									
1E-28E	79.43									
1E-29E	81.91									
1E-30E	84.42									
1E-31E	86.42									
1E-32E	88.43									
1E-33E	90.42									
1E-34E	92.43									
1E-35E	94.43									
1E-36E	96.43									
1E-37E	98.42									
1E-38E	100.43									
1E-39E	102.20									
1E-40E	104.50									
1E-41E	106.00									
1E-42E	108.10									
1E-43E	110.40									
1E-44E	113.40									
1E-45E	114.90									
1E-46E	117.80									
<i>Non-core catcher</i>										
1H-1 50-54	0.50	0.0	0.0	0.0	0.0	0.0	0.0	0.0	0.0	0.0
2H-1 80-84	2.85	4.1	0.1	0.0	0.0	0.0	0.0	1.2	0.8	15.4
2H-2 28-30	3.97	0.0	0.0	0.0	0.0	0.0	0.0	1.3	0.0	7.2
3H-2 50-52	7.15	12.7	2.9	0.0	0.1	0.0	0.0	0.9	1.0	27.1
4H-1 110-112	9.25	35.8	0.0	0.0	1.4	0.0	0.0	1.4	0.2	40.6
5H-1 30-32	11.45	0.0	0.0	0.0	0.0	0.0	0.0	0.0	0.0	0.0
5H-2 80-83	13.50	0.0	0.0	0.0	0.0	0.0	0.0	0.0	0.0	0.0
6H-2 0-3	15.70	0.0	0.0	0.0	0.0	0.0	0.0	0.0	0.0	0.0
7H-1 70-73	19.00	0.0	0.0	0.0	0.0	0.0	0.0	0.0	0.0	0.0
16E-2 60-63	44.90	13.3	2.4	0.2	1.7	0.0	0.0	1.6	0.5	37.3
18E-1 30-33	50.50	6.0	1.6	0.0	0.1	0.1	0.0	0.4	0.4	26.9
18E-2 80-83	52.45	2.3	0.0	0.0	0.0	0.0	0.0	1.8	0.2	25.2
20E-1 50-53	56.10	0.0	0.0	0.0	0.0	0.0	0.0	0.0	0.0	1.3
20E-2 100-103	57.72	1.3	0.2	0.0	0.0	0.0	0.0	0.4	0.2	92.2
21E-1 150-153	59.36	8.8	0.0	0.3	0.0	1.6	0.0	2.9	1.8	39.8
21E-2 120-123	60.39	19.1	0.7	0.0	0.0	0.0	0.0	1.1	0.3	21.3
22E-1 50-53	61.08	0.0	0.0	0.0	0.0	0.0	0.0	0.0	0.0	0.0
22E-2 100-103	62.84	0.0	0.0	0.0	0.0	0.0	0.0	0.0	0.0	0.0
23E-2 20-23	64.55	0.0	0.0	0.0	0.0	0.0	0.0	0.0	0.0	0.0
24E-1 67-70	66.21	0.0	0.0	0.0	0.0	0.0	0.0	0.0	0.0	0.0
24E-2 120-123	67.92	0.0	0.0	0.0	0.0	0.0	0.0	0.0	0.0	0.0
25E-2 30-33	69.48	0.0	0.0	0.0	0.0	0.0	0.0	0.0	0.0	0.0
26E-2 50-53	71.06	0.0	0.0	0.0	0.0	0.0	0.0	0.0	0.0	0.0
26E-2 100-103	72.72	58.0	3.1	0.4	0.0	0.0	0.0	2.5	0.4	65.2

Geological Society of America Special Papers

A quarter-million years of paleoenvironmental change at Bear Lake, Utah and Idaho

Darrell S Kaufman, Jordon Bright, Walter E Dean, et al.

Geological Society of America Special Papers 2009;450; 311-351
doi:10.1130/2009.2450(14)

E-mail alerting services click www.gsapubs.org/cgi/alerts to receive free e-mail alerts when new articles cite this article

Subscribe click www.gsapubs.org/subscriptions to subscribe to Geological Society of America Special Papers

Permission request click www.geosociety.org/pubs/copyrt.htm#gsa to contact GSA.

Copyright not claimed on content prepared wholly by U.S. government employees within scope of their employment. Individual scientists are hereby granted permission, without fees or further requests to GSA, to use a single figure, a single table, and/or a brief paragraph of text in subsequent works and to make unlimited copies of items in GSA's journals for noncommercial use in classrooms to further education and science. This file may not be posted to any Web site, but authors may post the abstracts only of their articles on their own or their organization's Web site providing the posting includes a reference to the article's full citation. GSA provides this and other forums for the presentation of diverse opinions and positions by scientists worldwide, regardless of their race, citizenship, gender, religion, or political viewpoint. Opinions presented in this publication do not reflect official positions of the Society.

Notes